Investigation of lateral diffusion as process for drug depot building in an artificial skin construct and human skin

Von der Fakultät für Lebenswissenschaften

der Technischen Universität Carolo-Wilhelmina

zu Braunschweig

zur Erlangung des Grades eines

Doktors der Naturwissenschaften

(Dr. rer. nat.)

genehmigte

D i s s e r t a t i o n

von Guido Schicksnus
aus Wolfsburg

1. Referentin: Professor Dr. Christel Müller-Goymann
2. Referent: Professor Dr. Jürgen Lademann
eingereicht am: 16.08.2010
mündliche Prüfung (Disputation) am: 04.11.2010

Druckjahr 2010

Für Tanja
und meine Familie

Preserve your illusions.

When they are gone you may still exist, but not live.

Mark Twain

Die vorliegende Arbeit entstand unter der Anleitung von Frau Prof. Dr. Christel Müller-Goymann am Institut für Pharmazeutische Technologie der Technischen Universität Carolo-Wilhelmina zu Braunschweig.

Frau Prof. Dr. Christel Müller-Goymann danke ich sehr herzlich für die Zuweisung des Themas, die erhaltene Unterstützung bei dessen Bearbeitung, sowie für die ständige Diskussionsbereitschaft und persönliche Betreuung. Darüber hinaus danke ich besonders für die langfristige Begleitung und Geduld.

Herrn Prof. Dr. Jürgen Lademann danke ich für die Anfertigung des Zweitgutachtens.

Allen Mitarbeiterinnen und Mitarbeitern des Institutes danke ich für die stets gute Zusammenarbeit und Unterstützung sowie für die herzliche und angenehme Arbeitsatmosphäre. Ich werde mich immer gern an die Zeit zurück erinnern!
Dabei gilt mein besonderer Dank Frau Britta Meier und Frau Dagmar Hahne für die zuverlässige Versorgung mit Hautkonstrukten aus der Zellkultur und Herrn Horst Wojahn für die Anfertigung des präzisen Stanzwerkzeugs zur Hautzerlegung.

Allen Doktoranden am unvergesslichen „Imsutut Tecloq“ danke ich sowohl für die vielen fachlichen Diskussionen als auch besonders für die großartige, freundschaftliche Grundstimmung der Zusammenarbeit mit viel Humor auf einzigartigem Niveau. Auch das macht die Zeit unvergesslich.

Ich möchte Herrn Dr. Peter-Jürgen Flory und den Braunschweiger Krankenhäusern für die Überlassung der humanen Spenderhaut danken.

Herrn Dr. Ulrich Schäfer vom Institut für Biopharmazie und Pharmazeutische Technologie an der Universität des Saarlands in Saarbrücken danke ich für das zur Verfügung stellen des Dermatoms, um definierte Schichtdicken der Hautproben zu erhalten.

Meiner Frau Tanja Schicksnus gilt meine Liebe und mein besonderer Dank für die langjährige, kontinuierliche Geduld, Unterstützung und Motivation und nicht zuletzt für das kritische Korrekturlesen der Arbeit. Auch meiner gesamten Familie möchte

ich für die fortwährende Unterstützung und die vielen kleinen Opfer herzlich danken. Vor allem danke ich dabei meinen Kindern Daniel und Noemi für das Verständnis, dass ich nicht immer soviel Zeit für sie hatte, wie ich hätte haben wollen.

Vorveröffentlichungen der Dissertation

Teilergebnisse aus dieser Arbeit wurden mit Genehmigung der Fakultät für Lebenswissenschaften, vertreten durch die Mentorin der Arbeit, in folgenden Beiträgen vorab veröffentlicht:

Publikationen

Schicksnus G, Müller-Goymann CC: Lateral drug diffusion in comparison of an artificial skin construct towards excised human stratum corneum; The Essential Stratum Corneum (Marks, Lèvêque & Voegeli) Martin Dunitz Ltd. (2002); 183-185

Schicksnus G, Müller-Goymann CC: Lateral diffusion of ibuprofen in human skin during permeation studies; Skin Pharmacol Appl Skin Physiol 2004; 17; 84-90

Tagungsbeiträge

Schicksnus G, Müller-Goymann CC: Lateral drug diffusion in comparison of an artificial skin construct towards excised human stratum corneum (Poster); Stratum Corneum III; Basel (2001)

Schicksnus G, Müller-Goymann CC: The influence of urea on lateral diffusion of ibuprofen acid in human skin (Poster); 4th World Meeting on Pharmaceutics, Biopharmaceutics, Pharmaceutical Technology; Florenz (2002)

Schicksnus G, Müller-Goymann CC: Influence of permeation enhancers on lateral diffusion in artificial skin constructs and excised human skin (Poster); Jahrestagung der Deutschen Pharmazeutischen Gesellschaft (DPhG); Würzburg (2003)

Table of contents

List of figures

List of tables

List of abbreviations

ASC	Artificial skin constructs
DMSO	Dimethyl sulfoxide
FHS	Full thickness excised human skin
HaCaT-cells	human adult keratinocytes, low calcium conditions, elevated temperature
HPLC - UV	High pressure liquid chromatography with ultraviolet spectrometry
NSAID	non-steroidal anti inflammatory drug
PHS	Planed excised human skin
TEM	transmission electron microscopy
TEWL	transepidermal water loss

1 Introduction

The transport of substances across the stratum corneum, forming the diffusion barrier of the human skin, is a highly complex process. Therefore multiple factors influencing the successful delivery of the active substance into or through the skin have to be considered during the development of drug formulations for topical application. Not only are the physicochemical characteristics of the active substance, but also the composition of the matrix with possible permeation enhancing effects, relevant to the interaction of the formulation with the skin. The diffusion process and the pathway of the molecules are largely influenced by the interaction of the three components drug, matrix and stratum corneum.

The great inter- and intrapersonal variability of skin structure causes additional difficulties in the comparative evaluation of formulations. This variability and the principle limitations of in vivo testing create the need to evaluate formulations using model systems providing standardized material.

These systems are supposed to simulate the human skin regarding the diffusive resistance and at the same time provide the basis for a standardized evaluation. Some of the more simplistic in vitro models reflect only a limited number of influencing factors and are suitable to characterize formulations or substances but have a limited correlation to in vivo results regarding delivery to the skin. Models focusing on the comparability to in vivo results commonly use animal skin, human skin from surgery or artificial skin models from cell culture. Due to their tissue structure they mimic the diffusion process in vivo more closely. While the use of native human or animal skin provides a greater total diffusion barrier the cell culture tissues show smaller variability of barrier properties between experiments.

A direct in vitro – in vivo correlation during formulation development is not necessary in most of the studies but correlation of an in vitro animal skin or cell culture model to an in vitro human skin is relevant to evaluate a therapeutic benefit.

This assessment is often done by the determination of drug permeation parameters using the same formulation. This purely vertical drug diffusion evaluation is sufficient in order to characterize the principle barrier property of the model. For more complex evaluations like for example drug depot building within the skin this approach is too simplistic. Modified methodologies need to be applied and the characteristics of the chosen model have a greater influence on the result.

The aim of this study was to characterize lateral drug diffusion in an artificial skin construct from cell culture in comparison to different types of human skin obtained from plastic surgery. Special focus was laid on the timely development of drug concentrations versus distance from site of application in order to investigate a depot building effect. If possible the observed profiles should be described by a mathematical function allowing a comparison of influencing parameters for the diffusion process in the respective skin types. The commercially available ibuprofen containing formulation Ibutop Creme was used directly and also modified with additional enhancers. Next to the lateral diffusion also drug permeation through the types of skin was determined using the same experimental setup.

2 Theoretical part

2.1 The skin

With a mass of up to 1/6th of the total body weight and a surface of nearly 2 m² the skin is the greatest human organ serving among others as interface to the environment. Because of the very large surface to volume coefficient and the variable demands depending on the localization the skin has to be considered a very diverse organ for example with regard to thickness, number of hairs or sensory cells.

2.1.1 Skin functions

2.1.1.1 Protection

Due to its elasticity and tensile strength it provides a very efficient mechanical protection. The skin also protects the body against chemical agents, radiation and desiccation.

2.1.1.2 Regulation

The regulation of the evaporation of water allows temperature control aided by the fatty tissue as isolating layer and the micro capillary system. Furthermore the skin has regulating functions for the immune system.

2.1.1.3 Perception

Various sensory cells allow the perception of heat, cold, pain, irritation and the sense of touch. The speed of stimulation transport as well as adaptation to persisting stimuli differs in dependence on the type of receptor.

2.1.2 Skin structure

The skin can anatomically be divided into three separate zones: the epidermis, dermis and hypodermis (more commonly also referred to as subcutis). Depending on the localization the thickness and also structure of each zone can differ considerably (fig. 2.1). While the subcutis with its fatty and connective tissue mainly functions as temperature isolating layer, the dermis' supporting connective tissue accounts for the mechanical robustness. The epidermis provides the barrier properties of the skin due to the corneocytes and multiple lipid bilayers.

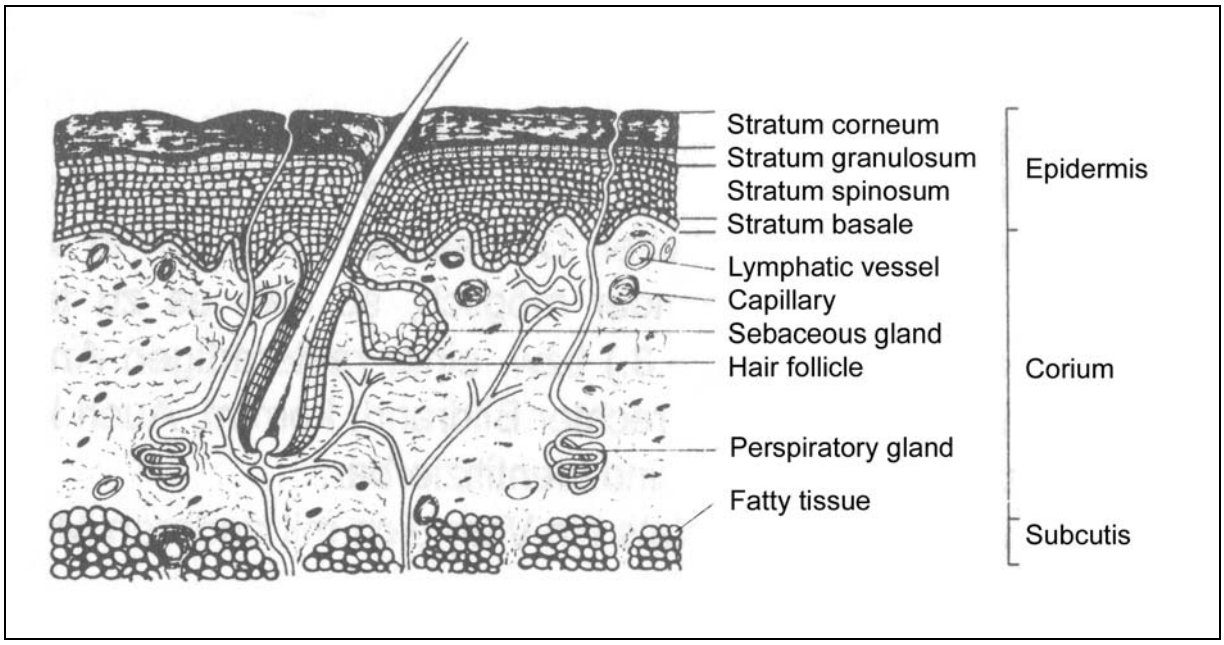

Fig. 2.1: Cross-sectional scheme of the human skin [Pfeifer et al., 1984]

2.1.2.1 Structure of the epidermis

The epidermis is a typical proliferation tissue of mainly (90 %) keratinocytes. Much less frequent also melanocytes, lymphocytes, Langerhans-cells and Merkel-cells are present. While due to the nature of the skin the proportions of the other cells varies the melanocytes appear in a preferred 1:36 ratio [Moll, 1989] and Langerhans-cells in a 1:53 ratio [Bauer et al., 2001]. Additionally, nerves but no blood vessels are found.

Due to the resulting need of passive nourishment the structure of the interface to the dermis is cone shaped for surface enlargement also providing better tensile strength.

Although different aspects for the segmentation of the epidermis based on mathematical considerations of cell layer organization are proposed also [Hoath and Leathy, 2002], most commonly the structuring is based on histological aspects. Inspite of earlier suggestions [Ryan, 1966] it is commonly accepted today that the direction of growth is directed from the epidermal-dermal borderline towards the body surface [Pinkus, 1970]. During their course of differentiation from keratinocytes into corneocytes the cells grow through microscopically distinguishable layers (fig. 2.2).

Starting at the borderline to the dermis the stratum basale is the mitotic active single layer of keratinocytes dispensing cells towards the following multi layered stratum spinosum. Here the cells gain in size, start to transform towards a polygonal leveled shape and start with keratin synthesis. When the cells are fully differentiated they have reached the stratum granulosum bearing up to three cell layers. The cornified envelopes are formed and apoptosis accompanied by the proteolytic degradation of the nucleus takes place leading to the release of the several proteins and lipids contained in the cell matrix. The end of the viable epidermis is reached.

Depending on the localization the subsequent layer of the stratum lucidum may be present or not. Typically this visually dense range of corneocytes is present at locations where also the following stratum corneum shows disproportionate thickness like at palms and the sole of the feet. While normally the stratum corneum consists of about 20 layers of desmosome connected corneocytes [Chapman and Walsh, 1990] providing a thickness of about 10 µm on hands and feet a size of about 500 µm is reported [Holbrook and Odland, 1974; Barry, 1983].

The outermost layers of the stratum corneum are ablated with time and newly differentiated cells have to replenish the loss of cellular material by desquamation. The total turnover time according to literature averages around 28 days and can be apportioned in 2-3 weeks for the viable epidermis and another two weeks for the stratum corneum. This process is not only driven by physical force but is an actively regulated protein and enzyme linked procedure [Lundström et al., 1994; Suzuki et al., 1994] influenced by various factors like pH, humidity, ionic strength, temperature, etc. [Bernard et al., 2002 and 2003; Öhman and Vahlquist, 1994].

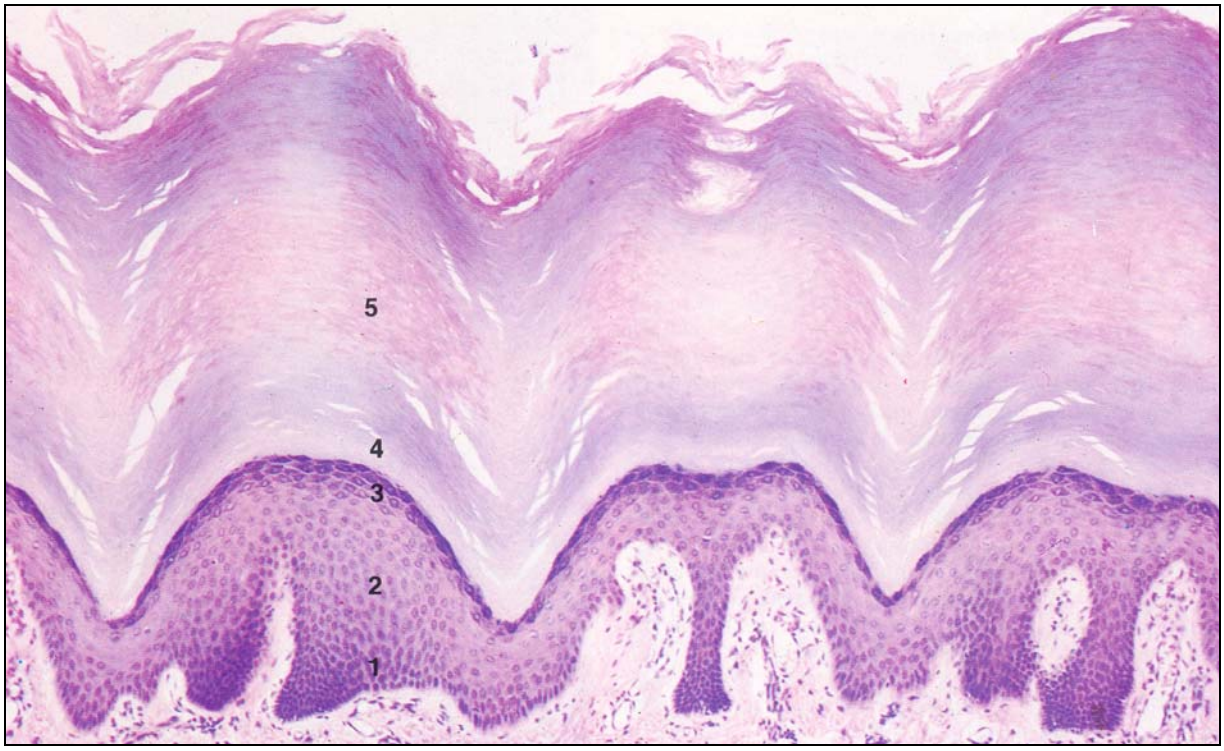

Fig. 2.2: Cross section of the epidermis (1 Stratum basale, 2 Stratum spinosum, 3 Stratum granulosum, 4 Stratum lucidum, 5 Stratum corneum) [Wheater et al. 1987]

2.1.2.2 Structure of the dermis

The most dominant cell type of the dermis is the fibroblast. Furthermore quite common are histiocytes like macrophages and also sporadic mastocytes and infrequent melanocytes. Functionally important are the several types of fibers forming a mechanically stable net based on mainly collagen type I.

The dermis consists of two histologic layers, the stratum papillare and the stratum reticulare. The former is rather thin and provides for the connection of the dermis to the epidermis with frequent elastic fibrils. The latter contains the collagen fiber network and as well the hair follicles as the perspiratory glands originate here.

The vascularization is subdivided into two connected layers. On the borderline to the subcutis the deep dermal plexus of small to mid-sized veins and arteries provides the basis for the sub-epidermal plexus of capillary blood vessels located in the stratum pallilare. This plexus guarantees for the nourishment of the viable epidermis and moreover regulates body temperature and blood pressure.

2.1.2.3 Structure of the subcutis

The subcutis consists of fatty tissue which is segregated by loose, lamelliform arranged connective tissue. It functions as an insulating layer, mechanical cushion and energy reservoir.

2.2 Barrier function of the stratum corneum

It is commonly acknowledged that the diffusion barrier of the skin lies within the stratum corneum [Scheuplein, 1976] preventing both water loss by evaporation and uptake of xenobiotics. The composition and the structure of the lipid phase within the stratum corneum are held accountable for the limitation of molecular transport. The

concepts explaining the high barrier function range from the standard “brick and mortar” model [Barry, 1987] to more sophisticated models like the “mosaic model” [Forslind, 1994], “sandwich model” [Bowstra et al., 2000] and the “single gel phase model” [Norlen, 2001]. The basic principle to all these models is the organization of the lipid phase into lamellar phases of 6 nm and 13 nm repeat distance [Bouwstra et al., 2003] containing crystalline regions. This principle is also supported by transmission electron microscopy (TEM) pictures from morphological studies (fig. 2.3).

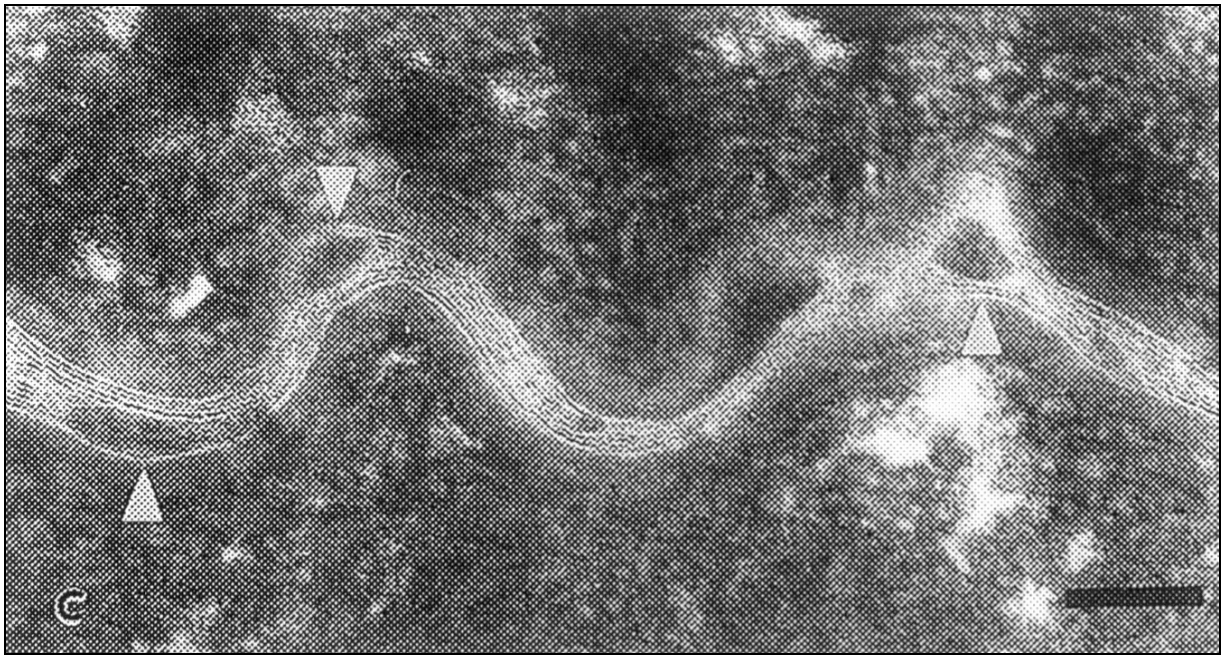

Fig 2.3: TEM picture of intercorneocyte spaces in normal human stratum corneum (arrows: corneodesmosomes; bar = 100 nm) [Haftek, 2002]

Studies on the formation of the intercorneocyte lamellar structure revealed that the mechanism is identical for mammals, birds and reptiles starting with lipid containing lamellar granules (fig. 2.4) in the uppermost living cells.

These granules are then discharged into the intercellular space forming short disks like a flattened unilamellar liposome. During the terminal differentiation of the

keratinocytes these disks are transformed into continuous sheets of lipid bilayers through a membrane-fusion process. [Landmann, 1986]

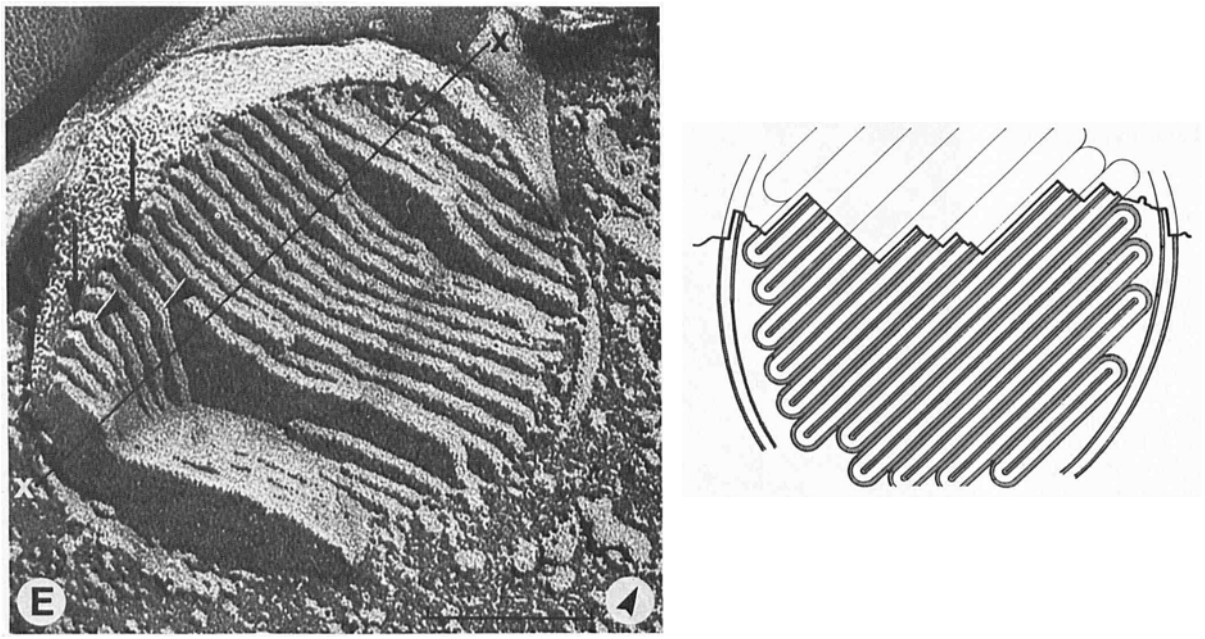

Fig 2.4: Lamellar granule disks from freeze fracture study (left) and profile of the fracture face along the X-X line (right); bar = 0.1 µm [Landmann, 1986]

Since drug transport through the skin is not an active transport process but is passively driven by diffusion these stacked sheets of lipid bilayers with their alternating hydrophilic and hydrophobic regions function as the main barrier.

2.2.1 Diffusion pathways

For a local or systemic therapy with an active substance via the skin the molecules in a first step have to permeate through the stratum corneum before penetrating into the viable epidermis or deeper into the dermis where the targets for local therapy are. Diffusing into the blood capillary plexus of the dermis leads to a quick drainage and a systemic therapeutic effect. The physicochemical characteristics of the active substance largely determine if a local or systemic transdermal use is possible. Since the principle function of the stratum corneum is to hinder the infiltration of exogenic molecules most substances are not suitable for dermal application. Although

controversial discussion exists about the influence of molecular size or volume [Tayar et al., 1991; Guy and Potts, 1992] it is commonly accepted that smaller molecules of sufficient lipophilic character have the best ability to penetrate into the stratum corneum [Bunge and Cleek, 1995] due to its high lipid content. The more hydrophilic a substance is the more effective is the barrier function of the stratum corneum. Yet for extremely lipophilic substances with a resulting low partition into the viable tissue, containing greater amounts of water, an accumulation in the lower layers of the stratum corneum is described [Wiechers, 1989; Bock et al., 2004]. Hence the epidermis in total is a good barrier for both highly hydrophilic and lipophilic molecules while amphiphilic or slight to medium lipophilic molecules show the best ability for transdermal delivery. A good proven indicator for permeation capability of a substance is the octanol / water partition coefficient [Bunge and Cleek, 1995; Potts and Guy, 1995] but also other partition coefficients are referenced [Abraham et al., 2004].

For the passage through the stratum corneum principally three different routes can be differentiated and largely the molecular characteristics determine which of the routes predominantly is chosen. For most molecules either the intercellular or the transcellular route as shown in fig. 2.5 are relevant while the shunt route via the hair follicles and perspiratory and/or sebaceous glands is generally of minor importance at any rate already due to its small fraction of only about 0.1% of the human skin surface.

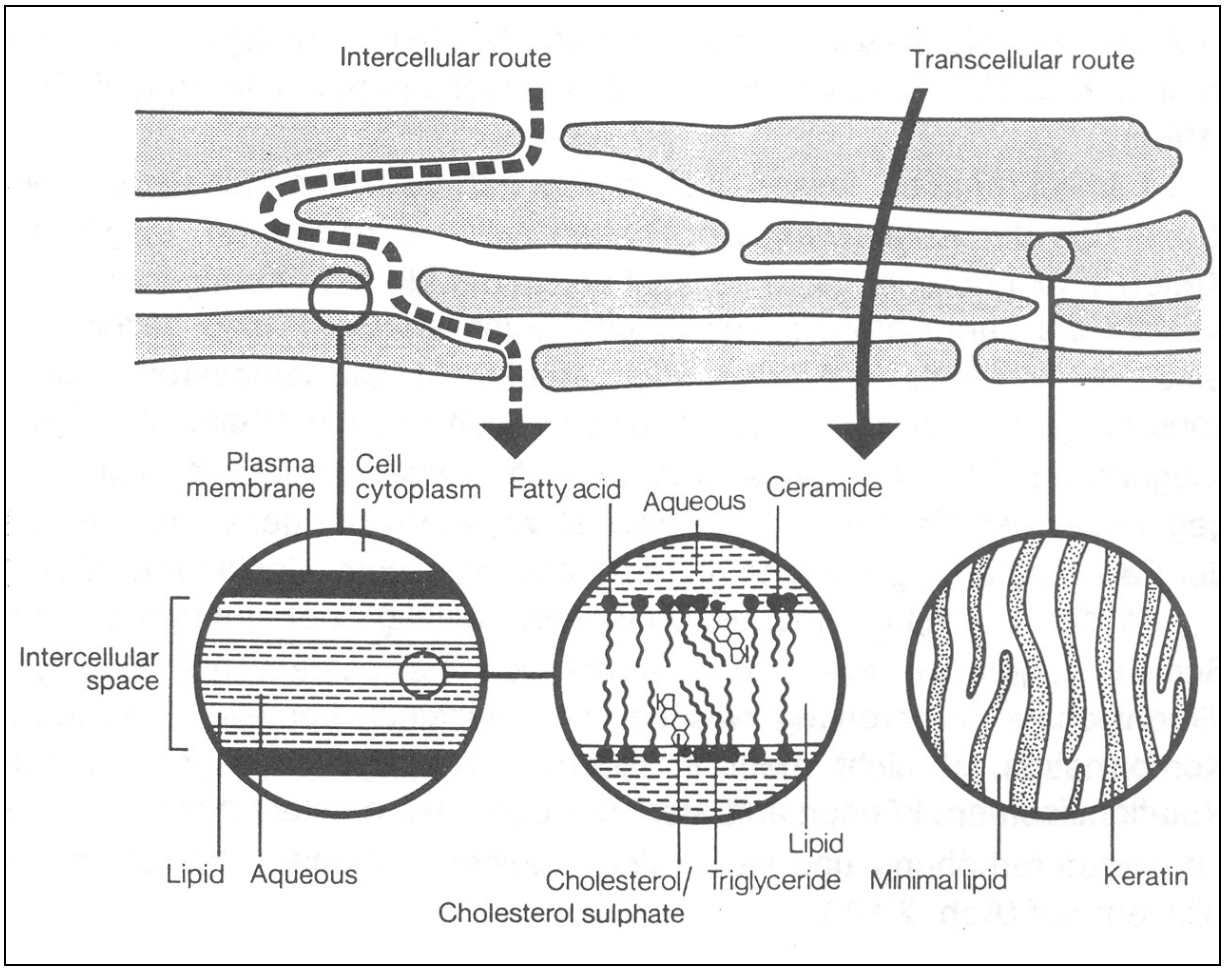

Fig. 2.5: Schematic view on the intercellular and transcellular route [Elias 1981]

2.2.1.1 Transcellular route

The diffusion across the corneocytes was the first suggested mechanism [Scheuplein, 1976] and is accountable mainly for the permeation of hydrophilic molecules. Though in some model evaluations also the primary mechanism for hydrophilic solutes is viewed as a diffusion process through imperfections / defects that occur between / within the lipid lamellar organization of the stratum corneum [Tezel and Mitragotri, 2003], it could be shown by fluorescence microscopy that diffusion through the corneocytes occurs [Yu et al., 2003]. This transcellular route is sometimes also referred to as “the porous pathway” or diffusion through “aqueous pores”. A hydrophilic molecule following this route can diffuse a large part of the

distance across the stratum corneum through the hydrophilic regions within the corneocytes but still has to cross the lipid lamellae between the corneocytes. The distance within the lipid phase is thus significantly reduced yet it is the rate limiting step leading to a noticeable lag time [Barbero and Frasch, 2006].

2.2.1.2 Intercellular route

The intercellular route is widely considered to be the most relevant for the topically applied drugs. In recent years it was even proposed to be the only relevant mechanism since the drug substance transport could be modeled for a variety of solutes including hydrophilic ones taking solely physical properties of the substances like molecular volume and hydrogen bond donor and acceptor activity into account [Potts and Guy, 1995; Abraham et al., 1995].

After partitioning into the lipid phase the molecules face a tortuous path along the intercellular channels containing structured lipid bilayers having to cross sequentially lipophilic and hydrophilic domains or diffusing within the sheet layers.

2.2.1.3 Shunt route

The permeation through hair follicles, sebaceous glands or perspiratory glands is in combination referred to as following the shunt route. This path is mainly a bypass for very large molecules or ionic solutes. Although it only plays a minor role for topically applied drugs from creams or ointments it could be shown that it is of significant importance for iontophoretic drug transport [Cullander and Guy, 1991]. Further modern concepts for targeted drug delivery of for instance liposomes or even solid particles were recently reviewed [Knorr et al., 2009].

2.2.2 Possibilities for modifying the barrier function

One of the physiological functions of the stratum corneum is to limit water evaporation. The determination of the transepidermal water loss (TEWL) shows different magnitudes of water evaporation for varying sites of the human body in good correlation to the determined drug penetration at the same site [Lotte et al., 1987]. It is commonly accepted that TEWL is a reliable indicator for the quality of the barrier function [Shimada et al., 2008] and thus is widely used to characterize the stratum corneum barrier function [Savi et al., 2007; Kuntsche et al., 2008] although it might not be directly related to it per se [Chilcott and Emanuel, 2000].

From the regional physiological differences for varying diffusive resistance like thickness of the stratum corneum layer, amount of perspiratory glands or local lipid composition [Lampe et al., 1983] especially the latter one gives way to an external modification of barrier properties. Multiple parameters influencing the permeability of the stratum corneum were studied. The effectiveness of most of these parameters is deriving from an alteration of the stratum corneum lipid organization [Lévêque, 2002 a] while mechanical deformation of the stratum corneum of up to 16 % extension which results in disruption of the corneocyte cell membrane from the lipid bilayers does not lead to increased TEWL rates [Takahashi and Marks, 1985; Lévêque et al., 2002 b].

If parameters with different mode of action as described in the following paragraphs are combined synergetic effects can be achieved [Hadgraft, 1999; Nicolazzo et al., 2005].

2.2.2.1 Water content

Water molecules change all the physical properties of the keratinized tissues and particularly increase the diffusion coefficient. The water content in the stratum corneum shows a gradient from the hydrous dermis to the relatively dry outer surface of the stratum corneum. The amount of water directly influences the organizational structure of the intercorneozyte lipids. Higher water levels allow a liquid crystalline structure and fluidization of the membranes [Alonso et al., 1995] while decreasing water concentrations provoke a gel state formation [Sparr and Wennerström, 2001]. This results in changing diffusion resistances along the water gradient. Since most substances rather partition into a liquid crystalline structure than into the gel state a significant increase in permeability can be gained from a greater hydration of the stratum corneum for instance by occlusion. Yet the potential effect also strongly depends on the characteristics of the active substance [Treffel et al., 1992; Cevc et al., 2008]. Therefore also the mechanism of a porous pathway for highly hydrophilic molecules was proposed [Tang et al., 2002].

2.2.2.2 Lipid extraction

As the natural, local variability of lipid composition in the stratum corneum determines the barrier quality any method of extracting lipids from the lipid bilayers will alter its microstructure and thus also modify the barrier function [Sweeney and Downing, 1970]. This can be an effect of the formulation’s matrix or can be caused by the mode of application. For instance is the effectiveness of low frequency sonophoresis attributed to an extraction of approximately 30 % of the intercellular lipids [Alvarez-Román et al., 2003] besides other alterations of the lipid structure [Chesnoy et al., 1996; Tang et al., 2001].

2.2.2.3 Enhancer

For increasing the delivery rate of active substance from a formulation additional excipients that interact with the stratum corneum are frequently used. These diffusion enhancing substances ideally possess the property that they reversibly reduce the barrier resistance of the horny layer, allowing the drug to reach the living tissues at a greater rate, without the enhancer damaging any cells. The enhancers can interact with stratum corneum lipids, proteins or improve partitioning of the drug, a co-enhancer or water into the tissue [Barry, 1991]. These effects can occur in any combination, depending on the physicochemical properties of the chosen enhancer. This will result in an enhanced permeation alongside the intercellular and / or the transcellular route, respectively.

In general the three possible sites as shown in figure 2.6 for interaction with the stratum corneum lipids affecting mainly the intercellular route are discussed.

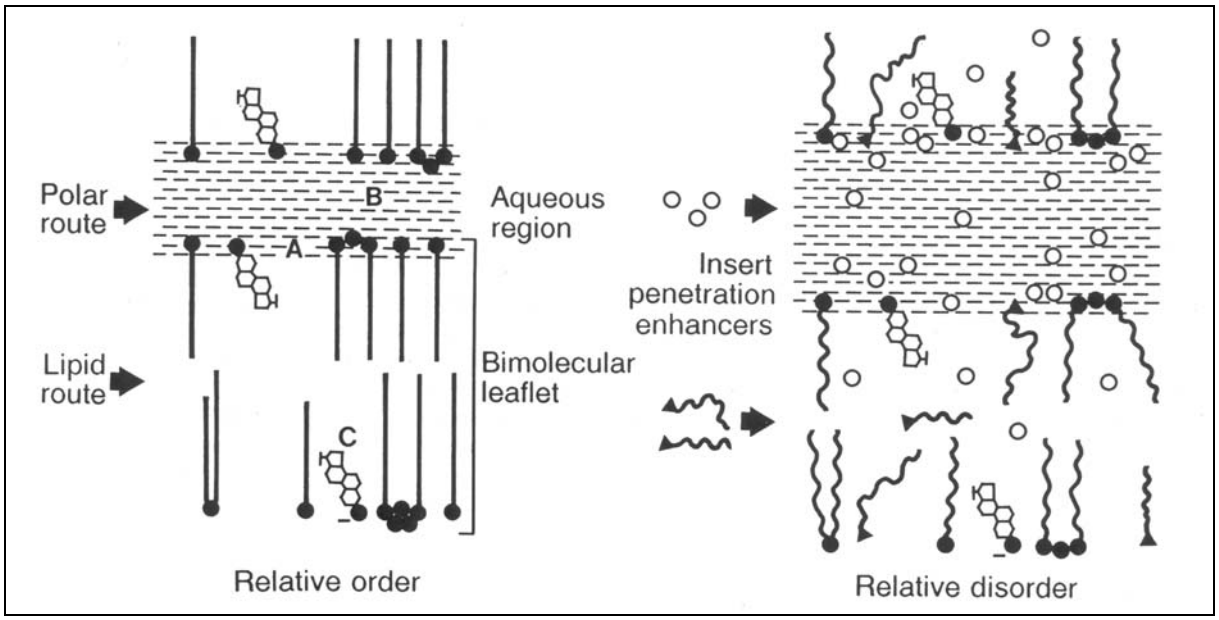

Fig. 2.6: Proposed action sites for accelerants in the intercellular space of the horny layer [Barry, 1991]

For the enhancers depicted in figure 2.6, linear chains represent e.g. azone, bent chains correspond to cis-unsaturated promoters and the circles stand for small polar solvents such as DMSO and its analogues.

- By interaction with the polar head groups of the lipids a disturbance of hydration spheres and head group interactions and thus a fluidization of this region can be reached. This will also increase the disorder within the lipid chains so that a lipophilic penetrant will then more readily permeate through this route.
- By absorption of enhancers which have a solvent characteristic into the stratum corneum the overall chemical constitution of both, the lipid and the aqueous region, can be changed. This modified lipid phase / enhancer mixture may increase the operating partition coefficient especially for oil soluble molecules.
- By intercalation between the lipid hydrophobic tails especially by structural changes lipophilic enhancers can increase disorder in lipid organization and thus also reduce polar head group interactions.

Influence on the transcellular route is mainly reached by interactions with the polar head groups of the semicrystalline keratin, relaxing the binding forces and altering the conformations of the helices. Extensive interaction may even form pore routes through the tissue.

Like the permeation abilities for active substances are estimated by their physicochemical properties the effect of potential enhancers is studied by structure-activity relationship [Warner et al., 2003]. This also allows the continuous

development of new classes of enhancer molecules [Akimoto and Nagase, 2003; Lee et al., 2004].

2.3 Drug diffusion through skin

Because drug passage through the skin along the routes described in 2.2.1 is not an active transport mechanism but a passive diffusion process the movement of the drug molecules is principally uninfluenced from any other molecules but depends on the physical parameters determining diffusion processes. Deriving from these parameters some general criteria a molecule should posses for successful permeation were formulated [Hadgraft, 2002]:

- Be small
- Have a low melting point
- Possess a log (octanol-water partition coefficient) ~ 2
- Have good solubility in both water and oils
- Have a minimum number of pendant functional groups capable of hydrogen bonding

The octanol-water partition coefficient is an indirect parameter for the expected solubility in the stratum corneum lipid phase which is proportional to the permeation rate at steady state [Tojo et al., 1987].

As for most molecules the diffusion through the stratum corneum will be the rate limiting step this is the most frequently examined step, yet for systemic delivery the skin has to be viewed as a three compartment tissue (stratum corneum, viable epidermis and dermis) with independent compartmental diffusion characteristics.

Furthermore the release from the formulation can be the limiting parameter if partition into the stratum corneum is faster than drug release.

2.3.1 Diffusion laws

The first Fick diffusion law describes what amount per time will pass through a defined area depending on the given concentration gradient.

$$\frac{dm}{dt} = -q \cdot D \cdot \frac{dc}{dx} \qquad \text{Eq. 2.1}$$

$\frac{dm}{dt} =$ Mass flow (mass difference per time)

$q =$ Area that the molecules pass through

$D =$ Diffusion coefficient [m^2/s]

$\frac{dc}{dx} =$ Concentration gradient (concentration difference over distance)

The only substance specific parameter in equation 2.1 is the diffusion coefficient which is a combined factor from numerous individual contributors as can be seen from equation 2.2.,

$$D = \frac{k \cdot T}{6 \cdot \pi \cdot \eta \cdot r} \qquad \text{Eq. 2.2}$$

$k =$ Boltzmann constant

$T =$ Absolute temperature

$\eta =$ Viscosity of surrounding medium

$r =$ Radius of the diffusing particle / molecule

Regarding drug substance parameters only the molecular size is accountable for the diffusion rate. As stated earlier (2.2.1.2) also the interaction with the lipid phase of the stratum corneum is of major influence. Therefore in permeation experiments the drug substance flux J [g/cm^2·s] is determined. The parameter estimates the drug amount permeating through a defined skin area per time unit at perfect sink conditions and thus includes interaction effects of drug substance molecules and lipid phase.

$$J = P \cdot C_0 \qquad \text{Eq. 2.3}$$

$P =$ Permeation coefficient [cm/s]

$C_0 =$ Donor drug concentration at start [g/cm³]

The permeation coefficient includes the diffusion coefficient from Eq. 2.2, the partition coefficient for formulation / skin partitioning and the thickness of the skin in the permeation experiment.

$$P = \frac{D \cdot K}{h} \qquad \text{Eq 2.4}$$

$D =$ Diffusion coefficient [cm²/s])

$K =$ Partition coefficient formulation / skin

$h =$ Effective thickness of the skin [cm]

The inverse value of the permeation coefficient is also sometimes used to express the diffusional resistance R of a tissue (R = 1/P).

2.3.2 Lateral drug diffusion

While for other bilayers systems like cell membranes the investigation of lateral diffusion within the bilayers is frequently done in order to determine for instance the

mobility of proteins, within the lipid bilayers system of the stratum corneum only little detailed research is available [Johnson et al., 1996]. Yet it is acknowledged that the lateral diffusion process in the bilayers is of high importance especially for the intercellular route of lipophilic drug transport [Johnson et al., 1997]. Due to the horizontal orientation of the corneocytes (with a height to width ratio of about 1:10) and thus also of the surrounding bilayers (see fig 2.7) molecules with preferred diffusion along the bilayers will show considerable lateral movement on the way towards deeper skin layers. This lateral diffusion is unimportant on a macroscopic level for permeation experiments where the total available skin area is in contact to the donor and acceptor compartment but for in vivo experiments a strong influence of lateral diffusion on the results has been demonstrated [Weigmann et al., 1999]. It has been shown in in vivo experiments with rats, using non occluded finite dose application of radio labeled compounds with different hydrophilicity that after only 30 minutes diffusion time considerable amounts of the drugs could be recovered 13 mm and even 29 mm away from the application area. The lateral diffusion was more pronounced for the model substance with greater lipophilic character. It was therefore concluded that in congruence with Johnson´s findings the lateral diffusion takes place mainly in the stratum corneum intercellular lipid phase. A lateral spreading of the formulation on the skin as accidental root cause was excluded [Simonsen et al., 2002].

A similar result was obtained in a human in vivo experiment studying the influence of the formulation using a radio labeled substance permeating for 8 h from two different matrices. Lateral diffusion of the drug was observed in both cases but the matrix delivering the greater applied dose to the contact site also showed greater lateral diffused amounts of drugs not only in total amount but also relative to the application area. So more than 10 % of the effectively applied drug amount were found in the

adjacent site. It was concluded that the greater permeation enhancing effect of the matrix also promoted lateral diffusion [Ashworth et al., 1988].

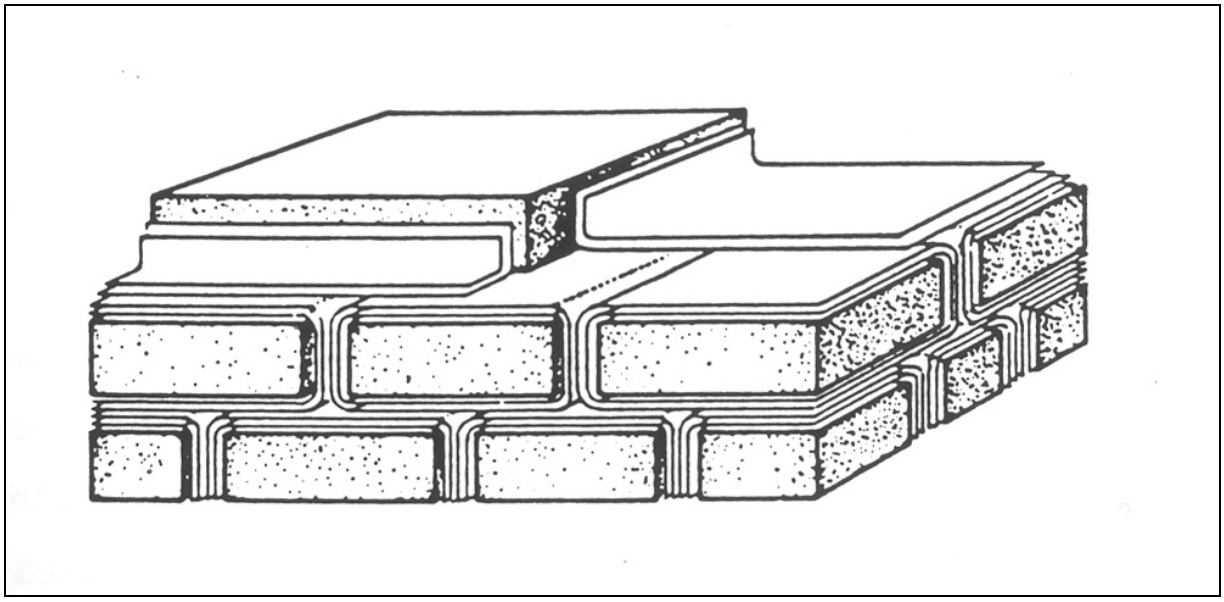

Fig. 2.7: Schematic view on surface parallel oriented corneocytes and lipid bilayers [Landmann, 1991]

Also by mathematical modeling a considerable influence on bioavailability of the drug substance by lateral diffusion was shown for a comparative simulation of permeation from a coherent donor to multiple distributed donors applying the same amount of active substance [Reddy and Bunge, 2000]. The lateral diffusion maintains the concentration gradient between donor and skin contact area as driving force for drug diffusion for a longer period of time.

When extrapolating in vitro results to in vivo use potential effects of the studies' methodological procedures neglecting the influence of lateral drug diffusion must be taken into account.

2.4 Common models

Several different approaches to study transdermal drug delivery are used. Depending on the aspect which is to be investigated a suitable level of complexity in the used model is necessary. Principally a simpler model can be used if a detailed parameter is to be assessed while more complex model are chosen to evaluate drug delivery in a more general perspective trying to mimic the in vivo situation as close as possible.

2.4.1 In silico (math models)

Mathematical models are used to simulate an observed experimental result by calculation based on as few parameters as possible. Often the model includes a hypothesis for a permeation mechanism. This approach can focus on very specific tasks like modeling the in vitro permeation of a special substance through a specific tissue [Coceani et al., 2003] or on the other hand try to predict drug delivery in general taking several influencing factors and pathways into account [Mitragotri, 2003]. Also a simulation of a single permeation pathway [Johnson et al., 1997; Mitragotri, 2002; Barbero and Frasch, 2006] or even prediction of transdermal drug delivery in vivo has been published [Chandrasekaran et al., 1978; Guy and Hadgraft, 1984; Lee et al., 1996]. Yet the overall extrapolation to in vivo conditions is viewed critically and requires experimental confirmation [Walters and Brain, 2000].

2.4.2 In vitro test models

2.4.2.1 Lipid mixtures

Since the intercellular lipids form the main barrier for drug permeation an artificial mixture of these lipids or analogous mixtures can be used for example to learn more about the stratum corneum lipid phase organization and behavior [Kitson et al., 1994]

or to study the interaction of drugs and/or excipients with the lipid phase during formulation development [Glombitza and Müller-Goymann, 2001]. In some set ups also additional corneocytes were added to the lipid mixture in order to generate a reconstituted stratum corneum membrane [Schendzielorz et al., 1997].

2.4.2.2 Siliconized membranes

For screening testing and optimizing the permeation of drugs siliconized membranes can be used. Since this very simple model cannot imitate any interactions between the formulation and the stratum corneum lipids the obtained results are generally not useful to directly extrapolate to an in vivo result [Herkenne et al., 2007].

2.4.2.3 Animal or human skin

A large variety of animal skins is used in publications on studying transdermal drug delivery. A practical reason for the use of animal skin models is the availability of animal or isolated animal skin compared to the availability of isolated human skin. Since the principle mechanism of forming the stratum corneum and its intercellular lipid phase is similar [Landmann, 1986] a large variety of different kinds of animals is used for transdermal drug diffusion testing. The selection is not only limited to mammalian animals like mouse, rat, rabbit or pig but also chicken and snake skin is used [Hirvonen et al., 1991]. Although there is principle similarity in stratum corneum structure significant differences in comparative experiments can occur due to morphological deviations (like skin thickness or amount of hairs) and different lipid composition.

The most frequently used animal skins appear to be rat and pig skin. For pig skin in recent years an acceptable correlation of results between pig in vitro to human in vitro [Schmook et al., 2001] and even human in vivo [Sekkat et al., 2002;

Herkenne et al., 2007] experiments could be shown. But also rabbits [Shah et al., 2006; Meshali et al., 2008] and rats [Yourick et al., 2008] are used for comparative studies towards human skin in vitro results. The use of rats or also frequently guinea pigs allows even for in vivo testing for more complex studies [Simonsen et al., 2002; Berner and Wagener, 1987].

Some more sophisticated animal skin in vitro models are developed to maintain tissue perfusion during the experiment so that drug elimination by simulated blood flow and even metabolic reactions can take place [Kietzman et al., 1993]. This helps to overcome the general tendency to find greater concentrations particularly of lipophilic drugs in the dermis in vitro compared to in vivo due to the missing elimination by blood perfusion [Zesch and Schaefer, 1975].

For the use of human skin for in vitro experiments the principle inter- and intra-individual variability of skin in combination with the limited availability do not allow the widespread use for formulation development. Nonetheless numerous set ups for transdermal drug delivery experiments using different types of pre-treated skin have been published [Franz, 1975; Wagner et al., 1998]. Depending on the aim of the study either full thickness skin, split thickness skin, heat separated skin or isolated stratum corneum, to name but a few, is used.

Direct comparability of results even from human skin in vitro to human skin in vivo experiments using skin from the identical individual is not always possible due to the influences of the experimental differences [Wagner et al., 2002]. Yet in some cases comparability could be shown [Bock et al., 2004] and for a comparison of drug delivery from several formulations [Hadgraft et al., 2003; Lombardi Borgia et al., 2008] or of enhancing effects [Vávrová et al., 2008] using the same methodology the human skin in vitro testing is very appropriate.

2.4.2.4 Artificial skin constructs

Artificial skin constructs (also frequently referred to as reconstructed human skin) are multilayered tissues built from various cell lines which are grown in cell culture. These immortalized cells undergo to some extent normal differentiation during the skin constructs cultivation period and thus form artificial tissue regions depending on the respective cell types. Due to the differentiation and construct geometry good simulation of native human skin tissue can be obtained for some aspects like biotransformation of active substances in the tissue [Gysler et al., 1999]. On the other hand the constructs' sizes in diameter are generally smaller and the robustness cannot compare to natural skin. This leads to necessary changes in methodology conducting in vitro experiments [Dreher et al., 2002].

A controversial discussion is led about the suitability of artificial skin constructs for experiments studying drug transport processes. While some publications assign good correlations with human skin and only a ten-fold difference in barrier quality [Doucet, 1998] up to the conclusion that an extrapolation to in vivo results is possible [Wagner et al., 2001] it is generally acknowledged that the barrier properties of skin constructs is some magnitudes lower than from native stratum corneum so that for instance Schmook et al. [2001] conclude that porcine skin is the better in vitro model.

A review on commercially available skin constructs also outlines that the designated areas of phototoxicity, corrosivity and irritancy testing are promising but the barrier property needs to be improved [Netzlaff et al., 2005]. In direct comparison of one commercial product to several types of human skin a difference in lipid composition was noticed and the differentiation by the diffusion barrier between two drug models on permeation experiments was insufficient [Netzlaff et al., 2007].

One the other hand the lower barrier function allows for more sensitive testing and guarantees shorter experiment times, which is especially useful in large screening studies.

2.5 Substances

2.5.1 Active substance

2.5.1.1 Ibuprofen

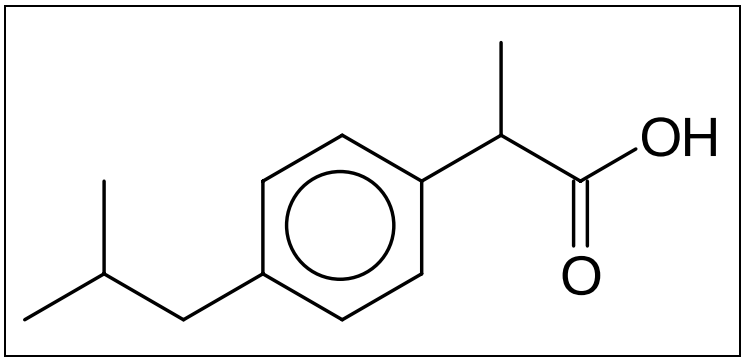

Molecular weight:

M_r = 206.27

Octanol / water partition coefficient:

log P_{oct} = 3.87

Fig 2.8: Molecular structure of ibuprofen and relevant data [Bouchard et al., 2003]

Ibuprofen belongs to the group of non-steroidal anti inflammatory drugs (NSAID) and is a racemic mixture of the (R)-(-)- and the (S)-(+)-isomer. Although the pharmacological activity is almost exclusively deriving from the (S)-(+)-ibuprofen the racemic mixture is therapeutically applied. This is reasonable since the (R)-(-)-isomer is transformed to about 60 % into the (S)-(+)-ibuprofen within the human body without observable back conversion.

Since the anti inflammatory effect shows good correlation with the inhibition of the enzyme cyclooxygenase this inhibition is the accepted main mode of action.

During local percutaneous treatment frequent (> 1/100) erythema, itching / burning sensation and eczema (also showing pustules and wheals) is reported. Yet from toxicity evaluation ibuprofen is rated to be of low irritancy in localized treatment.

After percutaneous application ibuprofen permeates from the respective formulation into deeper skin layers, joints and synovial fluid and reaches therapeutically relevant concentrations if suggested dosing is followed. Ibuprofen is therefore indicated for stand-alone or supportive topical treatment of several inflammatory and / or painful diseases. Daily 3 - 4 times application of 2 – 5 g of a formulation containing 5 % of ibuprofen (accounting to 100 – 250 mg ibuprofen / dose and up to 1000 mg / day, respectively) is suggested. Depending on the formulation the usual absorption rate is about 5 - 7.4 % [ABDATA, 2007]. The use of an occlusive patch can improve the therapeutic benefit. Greater penetration rates of ibuprofen can be achieved by iontophoresis or phonophoresis [Meshali et al., 2008].

Ibuprofen is a small molecule with sufficient lipophilic characteristics due to a log octanol-water partition coefficient (P) of around 4, and can therefore reach its site of action clearly beneath the transport-limiting barriers of the skin. Since the stratum corneum is the major barrier to permeation of NSAIDs, and it is essentially a dead tissue, in vitro experiments can provide relevant information about how effectively the NSAID will permeate in vivo. The impact of different formulation types like spray, mousse, cream and gel has been investigated [Herkenne et al., 2007] as well as differences within the same type of formulation [Hadgraft et al., 2003].

Ibuprofen is also commonly used as model drug for numerous other types of studies investigating for instance permeation enhancement, [González and Sumano, 2007] the influence of physicochemical formulation parameters on diffusion [Zgoda et al., 2007] or interaction effects with a second active substance on diffusion [Gu et al., 2008]. For the evaluation of lateral diffusion in membranes like multi-lamellar liposomes ibuprofen was also used [Gaede and Gawrisch, 2003].

2.5.2 Enhancer

2.5.2.1 Dimethyl sulfoxide (DMSO)

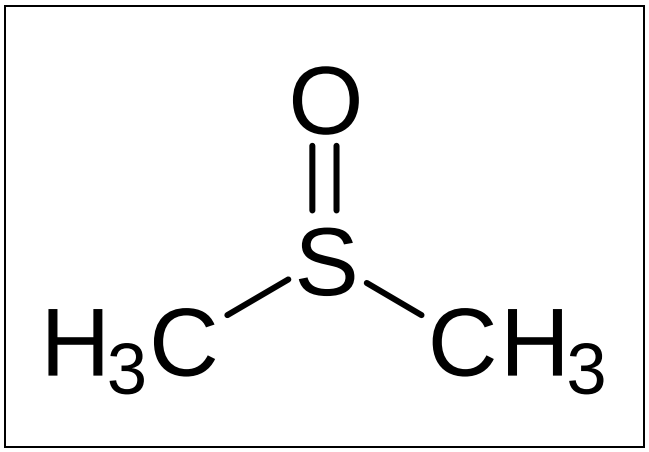

Molecular weight:

M_r = 78.13

Melting point:

18.55° C

Soluble in: water, ethanol, acetone, diethyl ether and chloroform

Fig 2.9: Molecular structure of DMSO and relevant data

Due to its physicochemical properties as aprotic solvent DMSO can interact with the skin intercellular lipids in a way that the solubilizing ability of the aqueous phase may increase. As an intercalating molecule it influences all three target domains for enhancers affecting the intercellular route and the result is that the operational partition coefficient now favours the development of a high drug concentration in the skin. But DMSO also shows influence on the intracellular route. Here interactions with polar groups, relaxation of binding forces and helical conformation changes are proposed. At higher concentrations even pore forming may appear [Barry, 1991]. The accumulation of DMSO in the stratum corneum leads to an increased partitioning of drug and / or co-enhancer like for instance propylene glycol in the case of Ibutop Creme from the formulation.

For permeation enhancing use DMSO is normally used in formulations up to concentrations of 10 – 15 %. In therapeutic use for the treatment of acute reflex sympathetic dystrophy even a concentration of 50 % is used [Zuurmond et al., 1996].

2.5.2.2 Urea

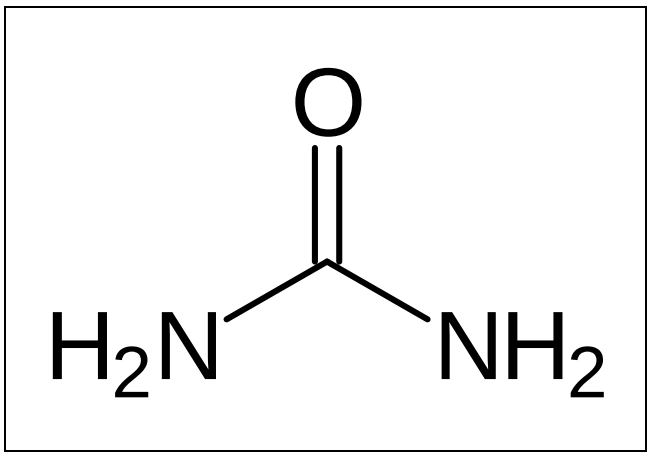

Molecular weight:

M_r = 60.06

Melting point:

132.7° C

Soluble in: water, ethanol, methanol, glycerol

Fig 2.10: Molecular structure of urea and relevant data

The permeation enhancing mechanism of urea is assumed to derive from its keratolytic abilities, which is also supported by the finding of a threshold concentration for an enhancing effect [Shah et al., 2006]. The efficiency is relatively small compared to other typical enhancers. More often urea is used as a moisturizer in topical formulations.

3 Materials and methods

3.1 Materials

3.1.1 Commercial formulation Ibutop Creme

As basic formulation for all experiments Ibutop Creme (Deutsche Chefaro Pharma GmbH, Waltrop, Germany) containing 5 % ibuprofen was used. Further excipients (and their functions) are:

- propylene glycol (permeation enhancer),
- methyl-4-hydroxybenzoate-Na (preservative),
- middle-chain triglycerides (fatty component),
- macrogol-glycerol fatty acid ester (surfactant),
- glycerol fatty acid ester (surfactant),
- macrogol stearic acid ester (surfactant),
- xanthan gum (thickening agent) and
- water.

3.1.2 Ibuprofen acid

For the calibration of the HPLC analysis racemic ibuprofen acid in pharmacopoeal quality from Caesar & Loretz GmbH, Hilden, Germany was used. The content measured by Caesar & Loretz using HPLC was 99.9 %.

3.1.3 Dimethyl sulfoxide (DMSO)

DMSO from Caesar & Loretz GmbH, Hilden, Germany was used.

3.1.4 Urea

The urea was purchased from Caesar & Loretz GmbH, Hilden, Germany.

3.1.5 Water

Water of double distilled quality was used.

3.1.6 HPLC-Mobile phase

Acetonitrile and glacial acetic acid (both HPLC quality) were purchased from J.T. Baker, Deventer, Netherlands.

3.1.7 Buffer pH 7.4

By solving 2.38 g sodium monohydrogen phosphate (Merck, Darmstadt, Germany) and 0.19 g potassium dihydrogen phosphate (Merck, Darmstadt, Germany) in one liter double distilled water a phosphate buffer system was prepared. To adjust the pH-value to 7.4 (3.2.3) further potassium dihydrogen phosphate was added.

3.1.8 Methanol as extraction medium

For the extraction of ibuprofen from the skin samples methanol of HPLC grade from Fluka, Neu-Ulm, Germany was used.

3.1.9 Reinforcement rings

Adhesive reinforcement rings to provide a constant application area of 19.6 mm^2 for the different formulations on the several skin types were purchased from Avery Dennison Zweckform, Holzkirchen, Germany.

3.1.10 Biopsy punches

Custom made steel punches 5, 10, 15, 20 and 24 mm in diameter, respectively, were used to segment skin samples. To ensure the separation into concentric rings the four smaller punches could be inserted in the central opening of the 24 mm punch.

3.1.11 Dermatome

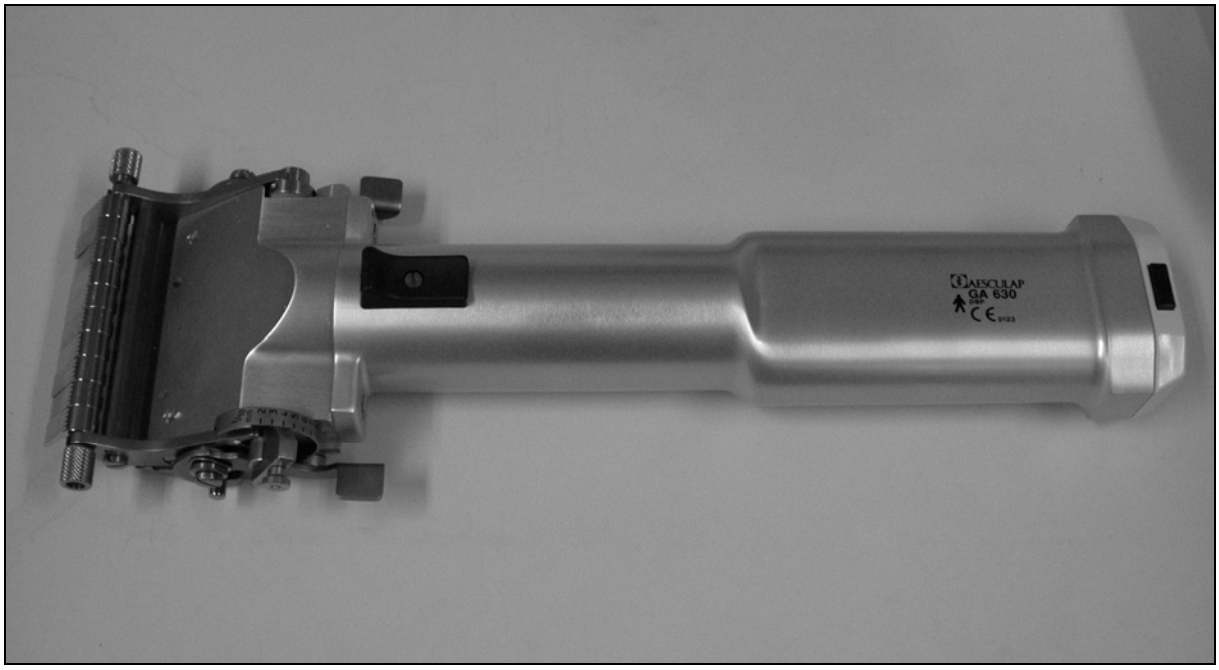

Fig 3.1: Aesculap dermatome GA 630

To obtain human skin samples of defined thickness, the dermatome GA 630 from Aesculap, Tuttlingen, Germany was used which was kindly provided by Dr. Ulrich Schäfer of the Department of Biopharmaceutics and Pharmaceutical Technology of the Saarland University, Saarbrücken, Germany.

The dermatome allows adjustment of skin sample width as well as thickness by mechanical levers largely independent from the force or pressure during the planing process.

3.2 Methods

3.2.1 High performance liquid chromatography (HPLC)

The HPLC system consisted of two 515 HPLC pumps, a 712 plus autosampler and a 486 tunable absorbance detector, all from Waters, Milford MA, USA.

The analytical software Millenium 32 from Waters, Milford MA, USA was used for peak identification and integration.

As analytical column a Hypersil ODS (particle size 5 µm) column (125 mm x 4 mm) from Grom, Herrenberg, Germany connected in line with a 10 mm guard column of the same filling was used.

The mobile phase consisted of water, acetonitrile and glacial acetic acid (3.1.5 / 3.1.6) in a ratio of 54 : 46 : 2. By isocratic elution at a flow rate of 1.7 ml/min and 140 - 170 bar a retention time of 5.8 min for ibuprofen acid was achieved. The method was calibrated with an injection volume of 40 µl for the quantitation range of 0.2 - 10.0 µg/ml with a correlation coefficient of R^2=0.99983.

3.2.2 Preparation of Ibutop Creme variations

To obtain the enhancer containing variations of Ibutop Creme an Unguator from GAKO Konietzko GmbH, Bamberg, Germany was used whose homogenization efficacy is proven in literature [Zobel et al., 1997]. Approximately half of the Ibutop Creme was given into the container before the additional enhancer (3.1.3 / 3.1.4) was weighed in. Then the remaining amount of Ibutop creme was inserted into the container. The homogenization was achieved by a two minute stirring time at about 1000 rpm at room temperature while moving the container slowly up and down.

3.2.3 Determination of pH-value

Measurements of pH-values were carried out using a WTW pH 539 pH-meter from Wissenschaftliche Technische Werkstätten WTW, Weilheim, Germany. As pH-electrode the single unit electrode 405-60-S7/120 from Mettler Toledo, Uhrdorf, Switzerland was used. Prior to the measurements the system was calibrated using standard buffer solutions from Merck, Darmstadt, Germany at room temperature for a two point calibration.

3.2.4 Artificial skin constructs (ASC)

The artificial skin constructs with organotypic characteristics were kindly provided by the colleagues of the cell culture lab belonging to the institute.

The cultivation of the ASC was conducted according to Specht et al. [1998 a] with a last step modification [Wassermann and Müller-Goymann, 2000]. The human fibroblasts used to generate the dermis equivalent were obtained by isolation from newborn foreskin and were kindly supplied by Dr. Kriwet (Organogenesis, Camden, MA, USA). Prof. Dr. N. E. Fusenig (DKFZ, Heidelberg, Germany) supplied the transformed human HaCaT-cells (**h**uman **a**dult keratinocytes, low **ca**lcium conditions, elevated **t**emperature) which form the epidermis equivalent of the construct. Although these cells are transformed they show no tendency of malign growth and are fully capable to differentiate into all epithelial forms [Boukamp et al., 1988].

Standardized conditions according to Freshney [1990] were used to cultivate both cell lines, fibroblasts and keratinocytes, in Ready Mix (DMEM High Glucose, PAA, Linz, Austria) already containing 10 % fetal calf serum, 2 mmol L-glutamine, 100 U/ml penicillin G, 100 µg/ml streptomycin sulphate and 0.25 µg/ml amphotericin B.

The cultivation of the ASC took place in two steps, the first establishing the dermis equivalent and the second growing an epidermis equivalent on top of the dermis. An overview of the cultivation steps is given in figure 3.2. As cultivation equipment Transwell inserts placed into Sixwell cell culture plates (both from Costar, Fernwald, Germany) were used (fig. 3.2 I.) and in a later step complemented by a custom made metal plate bearing a six-fold boring to match the upper surface of the Sixwell [Wassermann and Müller-Goymann, 2000].

The forming of the dermis equivalent derived from the method of Bell et al. [1981] and started with a collagen-gel matrix, based on collagen type I gained from the extraction of rat tails, which was given into the Transwell inserts (fig. 3.2 II.).

For the filling of six Transwell inserts 5.6 ml of a gelatinizing mixture consisting of

1. 2.2 ml 10 x MEM (ICN, Eschwege, Germany),
2. 0.2 ml L-glutamine (Gibco, München, Germany),
3. 0.7 ml sodium hydrogen carbonate solution (71.2 mg/ml, Sigma, Deisenhofen, Germany)
4. 2.5 ml fetal calf serum (Gibco, München, Germany)

was used together with 19 ml collagen solution acidified with acetic acid (2.4 mg/ml sterile acetic acid 0.05 %). Prior to gelatinizing 2 ml of a fibroblast suspension, adjusted to about $2 \cdot 10^5$ cells/ml, was quickly added to the matrix of neutral pH due to the sodium hydrogen carbonate. After completion of the gel forming the Sixwell was filled up with medium and incubated for seven days leading to a slight contraction of the fibroblast-matrix construct proving the presence of living fibroblasts [Bell et al., 1981].

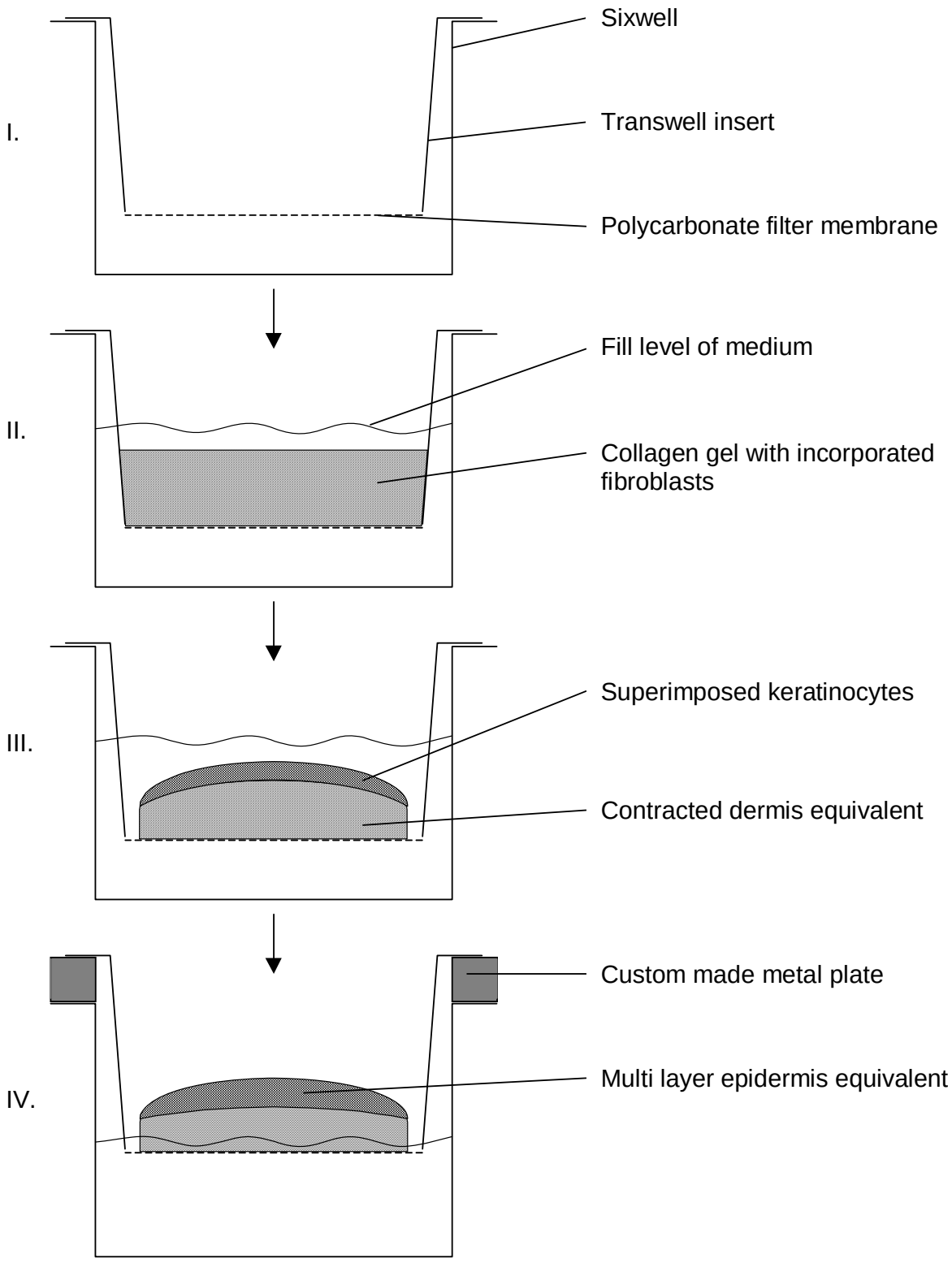

Fig 3.2: Overview on cultivation of the ASC [modified from Tegtmeyer et al., 2001]

Then 2 - 2.5·10^5 keratinocytes were allocated on top of each dermis equivalent and again kept in submerse cultivation for another seven days changing the medium every 2 - 3 days (fig. 3.2 III.).

In the following the construct was raised to the surface of the medium using the mentioned metal plate in order to simulate in vivo conditions by limiting the supply with nutrients to passive diffusion from the bottom surface (fig. 3.2 IV.).

In this position the construct was kept for another 14 days using a different medium consisting of

1. 75 % DMEM without glucose
2. 25 % Ham's F12 (both from Gibco, München, Germany) supplemented with
    - adenine (24.3 µg/ml),
    - insulin (5 µg/ml),
    - dexamethasone (0.4 µg/ml),
    - tri-iodine-thyronin (20 ppm, all from Sigma, Deisenhofen, Germany),
    - transferrin (5 µg/ml, ICN, Eschwege, Germany),
    - ethanolamine (6.1 µg/ml),
    - phosphorylethanolamine (14.1 µg/ml, both from Biochrom, Berlin, Germany),
    - selenious acid (6.8 ng/ml, Aldrich, Steinheim, Germany),
    - fetal calf serum (2 %, Gibco, München, Germany)
    - and the previously listed antibiotics.

3.2.5 Full thickness excised human skin (FHS)

The native tissue derived from plastic surgery of abdominal excess skin. Only physiologically healthy, normal skin from caucasian, female patients was used. Skin from seven different patients from 20 to 39 years of age was used.

Directly after reception the skin was cooled and the subcutaneous fatty tissue and connecting tissue were removed mechanically using a scalpel. The skin was used either directly or after shock freezing in melting nitrogen and storage at – 20° C until usage. The maximum storage duration for one specimen was six months which does not lead to any alteration of the barrier potential [Ainsworth, 1960; Bronaugh and Steward, 1986].

In order to verify the comparability of the diffusion characteristics a skin sample from each patient was used for qualification purpose. After applying Ibutop to the sample and an effective period of five hours penetration time, two biopsy samples were punched out and extracted. If the average content of ibuprofen per sample surface area was found to be between 500 and 800 µg/mm² the skin source was accepted.

3.2.6 Planed excised human skin (PHS)

In order to obtain skin samples of a defined thickness containing epidermis as well as dermis and also allowing drug permeation for some experiments the native tissue was prepared as described under 3.2.5 and then planed to a thickness of about 1 mm using the dermatome described in 3.1.11. For the planing process the frozen skin was positioned on a plastic board and immobilized on one side by a screw clamp. While slowly thawing, skin strips of about three centimeters in width were planed from the upper surface and immediately frozen again. The frozen strips were

visually inspected on possible holes and suitable areas were punched out with a biopsy puncher of 24 mm in diameter prior to use.

3.2.7 Lateral diffusion experiments

While several experimental setups are common for permeation experiments a new methodology had to be developed for the diffusion experiments in order to study the lateral diffusion of substances.

The main difference to the design of permeation experiments is that a rather small contact area between drug donor and skin is used while the larger skin area serves as diffusion compartment with contact to the buffer medium (acceptor) as visible from fig. 3.3.

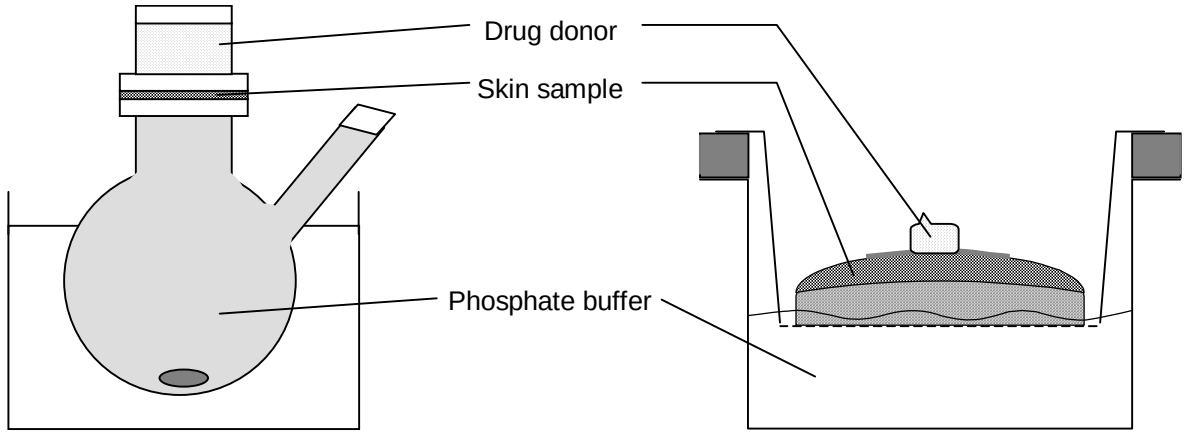

Fig 3.3: Comparison of Franz cell setup to lateral diffusion setup in Transwells

The preparation of the samples followed the workflow given in fig. 3.4:

A circular skin sample (Ø 24 mm) was either punched out of previously excised (FHS) or planed (PHS) human skin or grown in the Transwells by cell culture (ASC) to the necessary size. In order to achieve a controllable small application area

adhesive reinforcement rings were stuck in the center of the circular piece of skin (fig. 3.4-1).

The central hole of the reinforcement rings (Ø 5 mm) provides a constant application area of 19.6 mm² (3.1.9). The application of about 1.5 g ointment (3.1.1 / 3.2.2) on the skin (fig. 3.4-2) was done with a nasal application aid without any rubbing in of the cream. The systems were placed on the filter membrane of a Transwell on top of an isotonic phosphate buffer medium of pH 7.4 (3.1.7).

After a variety of different exposure times (fig. 3.4-3) the skin systems were frozen at - 20° C (fig. 3.4-4).

The removal of the formulation (fig. 3.4-5) and the adhesive ring as well as the segmentation into concentric rings (fig. 3.4-6) was carried out while the systems were frozen to prevent ongoing diffusion and to allow easier handling.

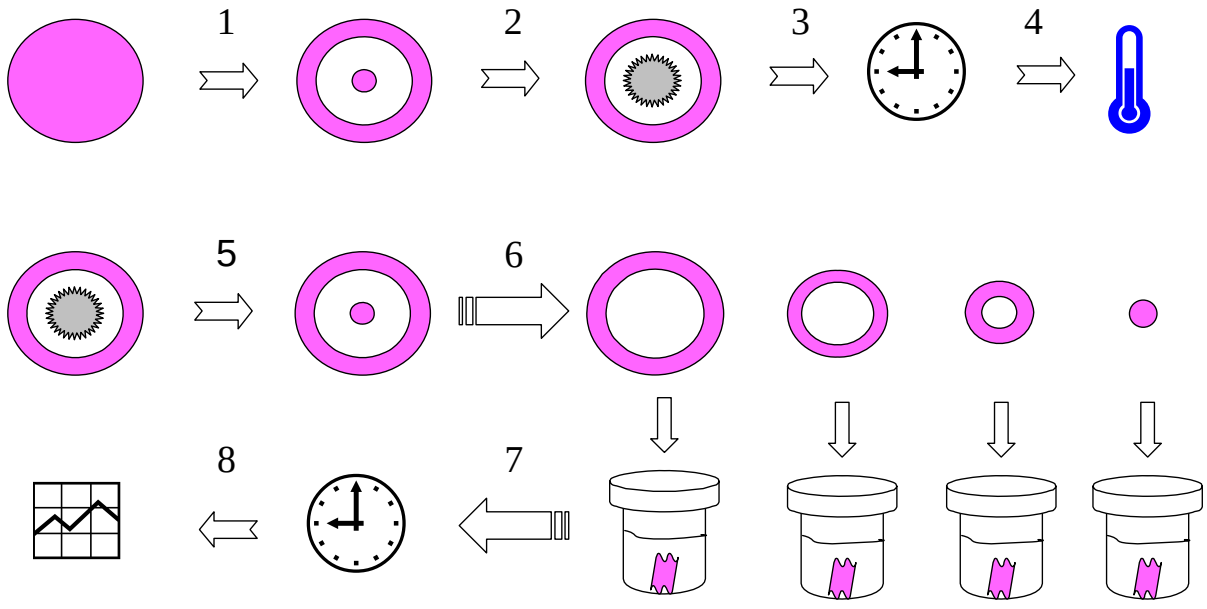

Fig 3.4: Sample preparation scheme for lateral diffusion experiments

Skin rings of 0 - 5, 5 - 10, 10 - 15, 15 - 20 and 20 - 24 mm in diameter were obtained by the use of custom made punching tools (3.1.10) and then extracted separately in

methanol for at least 5 hours (3.1.8) (fig. 3.4-7). The recovery of ibuprofen from the several skins by this extraction was 90 ± 5 %.

The amount of ibuprofen in the individual segments was determined by HPLC-UV analysis (3.2.1) against a blank extraction sample (fig. 3.4-8). For each series of measurements a set of at least five separate experiments was carried out.

For the presentation of the results a line diagram deriving from the averaged content of ibuprofen from the parallel diffusion experiments in one experimental set for the five individual ring segment values is used giving the determined drug amount in relation to the respective ring segment surface over the medium distance from the center of application. To each ring segment the standard deviation to the averaged ibuprofen content is displayed using error bars in the respective diagrams. Fig. 3.5 gives an exemplary overview of the connection. The numbers on the left half of the abscissa are inner and outer diameters of the skin sections while numbers on the right are median radius of the respective segment. The numbering from #1 – #5 from center to distal ring segment is used throughout this work to address individual rings.

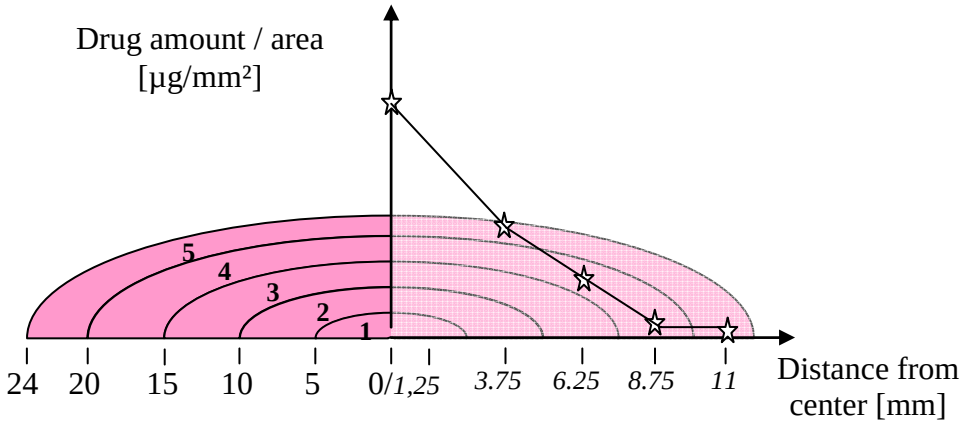

Fig 3.5: Depiction of the relation of result diagrams to the sample preparation

3.2.8 Permeation experiments

Although typically permeation experiments are carried out in modified Franz diffusion cells [Franz, 1975] for this study a different set-up was chosen in order to match the diffusion experiment conditions as closely as possible. So the permeation experiments were conducted directly in the Transwell inserts with circular skin samples of 24 mm in diameter at room temperature.

The Transwell inserts were placed in the Sixwell boxes each on top of 2.0 ml of an isotonic phosphate buffer medium of pH 7.4 (3.1.7). An adhesive reinforcement ring was applied to the center of the skin sample providing a defined contact area of 19.6 mm^2 for the test formulation. About 1.5 g of the respective formulation was administered maintaining a sufficient drug amount in the donor compartment. During the permeation time at regular intervals samples of 0.200 ml were taken from the buffer medium and replaced with fresh buffer solution using a 250 µl Hamilton syringe 1725 RN (Hamilton, Bonaduz, Switzerland). The ibuprofen content of these samples was then determined using the HPLC-UV method described in 3.2.1. The results of the analysis were entered into an excel sheet for the calculation of the absolute permeated amount of ibuprofen, taking the removed portions by sampling into account. A linear regression to the obtained averaged graph was conducted leading to the computational determination of flux (J) and permeation coefficient (P).

3.2.9 Statistical data evaluation

In order to evaluate if observed differences in results are substantial the respective data was assessed using a two sided t-test for two samples of different variance (heteroscedastic). The level of confidence for the assessment was 95% (α=0.05) and the resulting levels of significance (ρ) were calculated.

4 Results and discussion

4.1 Consideration of the model

The static or dynamic diffusion cells commonly used to perform bioavailability studies with human skin ex vivo provide an experimental set up for a precise determination of penetration or permeation rates only. Hence for studying the development and influence of lateral diffusion during drug penetration into skin (2.3.2) a modified experimental set up has to be chosen. In order to allow lateral diffusion an area of application smaller than the area in contact with the receptor fluid is necessary as shown in fig. 4.1. This methodology is considered to be resulting in inaccurate penetration rates compared to the standard penetration determination due to lateral diffusion [Dreher et al., 2002].

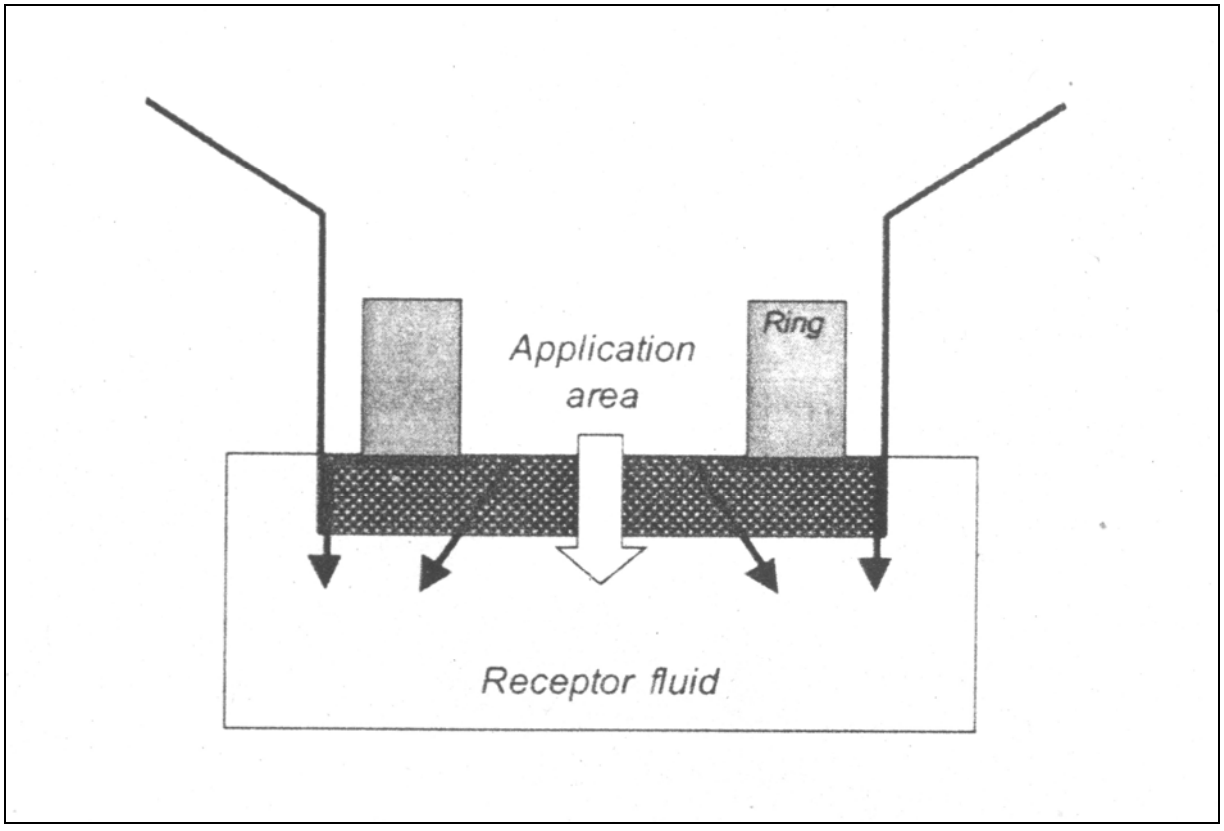

Fig. 4.1: Lateral diffusion as reason for inaccurate results in conventional permeation experiments [Dreher et al., 2002]

So for the developed experimental set up it was the aim to generate the biggest possible ratio from receptor contact area to formulation contact area in order not to limit lateral diffusion. With the chosen methodology (3.2.7) using a six-well plate this ratio is determined by the diameter of the transwell insert of 24 mm and the diameter of the application area limited to 5 mm by the glued ring. This allows for a distance for lateral diffusion of 9.5 mm in each direction. No limitation of the lateral diffusion by decreasing sink conditions in lateral orientation should occur as long as in the outermost ring segments of the used skin do not show significant drug amounts.

The permeation through the skin (2.2.) using this setup was also investigated in order to calculate the total amount of delivered drug to the skin. As stated above it is to be expected that permeation results will differ from conventionally determined permeation rates.

Since it is the aim of this work to compare the artificial skin construct's drug diffusion characteristics (2.4.2.4) to human skin characteristics (2.4.2.3) full thickness human skin as commonly used in several studies [Hadgraft et al., 2003; Netzlaff et al., 2007; Wagner et al., 2001] was employed. Additionally the planed human skin was chosen as model skin containing less dermis tissue since an influence of the viable epidermis and dermis tissue on specifically lipophilic molecules in vitro diffusion experiments, leading to an accumulation of the molecules in the stratum corneum, is described in literature [Wiechers, 1989].

As model drug substance ibuprofen (2.5.2) was chosen since it is commonly used as well for therapeutic comparison of formulations as for investigation of diffusion aspects. This frequent use is probably due to the sufficiently small size and lipophilic characteristics showing a log octanol-water partition coefficient (P) of about 4, which is an indirect parameter for the expected solubility in the stratum corneum lipid phase

[Tojo et al., 1987]. Furthermore the substance is readily available and easy to determine by HPLC analysis (3.2.1). Therefore the commercially available Ibutop Creme (3.1.1) was used as a standardized, ibuprofen containing basic formulation which was supplemented by DMSO (2.5.2.1) or urea (2.5.2.2) for the respective experiments.

4.2 Diffusion experiments

In this section the results for the effect of lateral diffusion in the different types of skin are presented deriving only from the determined drug concentrations at the end of the respective experiment directly within the skin. For this purpose full thickness human skin (FHS – 3.2.5), planed human skin (PHS – 3.2.6) and artificial skin constructs (ASC – 3.2.4) were selected. With each type of skin multiple diffusion experiments were performed as described in 3.2.7, respectively, with several different time periods available for drug diffusion. The data generated from these experiments is presented in the respective tables in the annex and is displayed in the several diagrams in this section.

4.2.1 Full thickness human skin (FHS)

The high barrier function of the native tissue causes a lag time of about 45 - 60 minutes until first noticeable amounts of ibuprofen could be registered at the direct site of ointment application. Hence, the use of FHS for lateral diffusion experiments requires relatively long permeation times of up to 390 minutes in order to develop the typical concentration gradient.

4.2.1.1 Ibutop on FHS

The following figure 4.2 shows the amount of drug substance determined per unit area [µg/mm²] of the several ring segments plotted versus the respective distance from the center of application [mm] following the principle diagram structure introduced in 3.2.7, figure 3.5. Each individual line represents a specific diffusion time period ranging from 90 – 390 minutes. The number of parallel experiments (n) is given in brackets. In order to establish a better understanding the zone reflecting the area with direct contact to the drug formulation is depicted as a grey layer.

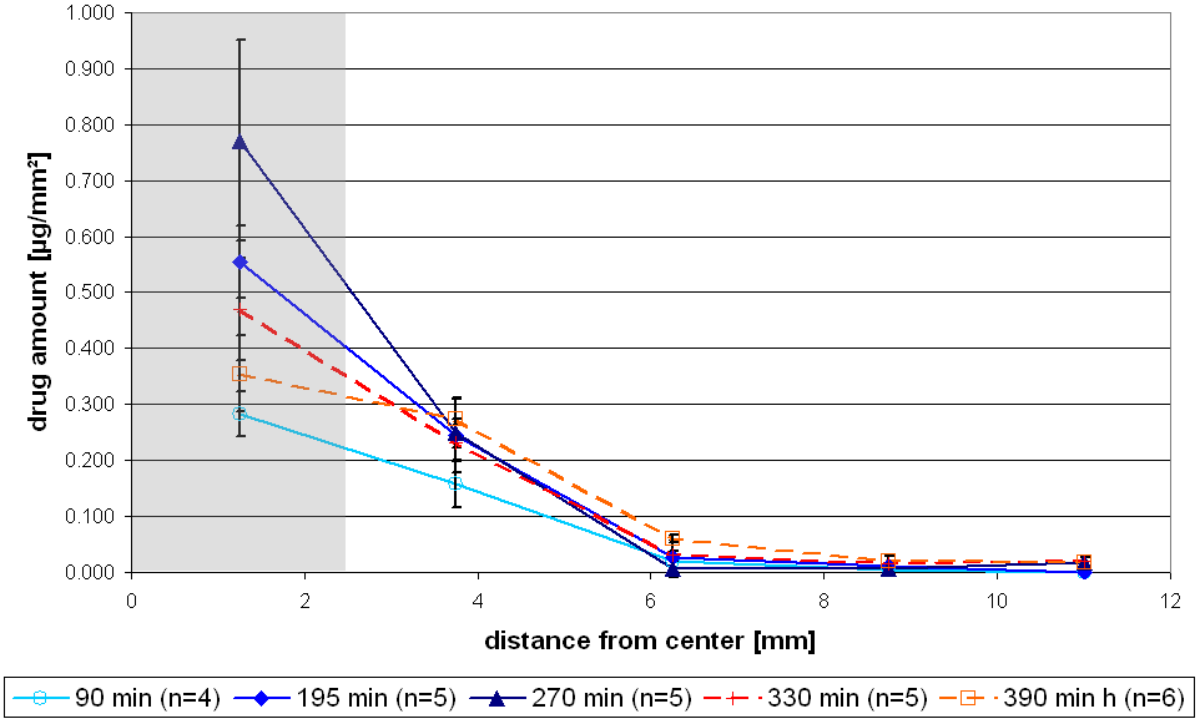

Fig. 4.2: Lateral diffusion profiles for Ibutop on full thickness human skin

Analyzing the concentration of ibuprofen in the several ring segments a characteristic concentration gradient development over time can be observed. These concentration gradients all show significant amounts of the model drug substance in the distal ring segments proving that lateral diffusion takes place.

In the beginning the concentration of ibuprofen in the central area with direct contact to the drug containing formulation rises rapidly with time. After reaching a maximum at about 270 minutes a gradual incline of concentration follows.

The region directly alongside of the application area (3.75 mm from center) also shows a quick increase with time but the concentration of ibuprofen is always distinctly lower than in the central section (#1). In contrast to the central segment no clear maximum in concentration development is noticeable but a tendency for a continuous increase.

For ring segment #3 (data points at 6.25 mm from center of application) no significant concentration development with timely resolution can be deducted from the experimental results. Yet the 390 minutes result indicates a tendency for a continuous concentration increase. This is supported by the results for the two outmost ring segments containing detectable amounts of ibuprofen.

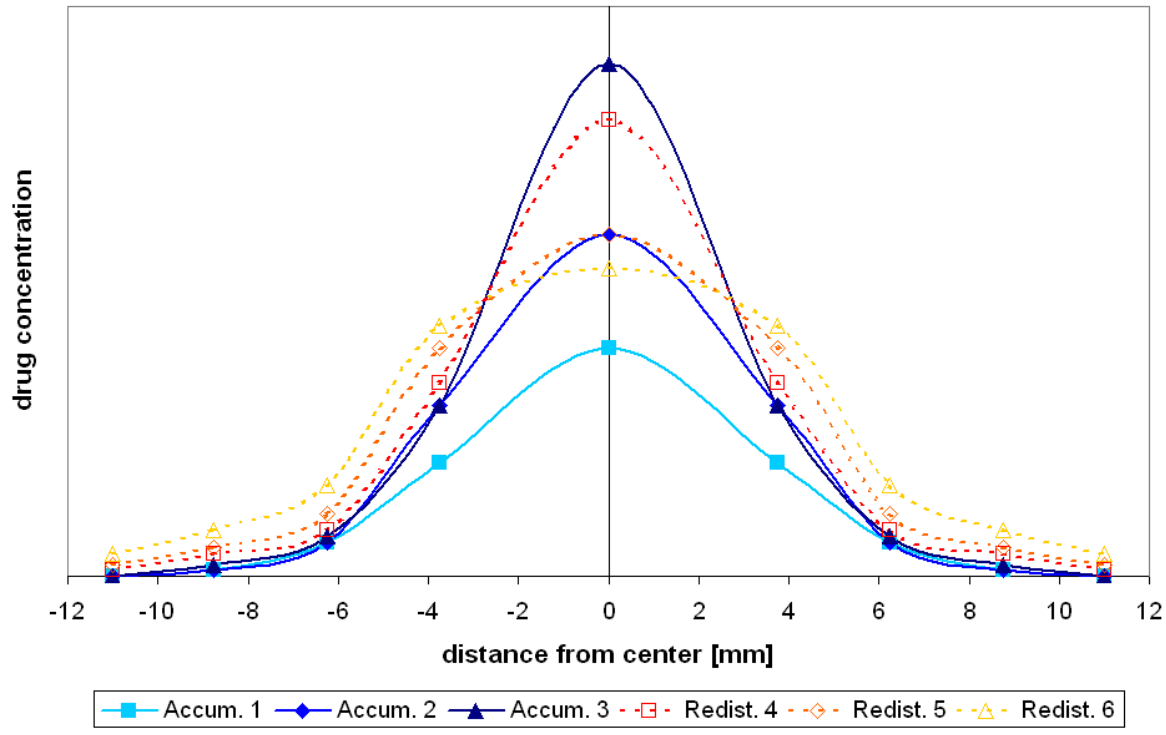

Fig. 4.3: Accumulation and redistribution phases during diffusion experiments

Due to the seen maximum in the drug concentration development within the skin directly in contact with the formulation the total diffusion time period can be separated into two stages. The first stage is characterized predominantly by drug penetration into the skin segment with direct formulation contact. In the second stage this diffusion process is less dominant but the effects of lateral diffusion attract notice. So in the first stage the initially penetrating drug amount accumulates in the central area of the skin and is then redistributed in the second stage leading to the decrease in central drug concentration. A schematic diagram emphasizing these two phases in the concentration development is shown in figure 4.3 where the accumulation phase is displayed by the blue curves and the redistribution phase is represented by the reddish colored curves.

In the following paragraphs of this chapter the results for each set of diffusion experiments are displayed separately in connection to the two phases accumulation and redistribution, respectively (see for example 4.2.1.1.1 and 4.2.1.1.2 for this set of experiments). This also allows for a better differentiation between diffusion durations due to a smaller number of graphs in one diagram.

4.2.1.1.1 Accumulation phase from Ibutop on FHS

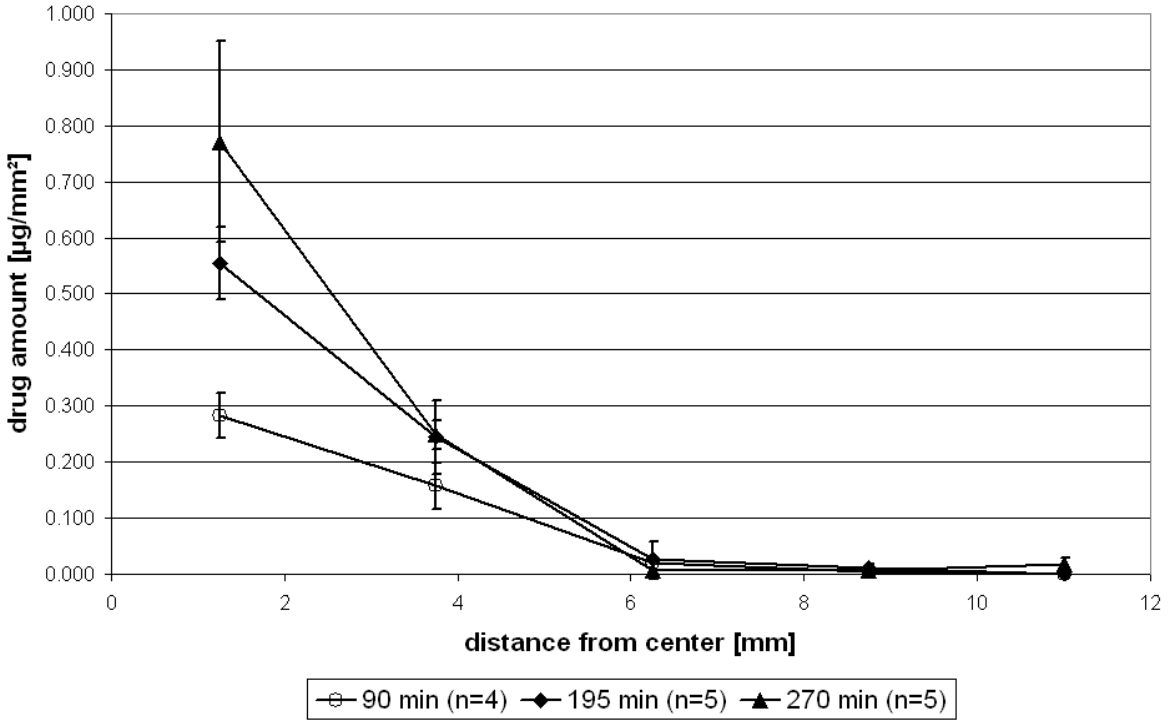

Fig. 4.4: Accumulation phase from Ibutop on FHS

In fig. 4.4 the profiles for the accumulation phase obtained from diffusion experiments with Ibutop on FHS are plotted as drug concentration per area unit [µg/mm²] over distance from the center [mm]. The shape of the profiles regarding the slope for the first three ring segments (#1 - #3) moves from a linear towards an exponential shaped curve.

After 90 minutes a quantifiable amount of ibuprofen is seen at the site of application as well as in ring #2. The drug concentration in the center increases constantly with time so that after about the double time the double drug amount is found. Yet during the next 90 minutes the increase slows down and a maximum concentration is reached. The relative drug concentration in the skin segment #2 compared to the center segment (#1) develops more slowly. While after 90 minutes about 60 % of the central concentration was recorded, after 195 minutes some 45 % of the central

concentration is found and after 270 minutes only about 30 % of the central concentration at the respective time is determined. The three outer segments (#3 - #5) only develop minimal drug concentrations within 270 minutes.

4.2.1.1.2 Redistribution phase from Ibutop on FHS

Figure 4.5 shows that 60 minutes later (330 min total diffusion time) the drug concentration within ring segment #1 decreases significantly ($\rho < 0.05$) while section #2 remains at the previously observed level. This tendency is confirmed by the finding of a decisively lower drug concentration in the center section (#1) after 390 minutes ($\rho < 0.01$). While the concentration in ring segment #2 at 390 minutes shows only a minimal tendency of increasing drug level a relevant relative rise in drug concentration is seen in comparison to the accumulation phase for segment #3 ($\rho < 0.001$).

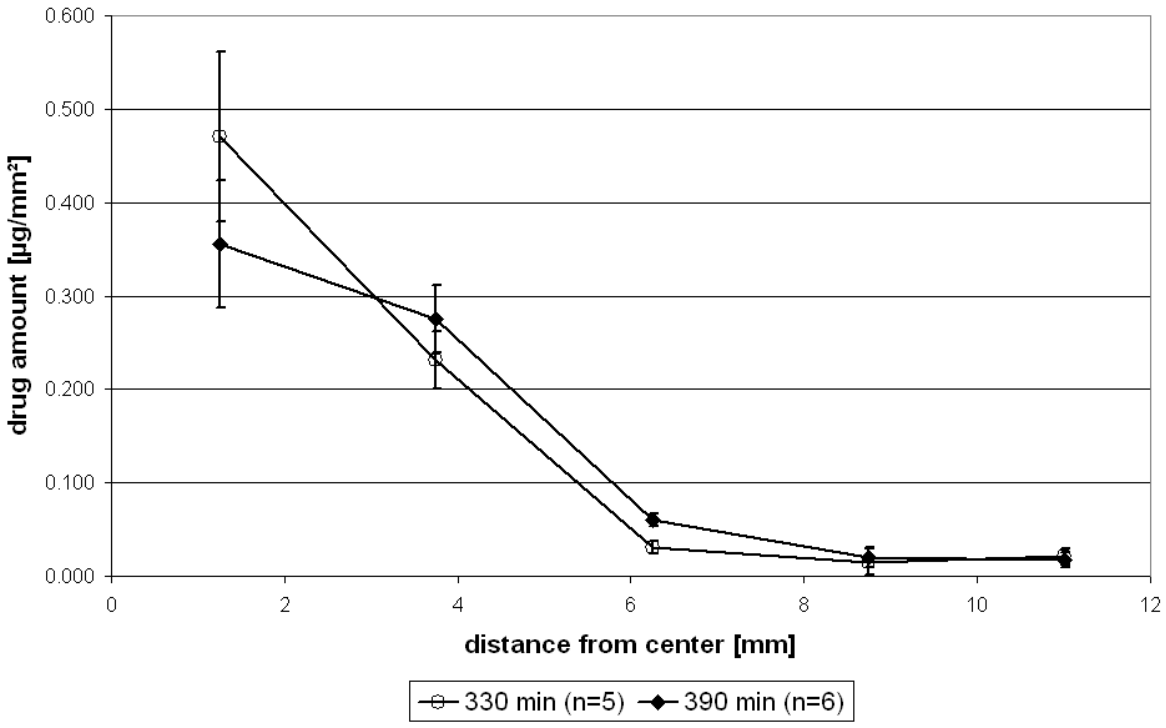

Fig. 4.5: Redistribution phase from Ibutop on FHS

The shape of the profiles develops from the exponential shape from the accumulation phase back towards a linear gradient at 330 minutes. This trend in development within the first three segments (#1 - #3) then leads to the forming of a shoulder at 390 minutes.

4.2.1.2 Ibutop + 5 % urea on FHS

4.2.1.2.1 Accumulation

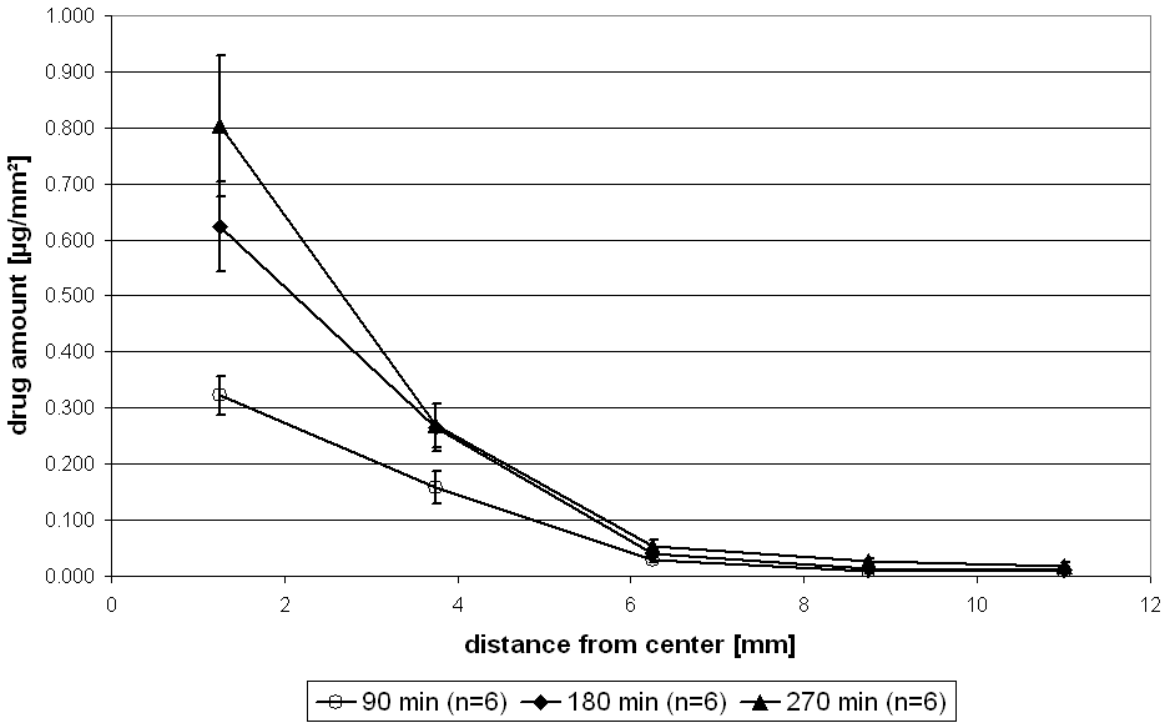

Fig. 4.6: Accumulation phase from Ibutop + 5 % urea on FHS

Compared to the application of Ibutop, using urea as additional permeation enhancer a slightly higher drug content at the central section (#1) already after 90 minutes is observed as can be seen in figure 4.6. At this point of time all other segments show results similar to the 90 minute profile of only Ibutop as donor. At later time points during the accumulation phase this trend can be seen to a greater extent leading to higher ibuprofen contents for segments #1 - #3. The drug amounts in segments #1

and #2 at about 180 min are at a level of about 10 % above the values from only Ibutop. Even more intense is the relative increase for segments #3 and #4 but due to rather high standard deviation this difference cannot be evaluated with sufficient significance ($\rho > 0.05$).

The profile shape for segments #1 - #3 again develops from linear slope to exponential slope but less distinctly compared to Ibutop only.

4.2.1.2.2 Redistribution

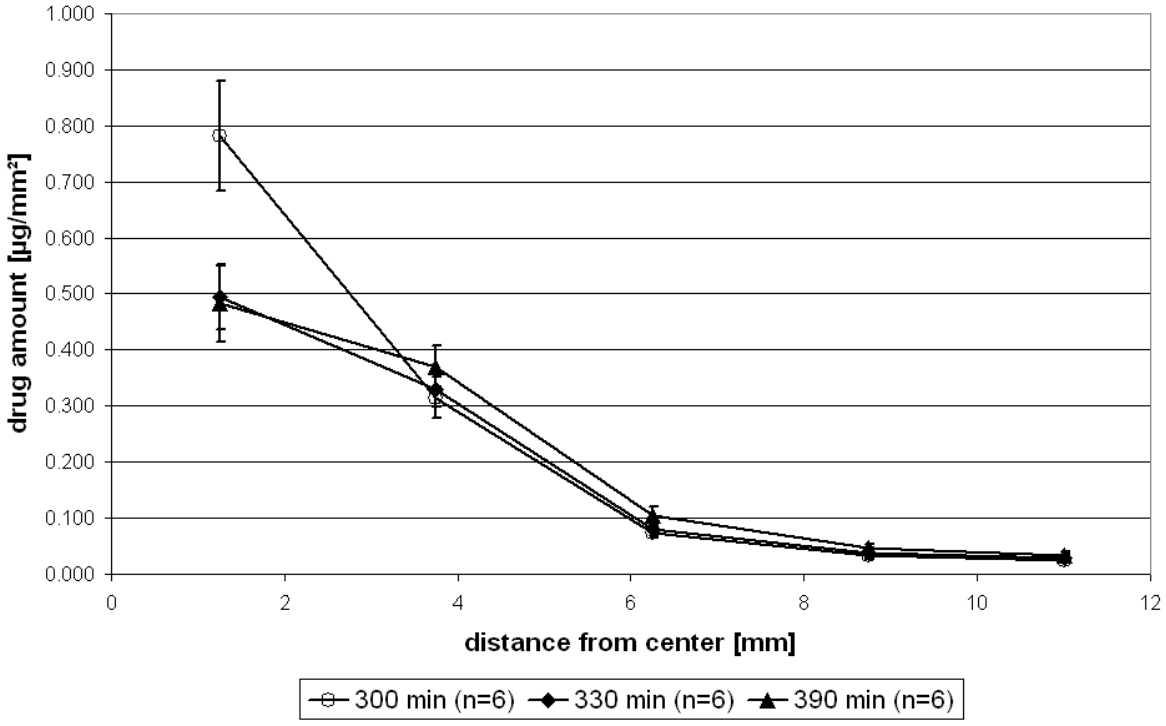

Fig. 4.7: Redistribution phase from Ibutop + 5 % urea on FHS

In order to determine the transition from accumulation to redistribution phase more precisely the additional time point of 300 minutes diffusion time was taken up for the FHS experiments. Compared to the 270 minutes profile the results show only a marginal decrease for section #1 while all other sections experience a slight increase in drug concentration. Hence it can be assumed that from this point of time on the redistribution process is the dominating mechanism.

Evaluating the 330 minutes and 390 minutes profiles against the results obtained with only Ibutop, especially the segments #3 - #5 appear to gain larger amounts of ibuprofen but also the segments #1 and #2 show higher drug contents.

4.2.1.3 Ibutop + 5 % DMSO on FHS

4.2.1.3.1 Accumulation

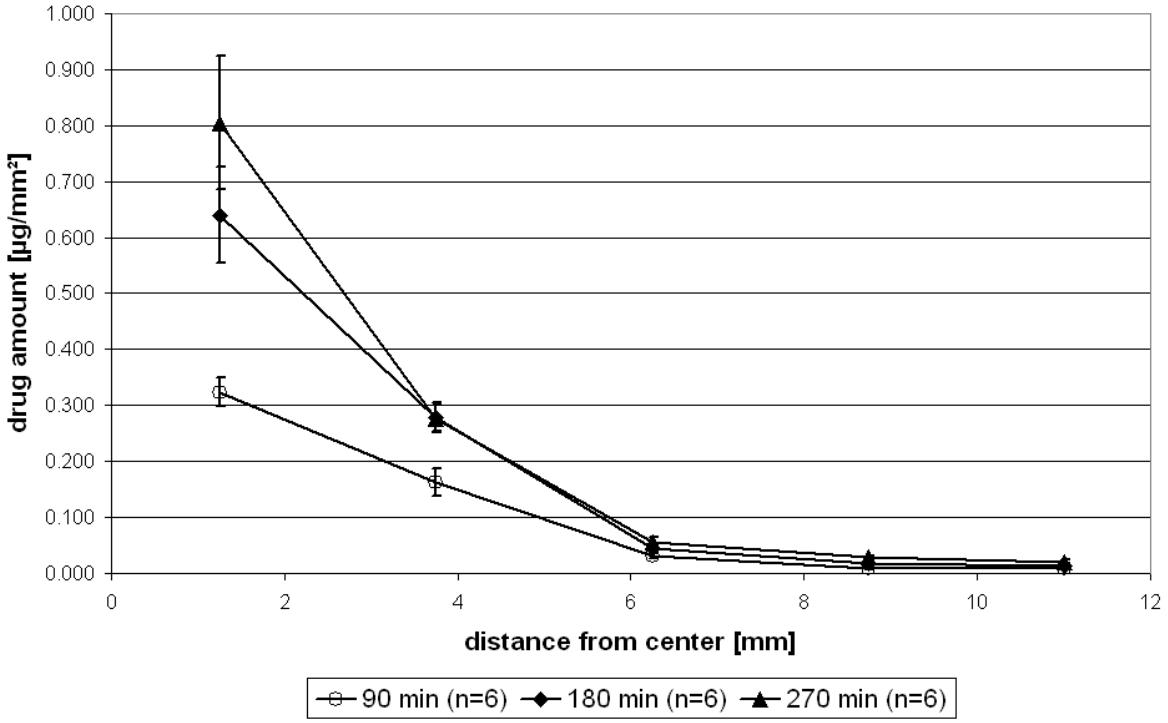

Fig. 4.8: Accumulation phase from Ibutop + 5 % DMSO on FHS

The use of DMSO, instead of urea as additional permeation enhancer, leads to an accumulation phase as can be seen in figure 4.8 with profiles which are quite similar for segments #1 and #2 to the profiles obtained using urea. Yet for sections #3 – #5 even higher drug concentrations are recorded. The drug content of sections #2 – #5 of the 270 minutes profile matches closely the results of the 390 minutes profile obtained with Ibutop only. Section #1 however shows the high content which is

typical for the end of the accumulation phase and no difference to the content resulting from the use of urea can be seen.

4.2.1.3.2 Redistribution

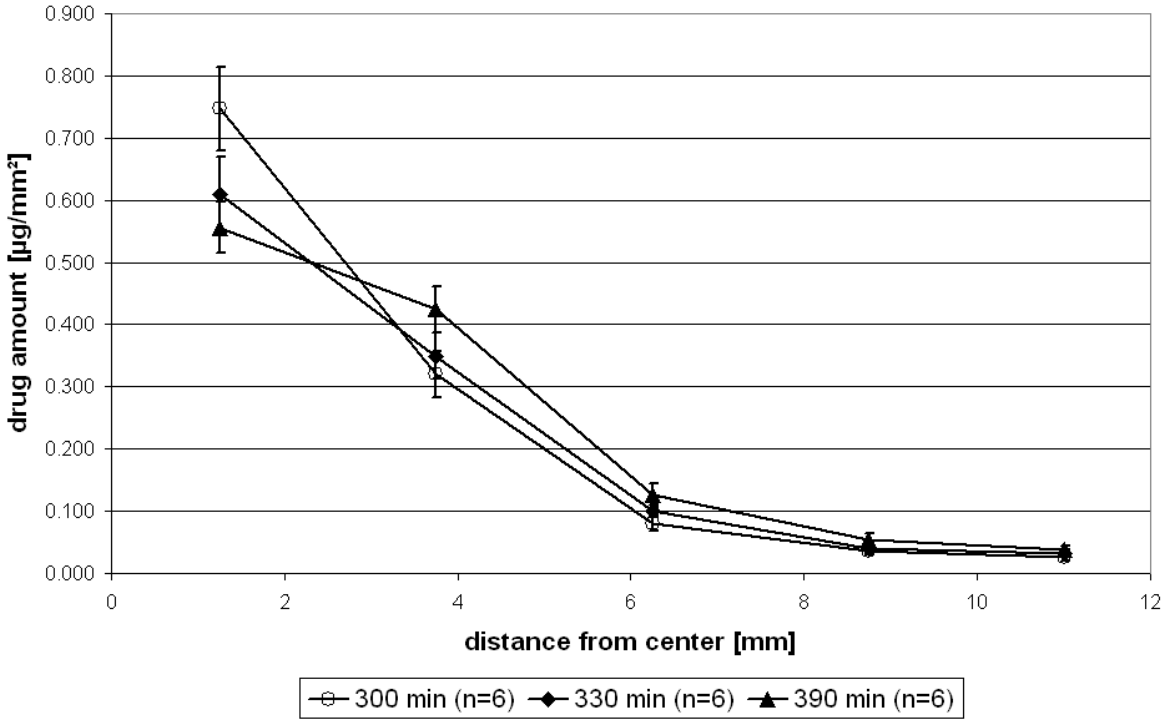

Fig. 4.9: Redistribution phase from Ibutop + 5 % DMSO on FHS

In general the redistribution phase using Ibutop + DMSO is quite similar to the one using Ibutop + urea as well as to Ibutop only regarding the profiles' slope change, respectively. Again the 300 minutes profile shows a slight decrease for section #1 while sections #2 – #5 continuously increase. The decrease of ibuprofen concentration in section #1 proceeds distinctly slower than during the redistribution phases of Ibutop or Ibutop + urea. On the other hand a still greater increase for sections #2 – #5 is seen.

4.2.1.4 Comparison of formulation effect on FHS

The following figures 4.10 – 4.13 show selected data obtained from the above experiments presented in 4.2.1.1 – 4.2.1.3 re-grouped in such a way that the influence of the formulation, and thus the contained enhancer (2.2.2.3 / 2.5.2.1 / 2.5.2.2), can be directly compared. For this overview the respective start and end data sets for the accumulation phase (90 and 270 minutes) and redistribution phase (330 and 390 minutes) were chosen.

After 90 minutes (fig. 4.10) of drug diffusion both enhancer containing formulations show a tendency to greater drug amounts in the central skin segment while all adjacent skin segments do not show any considerable differences.

At the end of the accumulation phase at about 270 minutes (fig. 4.11) with all formulations similar maximal drug contents were determined in the central segment. The ibuprofen concentration in ring segment #2 is also on the same level. Yet significant differences are seen for ring segments #3 and #4. Both additional enhancer containing formulations provoke a seven fold concentration ($\rho < 0.001$) in segment #3 and a four fold concentration ($\rho < 0.01$) in segment #4, respectively. No difference in drug amount is seen in ring #5.

Although no significant difference between the formulations was seen for the drug content in segment #1 during the accumulation phase, after 330 minutes the DMSO containing formulation shows an about 30 % greater drug level in this segment compared to Ibutop only ($\rho < 0.05$) as can be seen in figure 4.12. No relevant difference is seen for the urea enriched formulation ($\rho > 0.05$). For the ring segment #2 a 1.5 fold and for ring segments #3 and #4 a 2.5 – 3 fold greater ibuprofen content, respectively, was determined always with a slight advance for the DMSO formulation.

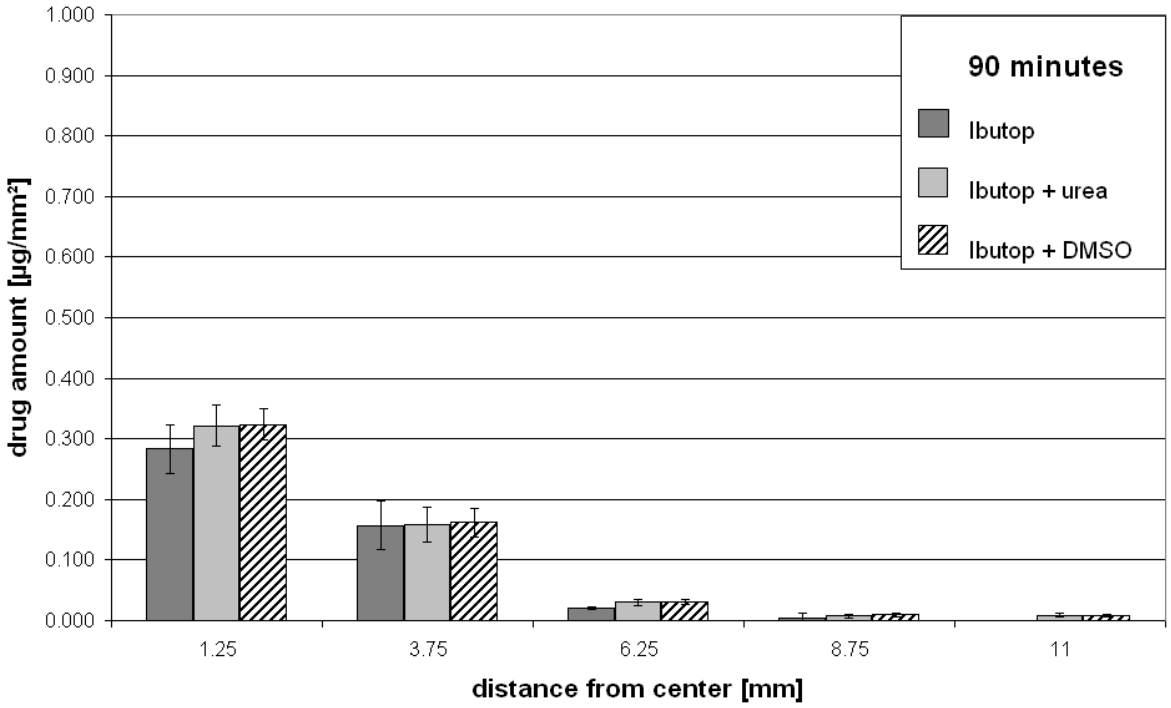

Fig. 4.10: Comparison of the permeation enhancing effect of urea and DMSO for ibuprofen from Ibutop on FHS after 90 minutes

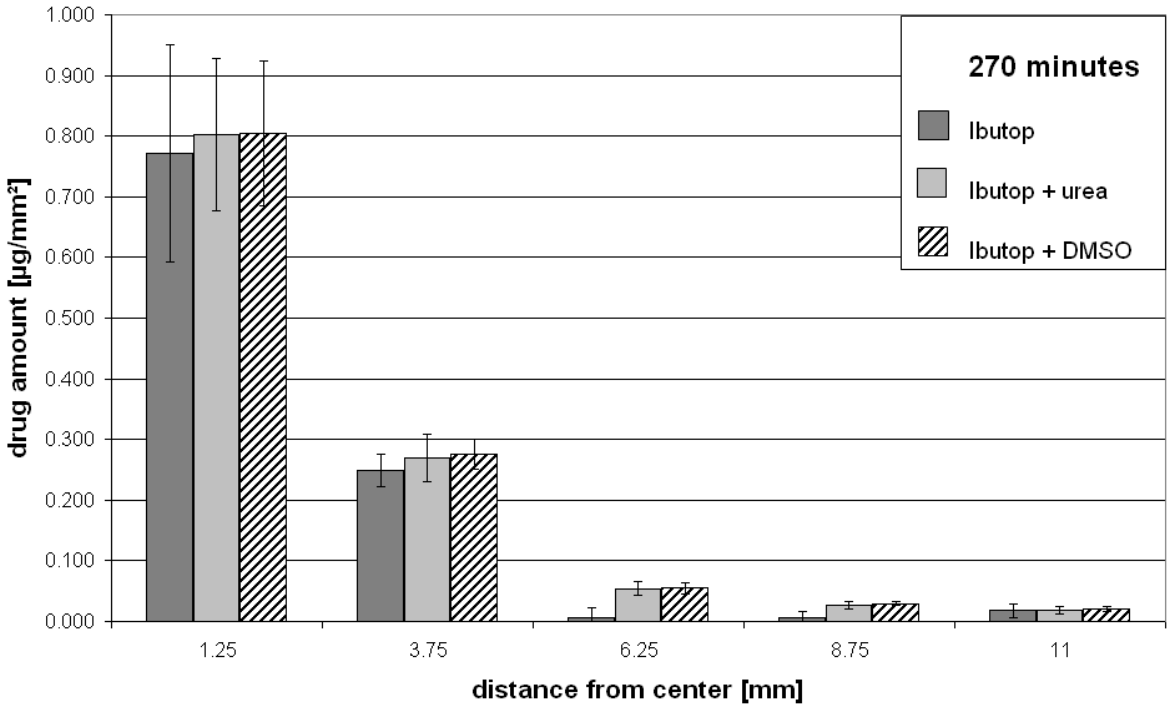

Fig. 4.11: Comparison of the permeation enhancing effect of urea and DMSO for ibuprofen from Ibutop on FHS after 270 minutes

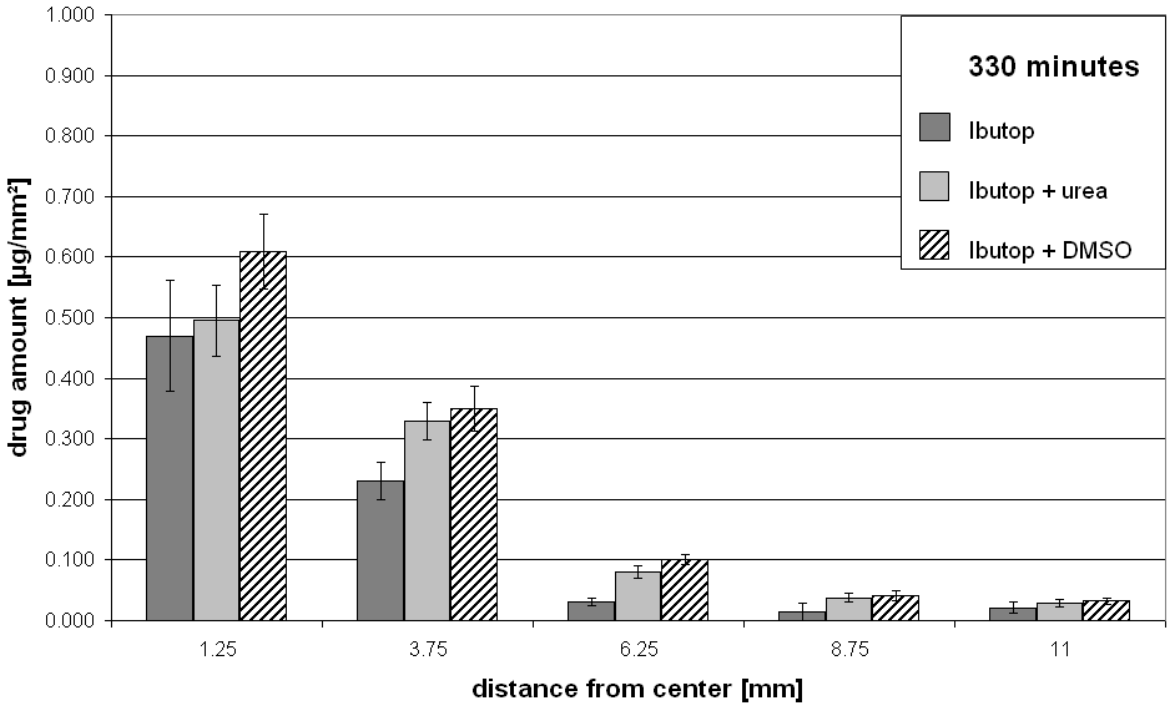

Fig. 4.12: Comparison of the permeation enhancing effect of urea and DMSO for ibuprofen from Ibutop on FHS after 330 minutes

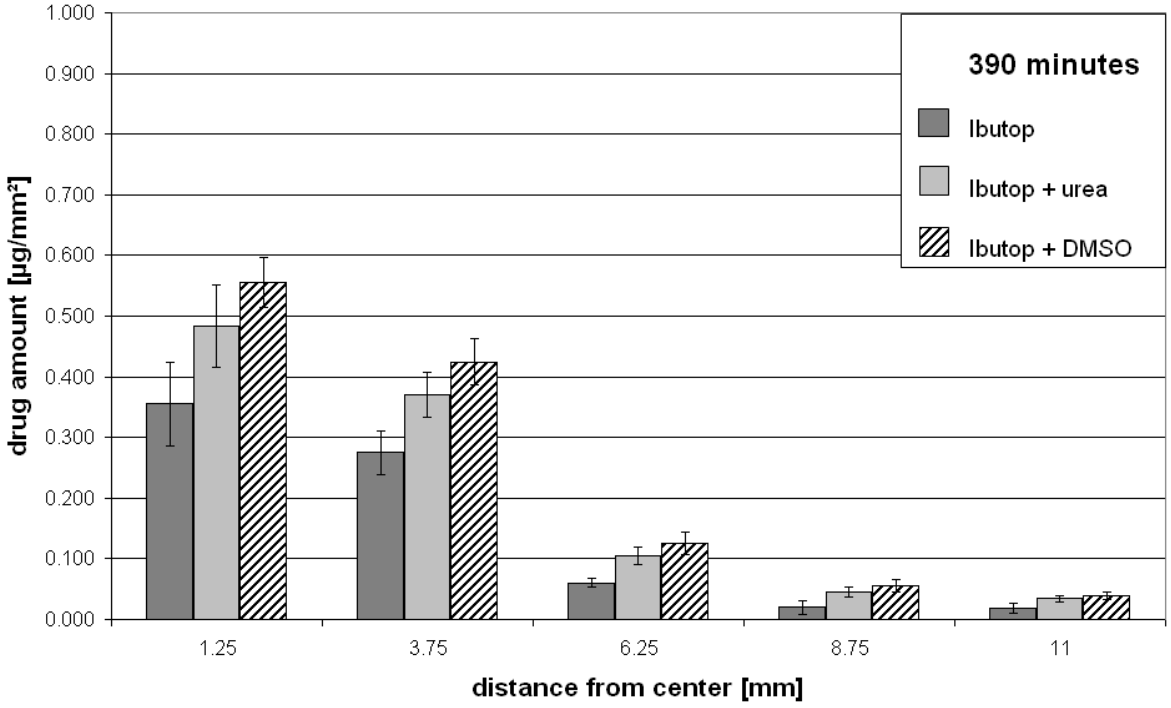

Fig. 4.13: Comparison of the permeation enhancing effect of urea and DMSO for ibuprofen from Ibutop on FHS after 390 minutes

This decline in relative drug concentration (between Ibutop and Ibutop + enhancer) for segments #3 and #4, from 7 fold and 4 fold after 270 minutes to 2.5 – 3 fold after 330 minutes, is not caused by lower absolute drug contents in these ring segments at 330 minutes for the enhancer containing formulations but mainly due to the faster relative increase (from 0.007 µg/mm² to 0.031 µg/mm²) for the Ibutop formulation without enhancers.

Figure 4.13 shows the comparison after 390 minutes where for both ring segments #1 and #2 a relevant drug level increase can be observed for the enhancer containing formulations. With additional urea about 35 % greater concentrations were achieved ($\rho < 0.01$ for ring #1 and #2) while DMSO even allows 55 % higher drug amounts in these two segments ($\rho < 0.001$). For the distal three sections (#3 - #5) an about two fold increased ibuprofen content is noted, again with slight but not significant advantage for the DMSO formulation.

In general comparison over the total diffusion times both enhancer containing formulations deploy their enhancing effect quite similar. A slight advantage for the DMSO containing formulation is seen the more pronounced the longer the diffusion time is. Most interestingly the first significant enhancer activity is the increase in the ring segments #3 and #4 and thus an enhancement of mainly the lateral diffusion at the end of the accumulation phase after about 270 minutes. It can be therefore concluded that the lateral diffusion in the stratum corneum lipid phase (2.2.1) is the main transport mechanism for a lipophilic molecule like ibuprofen and hence the permeation enhancing effect shows a larger impact on lateral drug movement compared to the vertical direction.

4.2.2 Planed human skin (PHS)

The planed human skin (3.2.6) lacks larger parts of the dermis and therefore has less viable tissue forming a diffusion barrier for lipophilic molecules (2.2.1). The same methodological set up as for full thickness human skin was used for the diffusion experiments. Also the identical type of diagram showing the amount of drug substance determined per unit area [µg/mm²] of the several ring segments plotted versus the respective distance from the center of application [mm] is used. The skin for the PHS experiments derived from only one source with quality differences only due to inter-individual variances of the skin at different body regions. Due to therefore limited availability of PHS fewer time points were investigated and special focus was laid on the transition from accumulation to redistribution phase with this type of skin. Also the urea containing formulation was omitted since DMSO showed to be the more efficient enhancer in the previous experiments with FHS.

4.2.2.1 Ibutop on PHS

Since with FHS at 90 minutes diffusion time no relevant differences between formulations with and without enhancer were seen the first diffusion time to be examined was 180 minutes. The next time points were chosen with an interval of 60 minutes from one another. Already after 300 minutes a decrease in central drug concentration was seen and therefore the curves from that time on attributed to the redistribution phase.

4.2.2.1.1 Accumulation

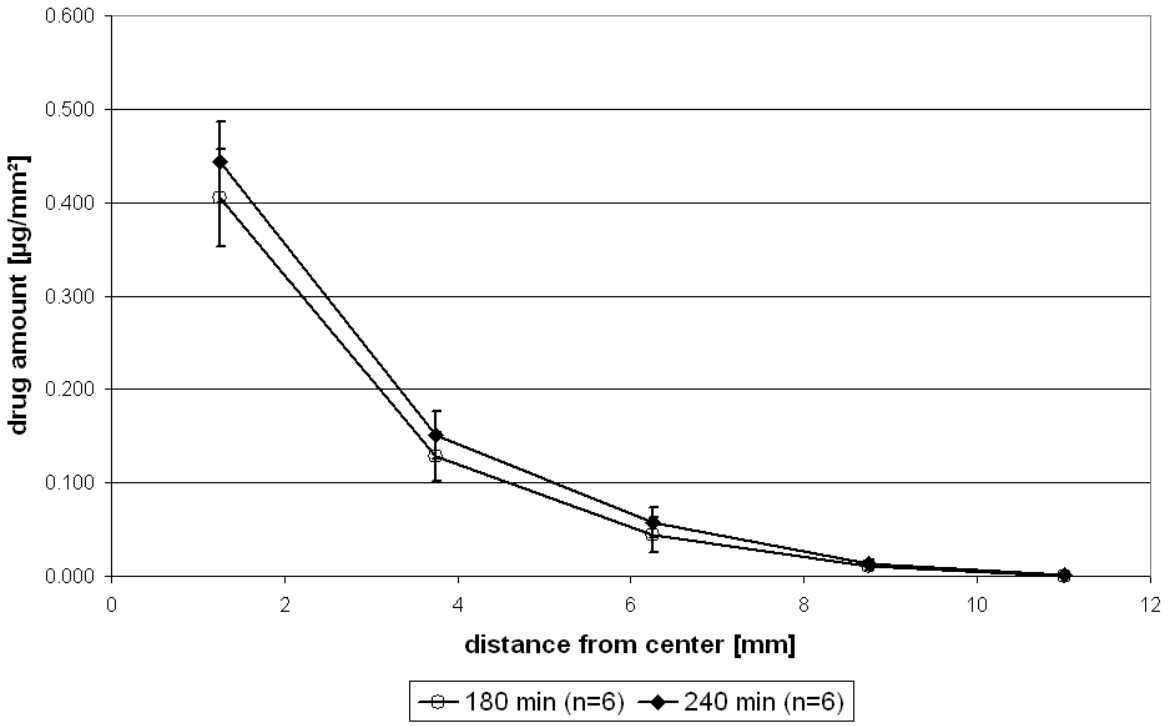

Fig. 4.14: Accumulation phase from Ibutop on PHS

Both of the curves in figure 4.14 from 180 and 240 minutes diffusion time, respectively, exhibit an exponential shape. The relatively small increase in drug concentration in the segment #1 from 180 to 240 minutes compared to the drug amount increase for the first three hours already indicates that after about 240 minutes the drug accumulation is reduced and the transition towards the redistribution phase starts.

4.2.2.1.2 Redistribution

The 300 minutes curve in figure 4.15 shows the significantly reduced ($\rho < 0.001$) drug amount in the central skin segment (#1) compared to the 240 minutes result and at the same time the curve shows a linear profile over the first three segments (#1 - #3) as was also seen with FHS. Consequently already 30 minutes later the forming of the

shoulder by noticeable increase ($\rho < 0.05$) of drug concentration in ring segment #3 starts.

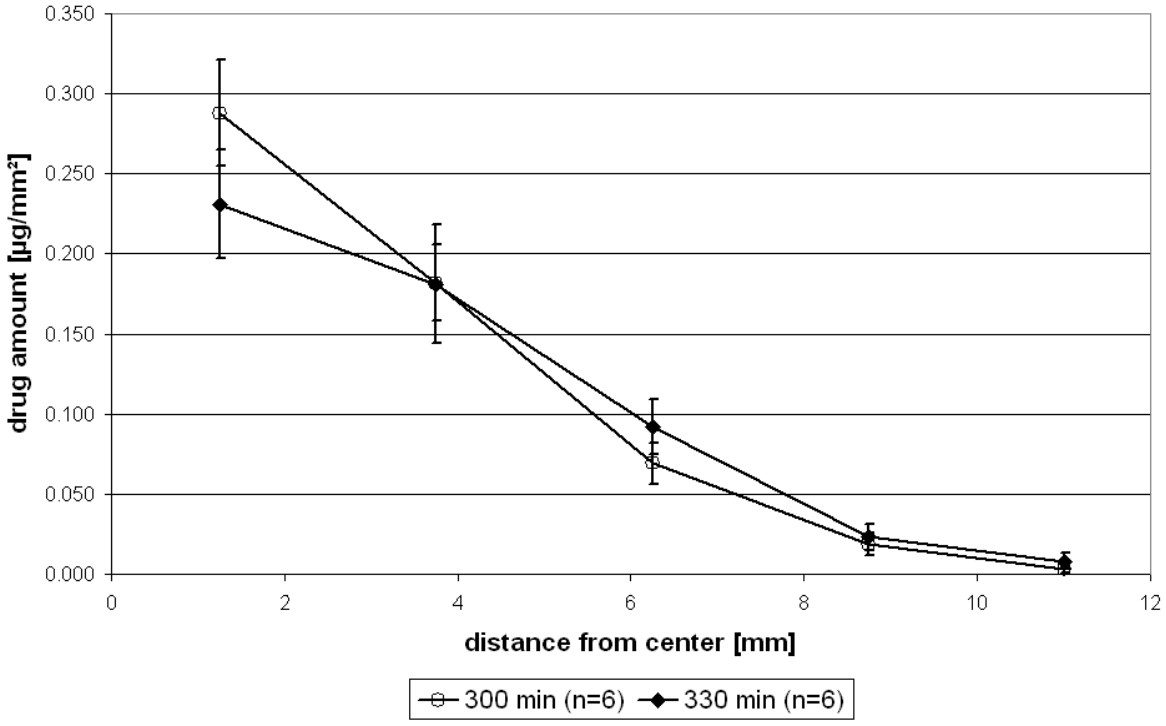

Fig. 4.15: Redistribution phase from Ibutop on PHS

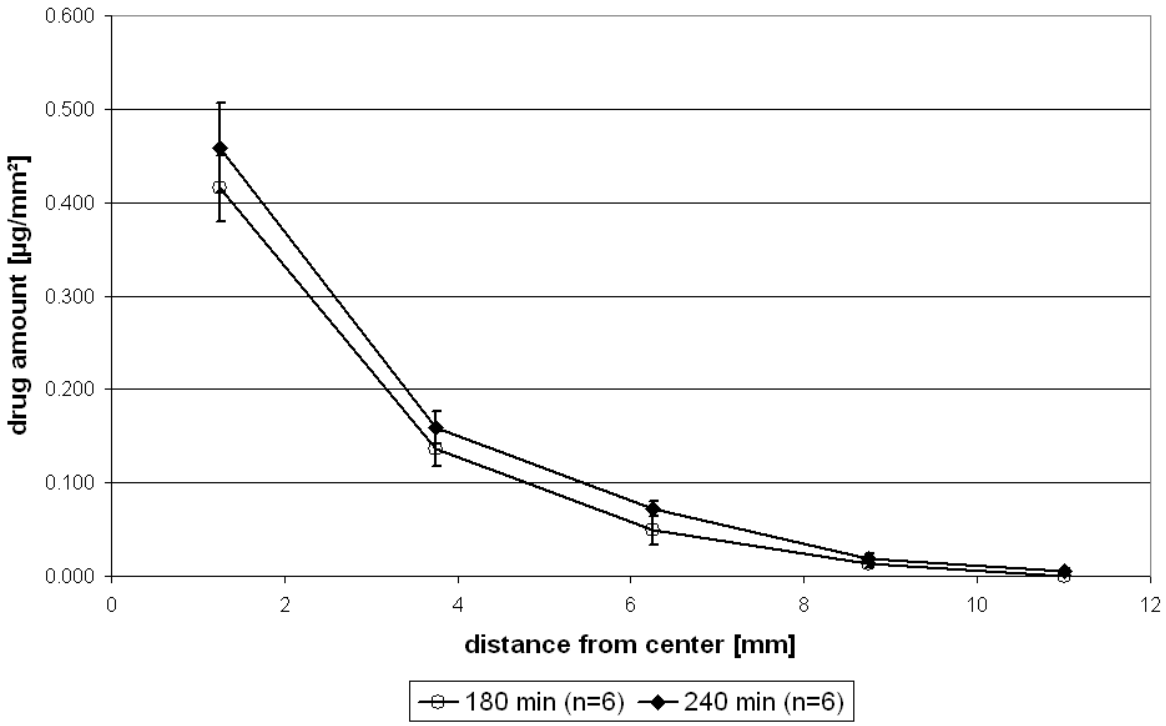

Fig. 4.16: Accumulation phase from Ibutop + 5 % DMSO on PHS

4.2.2.2 Ibutop + 5 % DMSO on PHS

4.2.2.2.1 Accumulation

Although the curves of figure 4.16 show close similarity to the ones obtained from Ibutop only in figure 4.14, a slightly bigger increase in ibuprofen concentration of segment #3 can be noticed. Both curves also present an exponential slope.

4.2.2.2.2 Redistribution

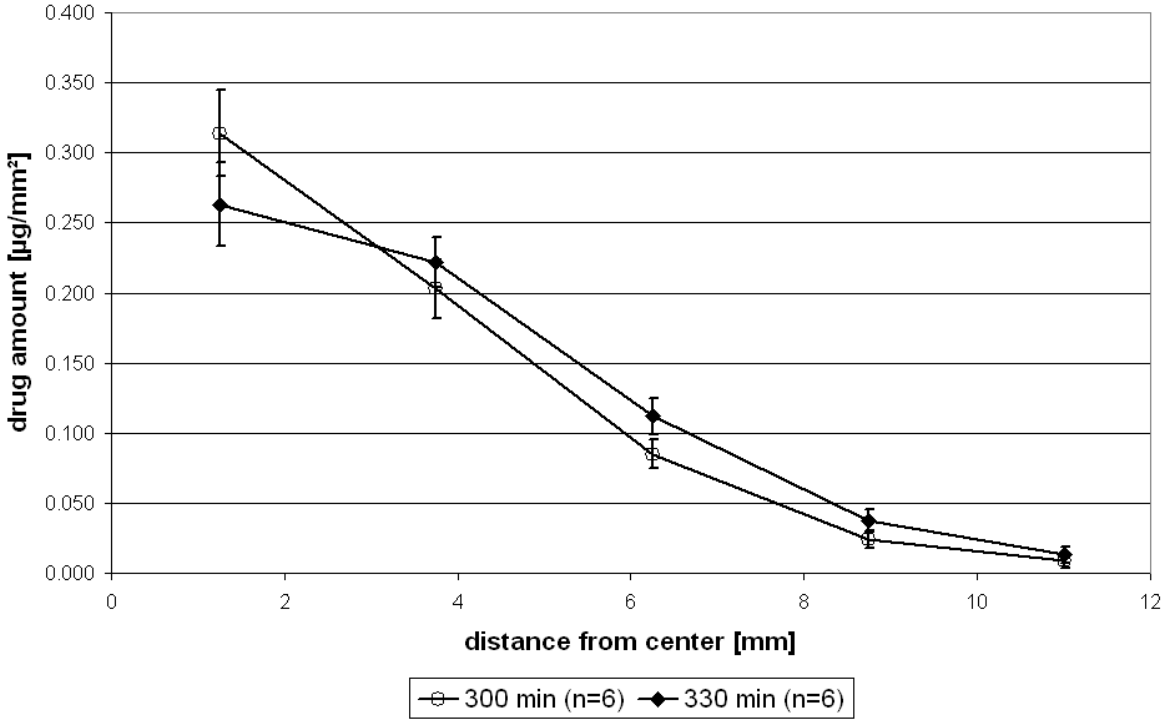

Fig. 4.17: Redistribution phase from Ibutop + 5 % DMSO on PHS

The 300 minutes curve in figure 4.17 shows reduced drug amounts in the central segment (#1) indicating that the redistribution phase is reached. Furthermore the curve has a linear profile for the first three segments (#1 - #3). The 330 minutes curve clearly exhibits increased drug levels in segments two ($\rho > 0.05$), three ($\rho < 0.01$) and four ($\rho < 0.05$) compared to the 300 minutes curve while segment #1

continues with the declining in ibuprofen concentration. This, again, produces the typical shoulder due to lateral diffusion.

4.2.2.3 Comparison of formulation effect on PHS

The previously shown data from 4.2.2.1 and 4.2.2.2 is presented in the following diagrams 4.18 to 4.21 in a re-grouped organization so that a direct comparison of the formulation related effects can be viewed.

During the accumulation phase (fig. 4.18 and 4.19) close similarity between the concentration profiles from both formulations can be seen with a tendency to greater permeated drug amounts for the DMSO containing formulation.

Also for the redistribution phase (fig. 4.20 and 4.21) still a resemblance of drug levels is seen but with a stronger tendency towards greater penetrated drug amounts for the DMSO containing formulation with longer diffusion duration.

One difference in profile development is noted between the 300 minutes to 330 minutes diagrams for ring segment #2. While with the Ibutop formulation a minimal decrease in the segment is observed, the DMSO added formulation generated a 10 % increase in drug content for this segment.

While for the first three ring segments (#1 - #3) an elevated ibuprofen concentration of up to 25 % is seen, increases of up to 60 % are determined for the DMSO formulation in ring segments #4 ($\rho < 0.05$ at 330 min) and #5 ($\rho < 0.05$ at 300 min). So generally the relative differences between the formulations are more intensely seen in the distal ring segments indicating that the enhancing effect of DMSO is primarily related to the improvement of lateral diffusion.

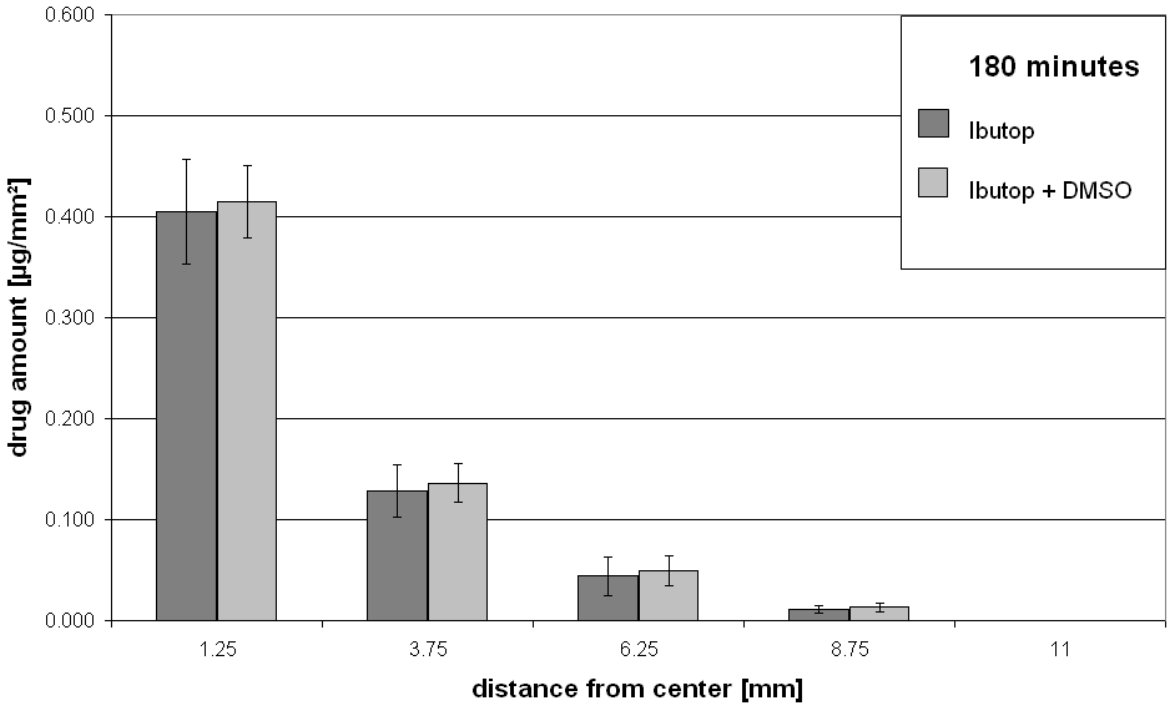

Fig. 4.18: Comparison of the permeation enhancing effect of DMSO for ibuprofen from Ibutop on PHS after 180 minutes

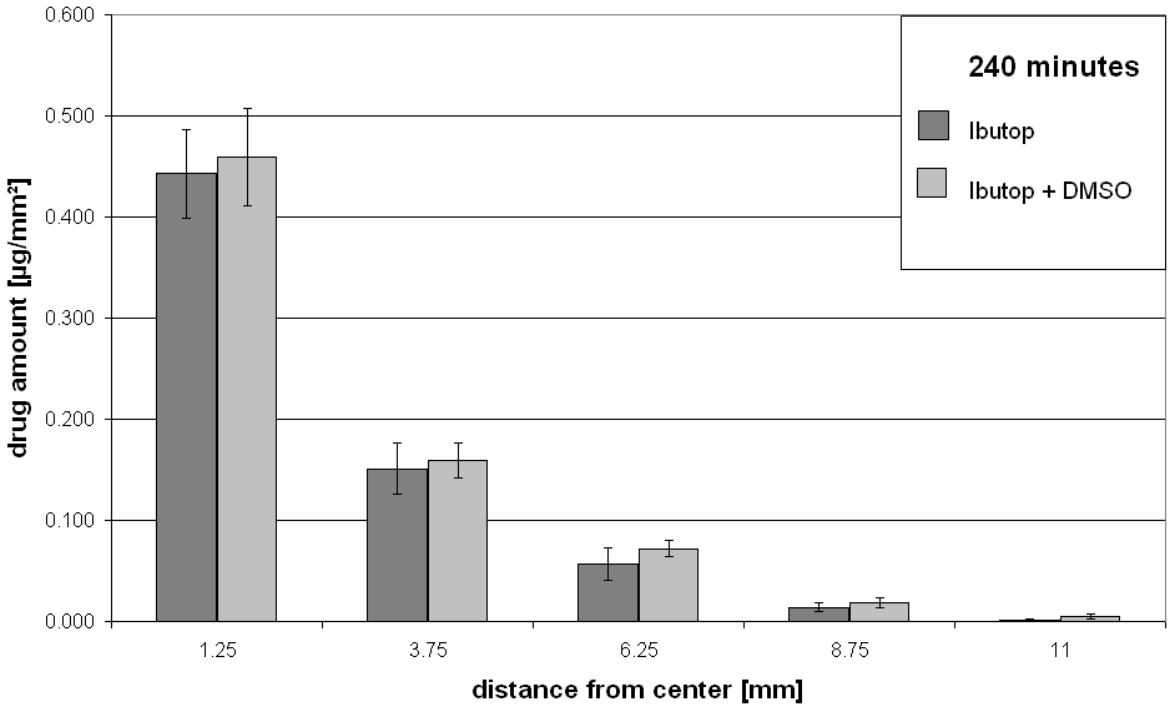

Fig. 4.19: Comparison of the permeation enhancing effect of DMSO for ibuprofen from Ibutop on PHS after 240 minutes

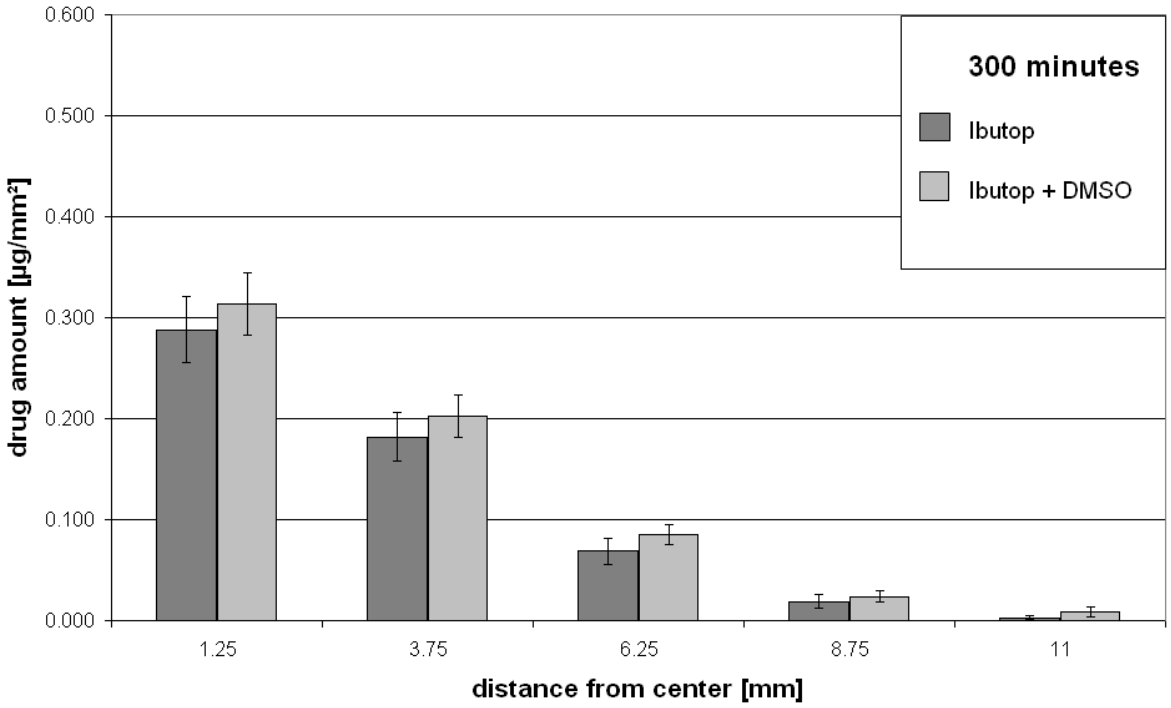

Fig. 4.20: Comparison of the permeation enhancing effect of DMSO for ibuprofen from Ibutop on PHS after 300 minutes

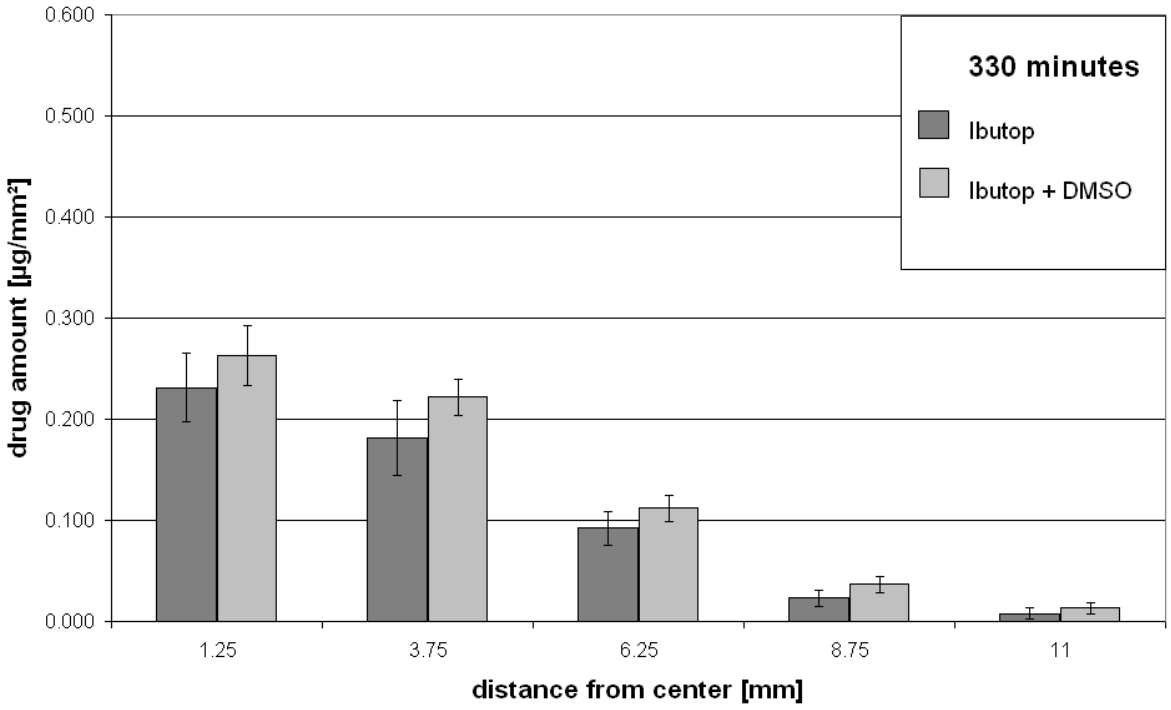

Fig. 4.21: Comparison of the permeation enhancing effect of DMSO for ibuprofen from Ibutop on PHS after 330 minutes

4.2.3 Artificial skin construct (ASC)

The artificial skin construct (3.2.4) consists of an artificial epidermis from keratinocytes and a dermis out of fibroblasts in a collagen gel matrix. So the principal tissue structure (2.1.2) is identical to native skin but a distinctly lower mechanical robustness is given. The thickness of the skin constructs is comparable to that of the planed skin.

While the native skin samples always had a diameter of 24 mm due to the biopsy punch the ASC show a smaller diameter. This is due to the constriction of the fibroblast/collagen gel dermis equivalent during the cultivation in the 24 mm transwells. Therefore the factual diameter of each construct was measured and the determined drug concentration from ring segment #5 was calculated with regard to the available respective ring segment surface. The experiments with ASC rely on separate batches of constructs for each individual diffusion time point. Due to a standardized cultivation of the ASC a sufficient equivalence of the single batches is granted.

Again the methodology described in 3.2.7 was used to generate the data presented in the following diagrams showing the amount of drug substance determined per unit area [µg/mm²] of the several ring segments plotted versus the respective distance from the center of application [mm].

4.2.3.1 Ibutop on ASC

Since it is known from previous permeation experiments using the ASC with various drug substances [Specht et al., 1998 a; Winkler, Müller-Goymann 2002] that the diffusion barrier properties of the construct is considerably lower than from human stratum corneum quicker diffusion of ibuprofen was to be expected (2.3.1 / 2.4.2.4).

Therefore shorter intervals for the several diffusion experiments were chosen. The experimental results indicate that the transition from accumulation phase to redistribution phase takes place between 60 - 120 minutes of diffusion time using ASC.

4.2.3.1.1 Accumulation

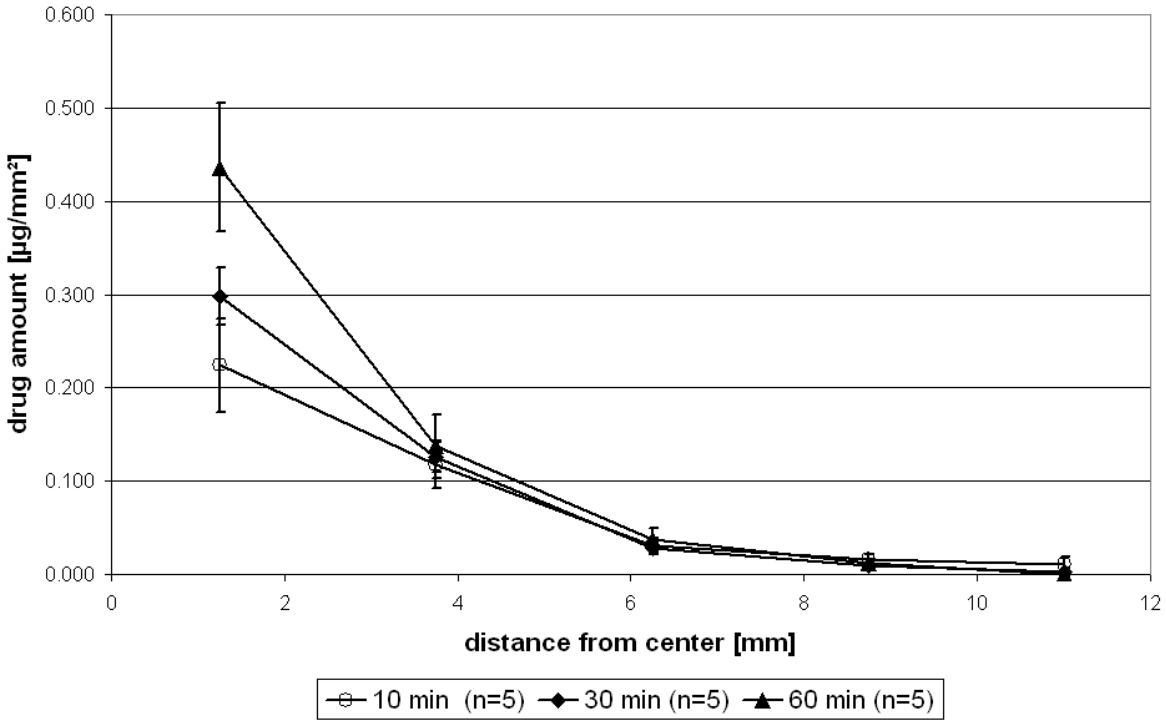

Fig. 4.22: Accumulation phase from Ibutop on ASC

As can be seen in figure 4.22 the drug concentration profile development in ASC also proves lateral drug diffusion starting with a linear concentration decrease for the first three segments (#1 - #3) and then developing towards an exponential graph structure towards the end of the accumulation phase at about 60 minutes. While already significant amounts of drug are determined in the ring segments #3 and #4 after 10 minutes only little change in concentration is observed over time for these segments.

4.2.3.1.2 Redistribution

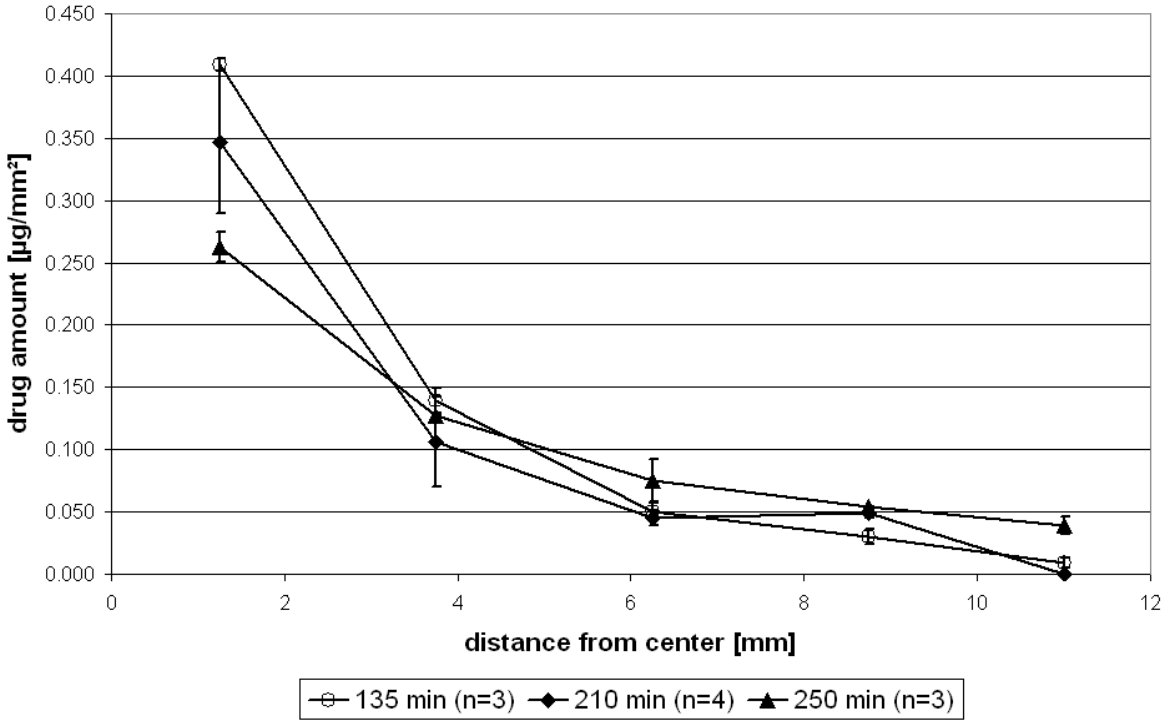

Fig. 4.23: Redistribution phase from Ibutop on ASC

Also for ASC the profile development is characterized by a drug decrease in section #1 while section #2 remains rather unchanged and sections #3 – #5 show a relevant increase of ibuprofen content (#3: $\rho > 0.05$; #4: $\rho < 0.05$; #5: $\rho < 0.01$). The shape of the profile also shows a tendency to develop backwards from exponential to linear drug concentration decrease over the first three segments (#1 - #3). Yet the formation of a shoulder is not clearly seen due to the little change in drug concentration of segment #2 although the trend of increasing concentrations at 250 minutes after previous decrease suggests that a shoulder might appear at later times.

The untypical dent in the 210 minutes curve for ring segments #3 to #5 may be attributed to a lack in precision during the dissection of the skins falsely transferring some of the higher drug concentration from ring #3 to ring #4.

4.2.3.2 Ibutop + 5 % DMSO on ASC

4.2.3.2.1 Accumulation

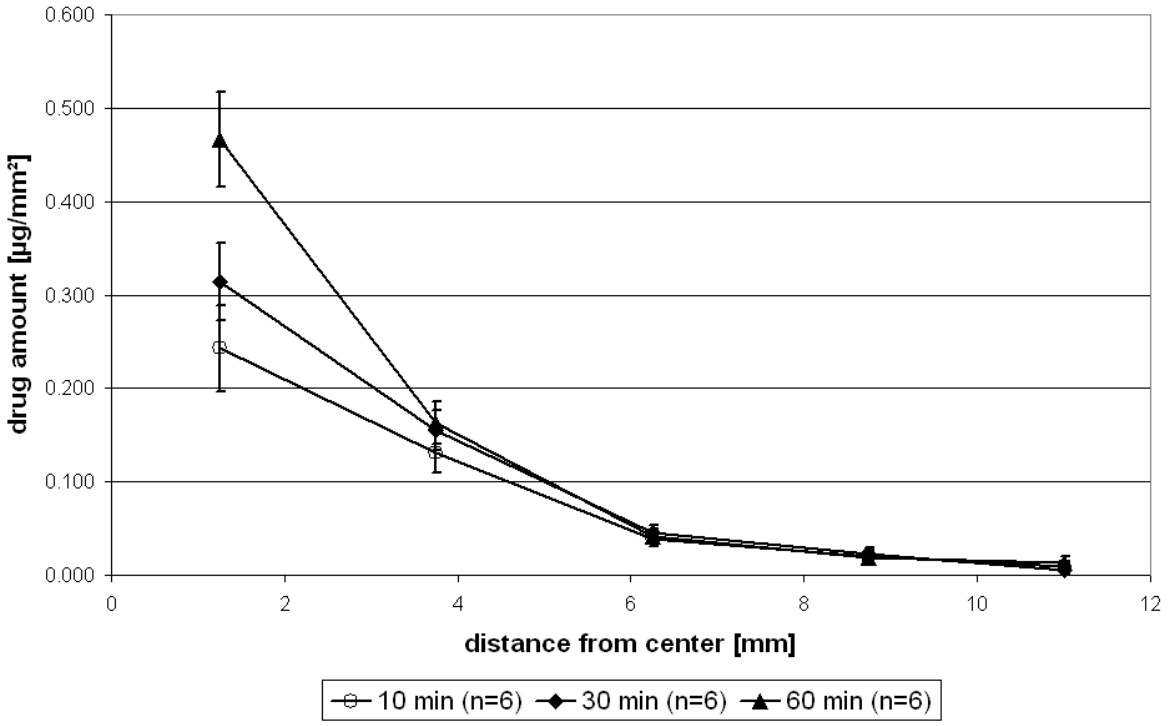

Fig. 4.24: Accumulation phase from Ibutop + 5 % DMSO on ASC

Again effects from lateral diffusion are noticeable already from the short term diffusion results. With DMSO also for ring segment #2 an increase in drug concentration over time is observable in figure 4.24. No significant change in drug levels is seen for segments #3 – #5.

4.2.3.2.2 Redistribution

The diffusion profile shape as depicted in figure 4.25 also develops from exponential to a more linear character for the first three ring segments (#1 - #3). Since the drug level in segment #2 remains unchanged no shoulder formation can be seen.

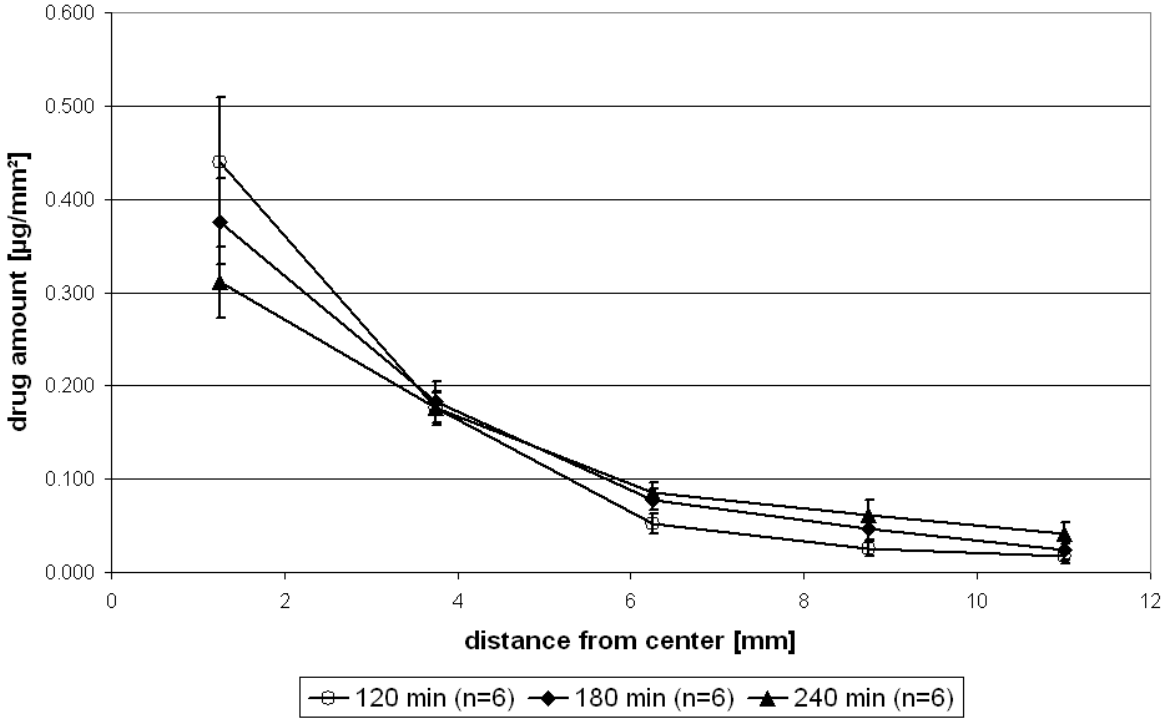

Fig. 4.25: Redistribution phase from Ibutop + 5 % DMSO on ASC

Comparing the 120 minutes to the 240 minutes curve significantly different ibuprofen concentrations are found for all segments but #2. So a significant reduction in drug content for the central segment (#1) was determined ($\rho < 0.01$) while segments #3 – #5 show a significant increase with more than doubled amounts for segments #4 and #5 (#3: $\rho < 0.001$; #4: $\rho < 0.001$; #5: $\rho < 0.01$).

4.2.3.3 Comparison of formulation effect on ASC

In order to compare the data shown in 4.2.3.1 and 4.2.3.2 evaluating the effect of DMSO as enhancer it has to be noticed that for the data during the redistribution phase not absolutely identical diffusion times were used. Since the respective differences are small compared to the absolute duration, comparability of the results is still assumed and the average of the time points is used for denomination.

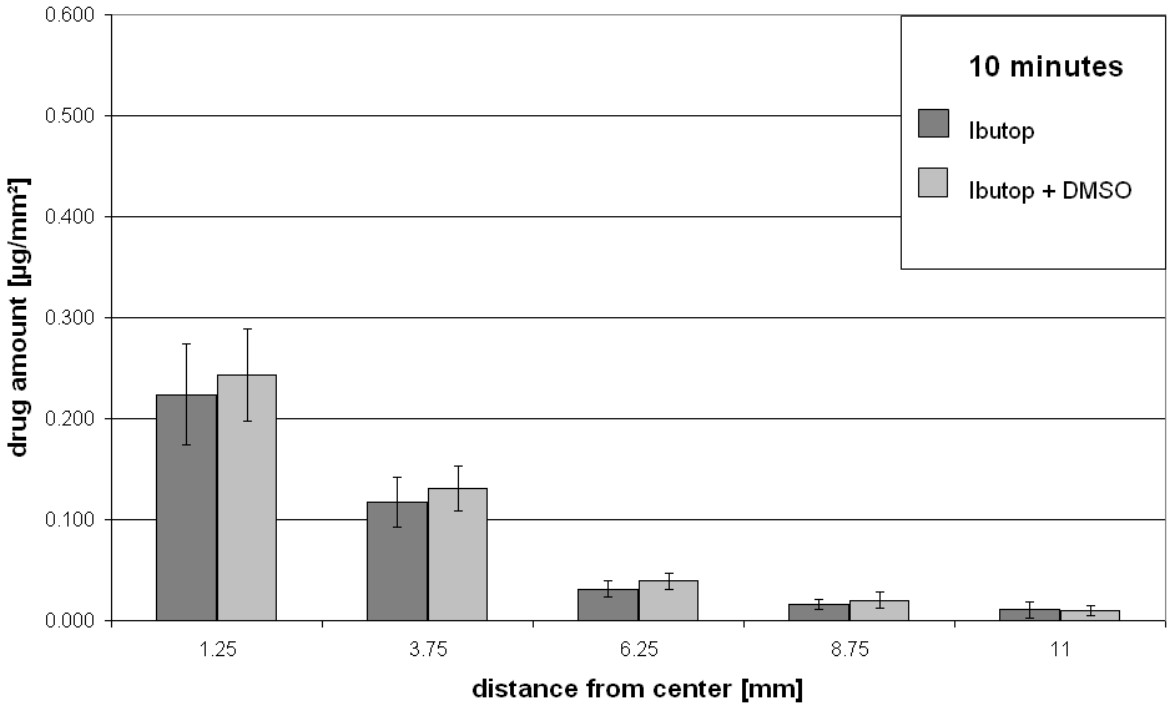

Fig. 4.26: Comparison of the permeation enhancing effect of DMSO for ibuprofen from Ibutop on ASC after 10 minutes

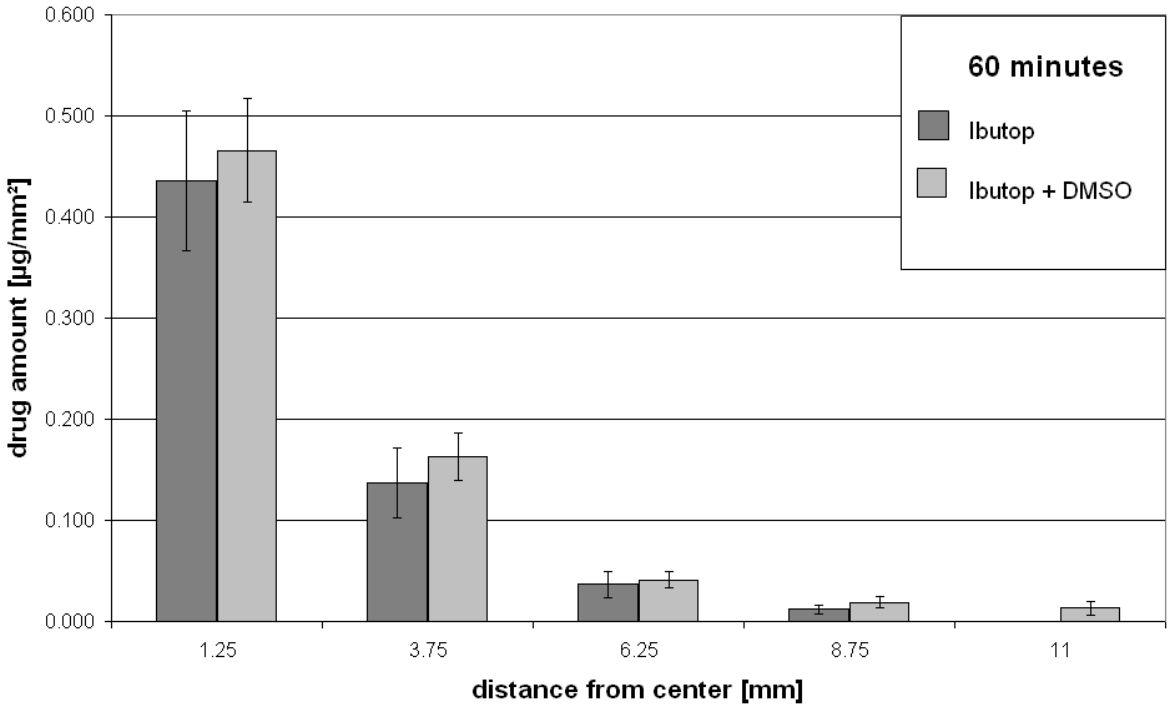

Fig. 4.27: Comparison of the permeation enhancing effect of DMSO for ibuprofen from Ibutop on ASC after 60 minutes

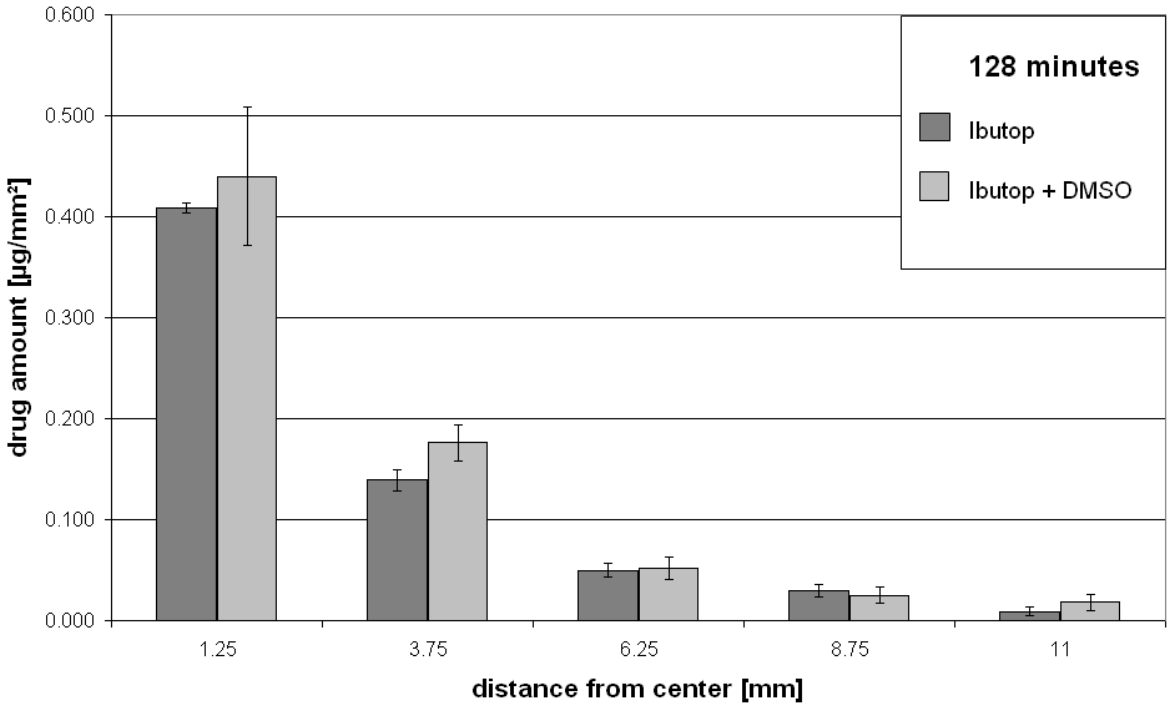

Fig. 4.28: Comparison of the permeation enhancing effect of DMSO for ibuprofen from Ibutop on ASC after 128 minutes

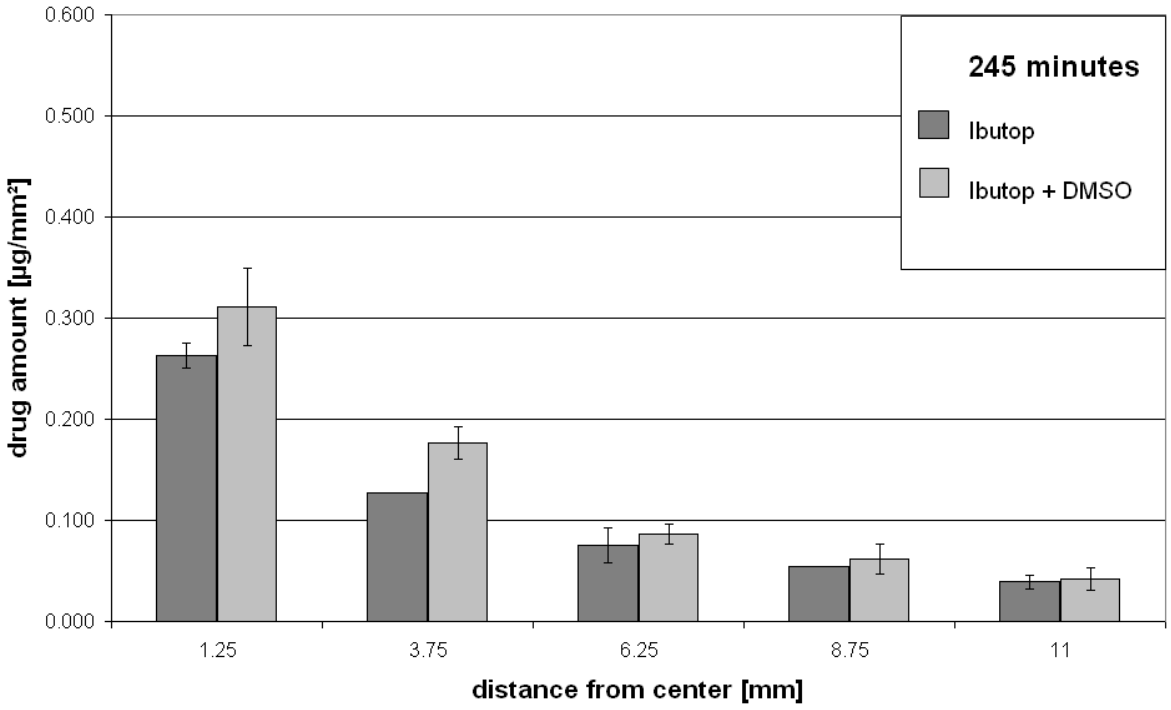

Fig. 4.29: Comparison of the permeation enhancing effect of DMSO for ibuprofen from Ibutop on ASC after 245 minutes

For the accumulation phase the principle tendency to increased drug amounts using the DMSO containing formulation can be seen in figures 4.26 and 4.27. For most ring segments the relative increase in ibuprofen concentration is at least 10 % with a trend to greater relative increase for distal ring segments.

On the other hand relevant to significant enhancement effects during the redistribution phase (fig 4.28 and 4.29) can only be seen for ring segments #1 ($\rho > 0.05$ at 128 min; $\rho < 0.05$ at 245 min) and #2 ($\rho < 0.01$ at 128 min; $\rho < 0.001$ at 245 min). In the segments #3 – #5 only for the long diffusion duration a slight effect from the enhancing effect of DMSO can be seen (fig. 4.29).

4.2.4 Comparison of diffusion results for the different types of skin

Since it is the aim of this work to evaluate the comparability of the artificial skin construct to human skin in vitro, the generated results are re-grouped into figures 4.30 – 4.33 to allow for a comparative assessment of the different types of skin regarding the diffusion profiles at the end of the accumulation phase and at the late redistribution phase from Ibutop and Ibutop + 5 % DMSO.

Over all the development of the ibuprofen concentration profiles follows the same pattern for all types of skin characterized by the two phases of accumulation and redistribution as described earlier (4.2.1.1). So in all types of skin the concentration gradient develops from a linear towards an exponential slope over the first three ring segments (#1 - #3) at the end of the accumulation phase (fig 4.30 and 4.32). After this phase the central concentration decreases in all skin types and by that transforms the slope from exponential to linear again. Then a difference from profile development from ASC to the human skins as shown in figures 4.31 and 4.33 can be observed: while in the native tissue a drug concentration shoulder is formed over ring segment #2 this phenomenon is not observed for the ASC profiles. This could be

related to either a different proceeding of the diffusion process or simply to an insufficient diffusion time in order to show the shoulder.

Comparing the time span until the estimated end of the accumulation phase for the types of skin, not surprisingly a clearly shorter period is found for the ASC which is related to the lower diffusion barrier of the tissue. Based on the ratio from time until end of accumulation phase to time until shoulder forming for FHS and PHS, it can be assumed that the time span for the ASC was sufficient as a shoulder forming would be expected already after about 90 minutes if the identical diffusion mechanism occurs (see table 4.1). The slight deviations from FHS to PHS concerning the absolute times may be attributed to individual differences of the skin donors.

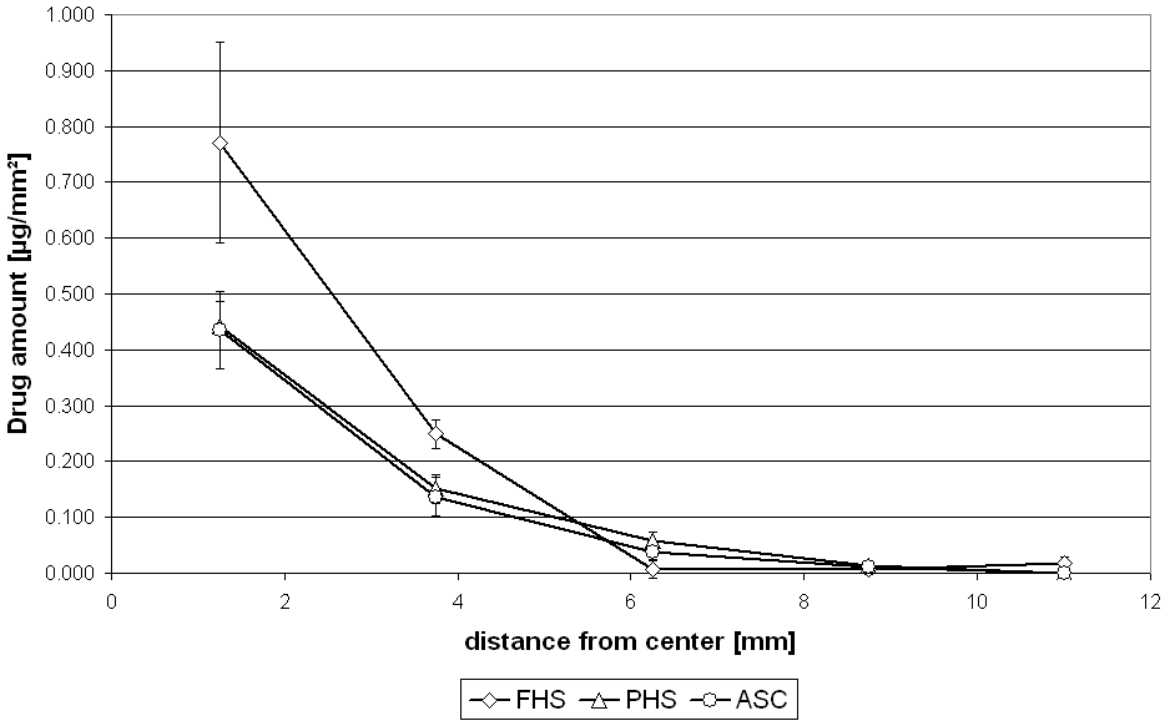

Fig. 4.30: Comparison of the profiles at the end of the accumulation phase from Ibutop

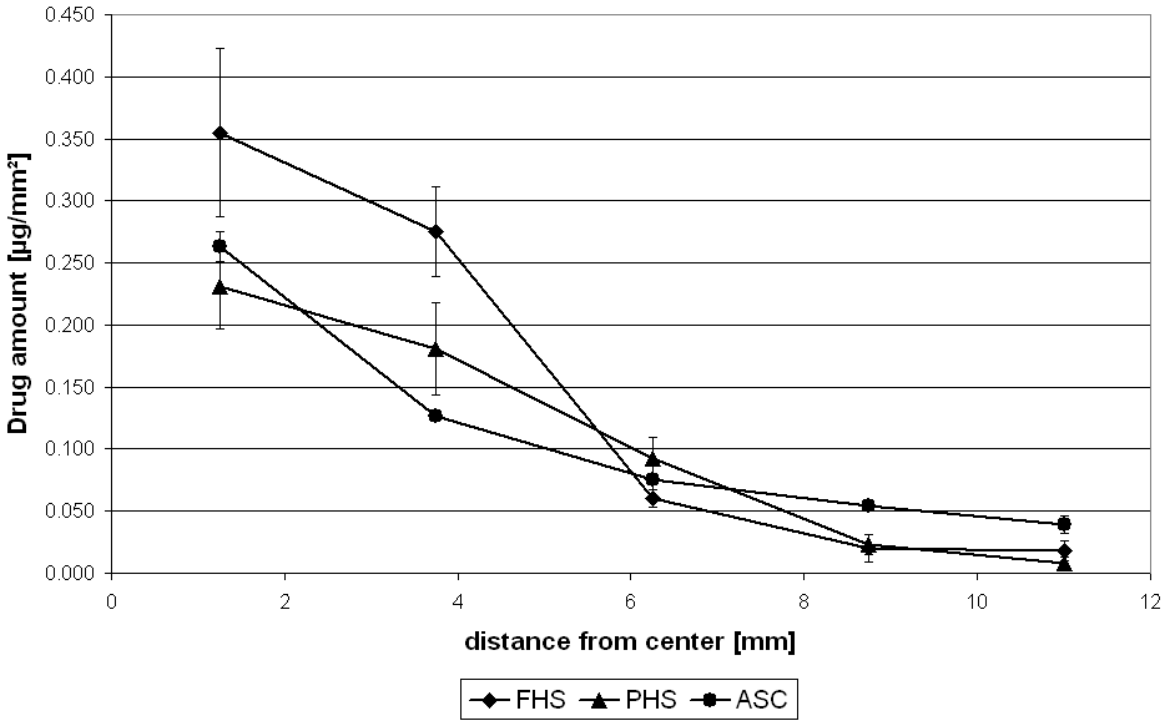

Fig. 4.31: Comparison of the profiles late in the redistribution phase from Ibutop

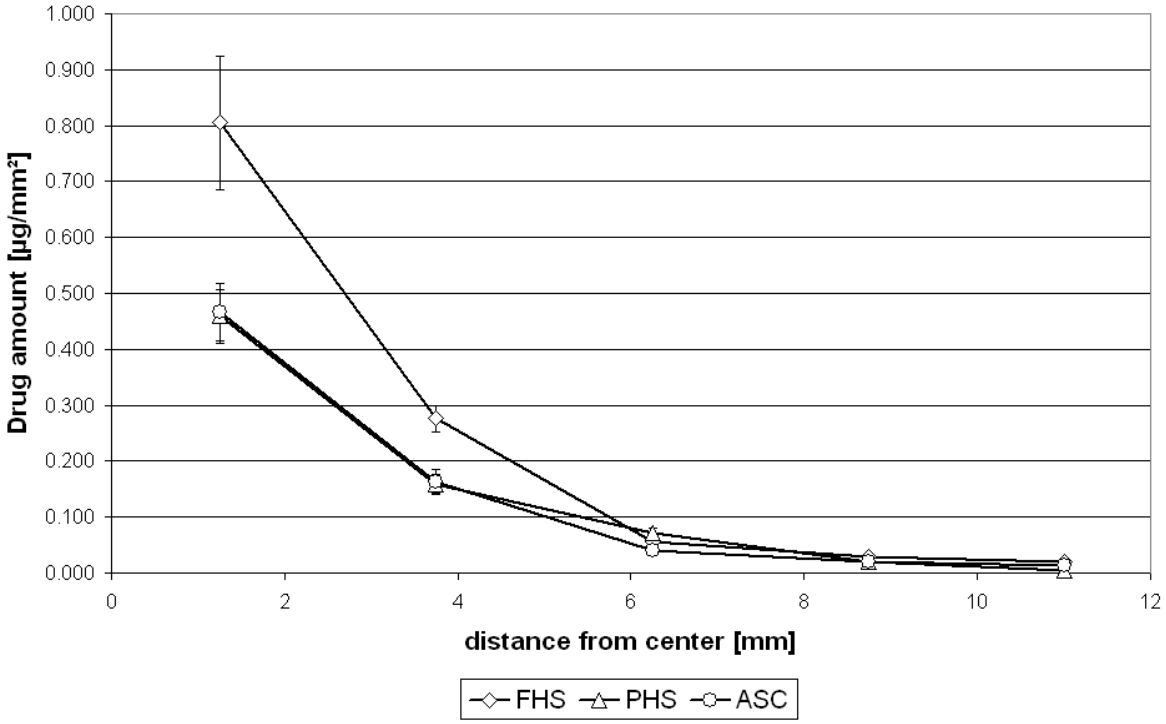

Fig. 4.32: Comparison of the profiles at the end of the accumulation phase from Ibutop + 5 % DMSO

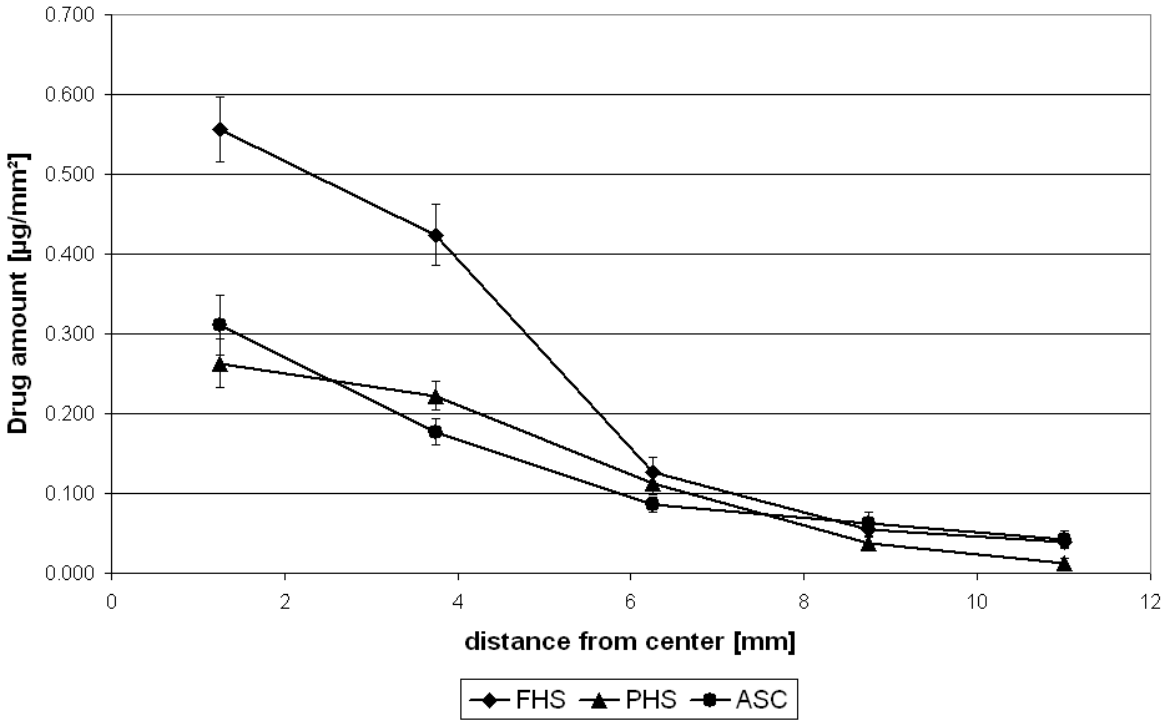

Fig. 4.33: Comparison of the profiles late in the redistribution phase from Ibutop + 5 % DMSO

A potent difference in the diffusion mechanism process could be a reuptake of ibuprofen from the acceptor medium during the experimental diffusion time. This should lead especially to increased drug contents in the distal rings due to lower intrinsic ibuprofen concentrations compared to the central segments. Thus a uniform increase in distal drug concentrations could cover up a slight shoulder forming. Due to the lower permeation barrier in ASC, larger drug amounts per time should permeate into the acceptor medium compared to PHS and it is therefore more likely to see influences of reuptake from the buffer using ASC.

A clear difference between the full thickness human skin to PHS and ASC is the significantly greater drug amount in the ring segments #1 and #2 in FHS. A logical explanation for this observation is that with FHS no permeation through the skin into the acceptor medium takes place (see also 4.4.1.1) but all penetrated ibuprofen remains in the skin as the viable epidermis and dermis are known to be a diffusion

barrier for lipophilic substances and additionally the thickness of this type of skin is bigger thus prolonging the pathway to the acceptor medium. With PHS and ASC, on the other hand, permeation occurs and the ibuprofen leaving the tissue into the acceptor medium cannot be detected by tissue extraction.

Table 4.1: Ratios of phase durations

	Duration of accumulation phase	**Time until shoulder is formed**	**Ratio**
FHS	270 min	390 min	1 : 1,4
PHS	240 min	330 min	1 : 1,4
ASC	60 min	> 245 min	1 : >4,1

This also has to be taken into account for the evaluation of the enhancer effects. Comparing the FHS results for drug concentration in the central segment (#1) a remarkably smaller decrease in concentration from end of accumulation phase to redistribution phase is observed using the DMSO containing formulation. The PHS and ASC results do not show a relevant difference for this aspect as can be seen from table 4.2.

Table 4.2: Decrease diminution from end of accumulation (EA) to late redistribution (LR) phase for segment #1

	Ibutop			**Ibutop + 5 % DMSO**			
	EA [µg/mm²]	**LR** [µg/mm²]	**Decrease** [µg/mm²]	**EA** [µg/mm²]	**LR** [µg/mm²]	**Decrease** [µg/mm²]	**Decrease diminution**
FHS	0.771	0.355	**0.416**	0.803	0.556	**0.247**	**41 %**
PHS	0.443	0.231	0.212	0.459	0.263	0.196	8 %
ASC	0.436	0.263	0.173	0.466	0.311	0.155	10 %

This indicates only a slightly improved solubility of ibuprofen in the skins leading to the minimal increase within ASC and PHS while the largely improved penetration without subsequent permeation causes the noticeable difference in FHS.

For all three types of skin, independently from the formulation, at least some 65 % of the contained ibuprofen resides outside of the central ring (#1) at the end of the accumulation phase. About 80 – 85 % of the total drug amount in the respective skin was found in the lateral ring segments #2 – #5 at the end of the experiments in late distribution phase. Yet the distribution of drug within the four lateral rings was more oriented towards the center with FHS than with PHS / ASC due to the larger total amount deriving from penetration. This uniformity in percentage development firstly emphasizes the relevance of the lateral diffusion and secondly underlines that the ASC provides results well comparable to human skin.

4.3 Diffusion model

Since great similarity in the concentration development for all skin types and formulations regarding the principle mechanism was observed from the results presented in this section (4.2) an attempt to match the spatiotemporal development on the basis of a mathematical function (2.4.1) was made.

The principal observation of two phases (accumulation and redistribution) with a strongly time dependent specificity has to be reflected in the three dimensional function by two separate terms, each one describing one of the respective phases in connection to the diffusion time. Because the lateral diffusion effect is also influenced by co-diffusion of enhancers it is a distance dependent function which has to be reflected in the respective term.

Expected influencing parameters for the total function are the maximal content of ibuprofen per area in the middle of ring segment #1 (C_{max}) and the point of time when this takes place (t_{max}) as discriminator for the shift between the phases. Furthermore some parameters compensating the individual skin and formulation characteristics need to be included.

The function that evolved from the above considerations empirically is given in equation 4.1 calculating the content $C_{(t,d)}$ [µg/mm²] against time t [min] and distance from center of application d [mm].

$$C_{(t,d)} = \frac{C_{max} \cdot a}{a + \left(t - t_{max}\right)^2} \cdot \frac{r + b^{\left(t - t_{max}\right)}}{r + b^{\left(t - t_{max}\right)} + d^s} \qquad \text{Eq. 4.1}$$

$t =$ Time [min] that the formulation is applied on the skin

$d =$ Distance [mm] from the center of formulation application

$C_{max} =$ Content maximum [µg/mm²] at application site during accumulation phase

$t_{max} =$ Diffusion time [min] until concentration maximum is observed

$a, b, r, s =$ Skin and formulation dependent parameters

For the determination of parameter settings in order to fit to a set of experimental results the observed values for C_{max} and t_{max} can be used only as initial approximations.

Regarding C_{max} it has to be taken into account that the mathematical function will require a greater value than it is observed for the central ring (#1). This is due to the fact that practically the average content for the total ring segment is determined and therefore reflects the content at 1.25 mm from the center while the function requires

the maximum directly in the center assuming a punctual application of the formulation.

With respect to the experimentally determined t_{max} it is obvious that choosing the ideal experimental diffusion time a priori is highly unlikely. The true value might therefore be as well earlier as later and can be estimated fitting the function to the obtained experimental data.

Besides the functional variables *t* [min] and *d* [mm] the four constants *a,b,r* and *s* had to be integrated into the function in order to allow for the best possible fit to the experimental results.

The constant *a* in the term for the accumulation phase determines the slope of the principally bell shaped content development in the central ring segment (#1) and therefore modulates how quickly the content increases and decreases over time.

The parameter *r* in the redistribution term together with *b* as basis for the exponential expression controls the shoulder forming process at later diffusion times. The principle slope of the content profiles (displayed as drug amount [µg/mm²] over distance [mm]) is largely influenced by the constant *s* towards either more exponential or linear shape over the first three ring segments (#1 - #3).

4.3.1 Parametrical fit to experimental results

The parameters were adapted as described above for each set of experiments carried out with Ibutop and Ibutop + DMSO in order to find a best match over all several diffusion time points belonging to one experimental set.

The following two diagrams show the experimental results for Ibutop on ASC in comparison to the model prediction (in dotted lines) separated into accumulation (fig. 4.34) and redistribution phases (fig. 4.35).

When evaluating the quality of the fit to the data set it has to be taken into account that for each time point a different batch of ASC was used and therefore certain variability is to be expected. Bearing this in mind the fitted curves in figure 4.34 are sufficiently matching the experimental data. Although it appears that for early time points the model overestimates the content in the central ring (#1) by trend all curves lie within the error bar range of the respective experimental curve.

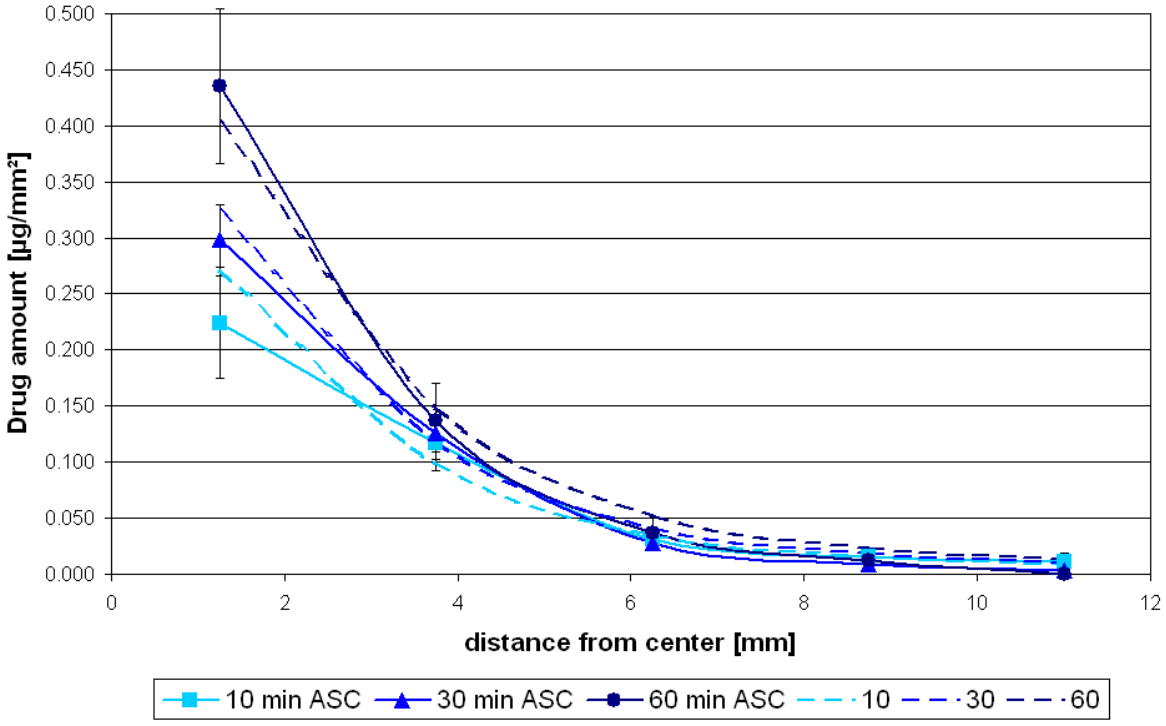

Fig. 4.34: Comparison of experimental results as solid lines / symbols for the accumulation phase from Ibutop on ASC to the respective time points in the mathematical fit, displayed in dotted lines

The 135 minutes diagram in figure 4.35 very closely matches the experimental correspondent except for a slightly bigger discrepancy in ring segment #2. A bigger deviation is seen after 210 minutes for the content in ring #1 which is calculated to contain less drug substance than was found in the experiment. On the other hand the unusual ripple seen from the ring #4 and #5 data most likely has to be attributed to an experimental handling error transferring drug amounts errantly to ring #4.

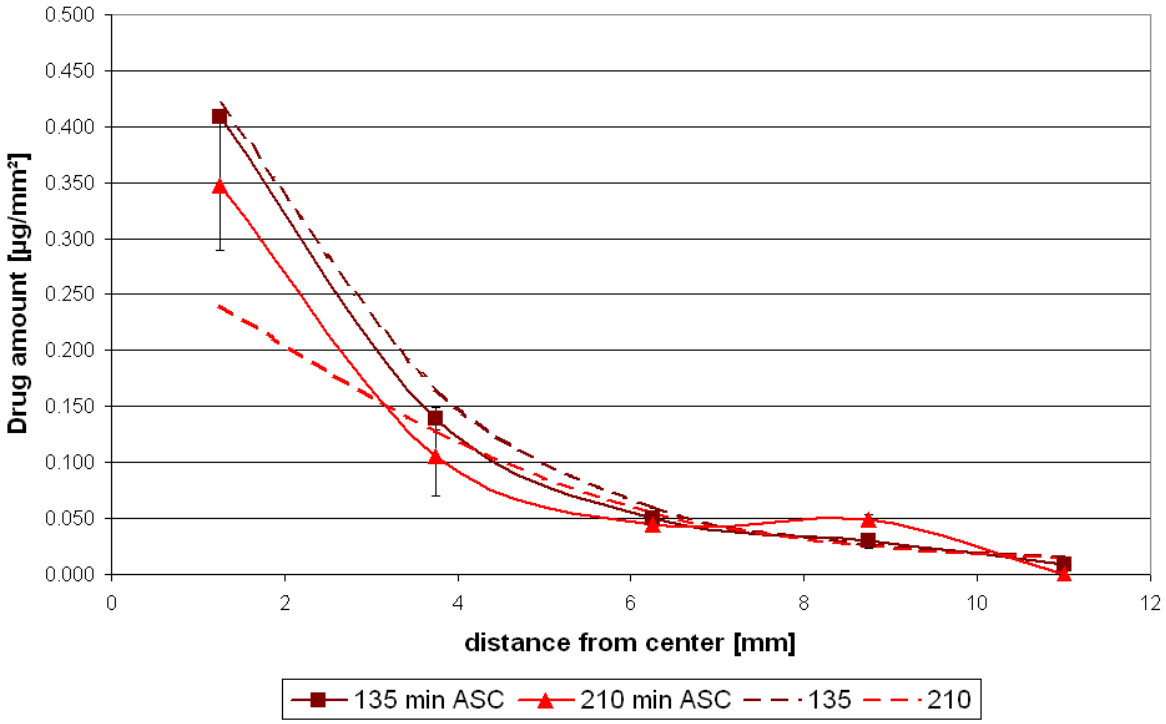

Fig. 4.35: Comparison of experimental results for the redistribution phase from Ibutop on ASC to the respective time points in the mathematical fit

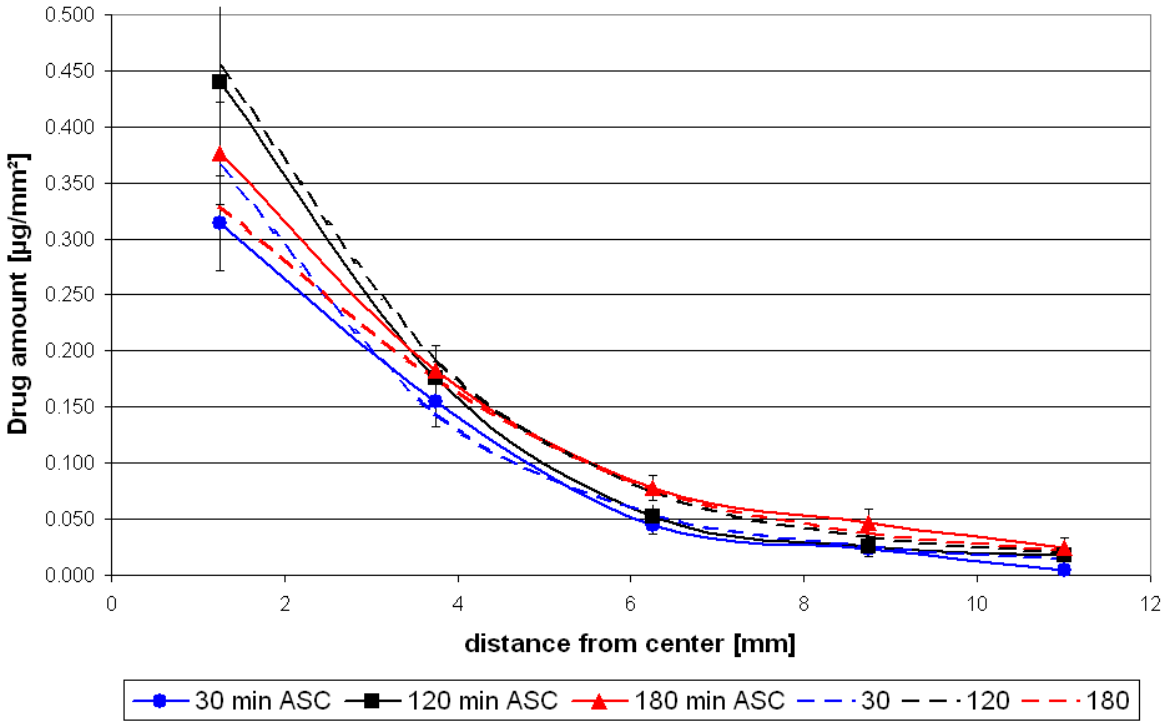

Fig. 4.36: Comparison of experimental results from Ibutop + DMSO on ASC to the respective time points in the mathematical fit

For the remainder of the experiments with the various types of skin using Ibutop and Ibutop + DMSO as formulation only one diagram per data set with relevant time points is presented in the following, starting with figure 4.36 for Ibutop + DMSO on ASC. As previously the curves of the mathematical fit are displayed in dotted lines. Again the content of ring #1 is slightly overestimated in the beginning and the opposite for later time points, yet within the error bar range.

Figures 4.37 and 4.38 contain the diagrams from the experiments with planed human skin. For this skin type no early accumulation phase data is available but a close match to the existing results was possible. The assumptions of the model for rings #1 - #3 are acceptable but for rings #4 and #5 higher contents were expected as shown in figure 4.37.

Using Ibutop + DMSO also the 180 and 300 minutes curves in figure 4.38 are matched sufficiently. For ring segments #1 - #3 in the 330 minutes diagram the fitted curve also ranges within the error bars but does not show the same extent of shoulder as assumed from the experimental data. The most distal rings (#4 and #5) were expected to contain more ibuprofen at later times.

The approximation to the experimental curves obtained from the full thickness human skin experiments as displayed in figures 4.39 and 4.40 shows good results for most curves. Yet the segment #3 from Ibutop on FHS (figure 4.39) is systematically calculated higher than the found results from praxis.

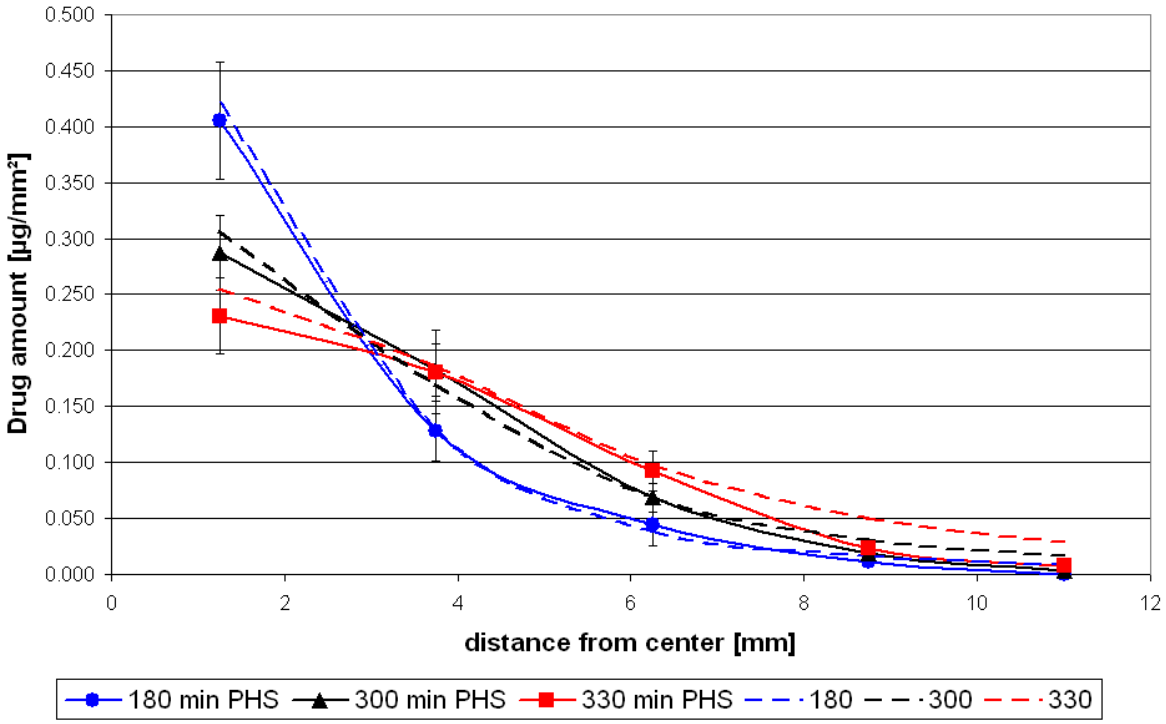

Fig. 4.37: Comparison of experimental results from Ibutop on PHS to the respective time points in the mathematical fit

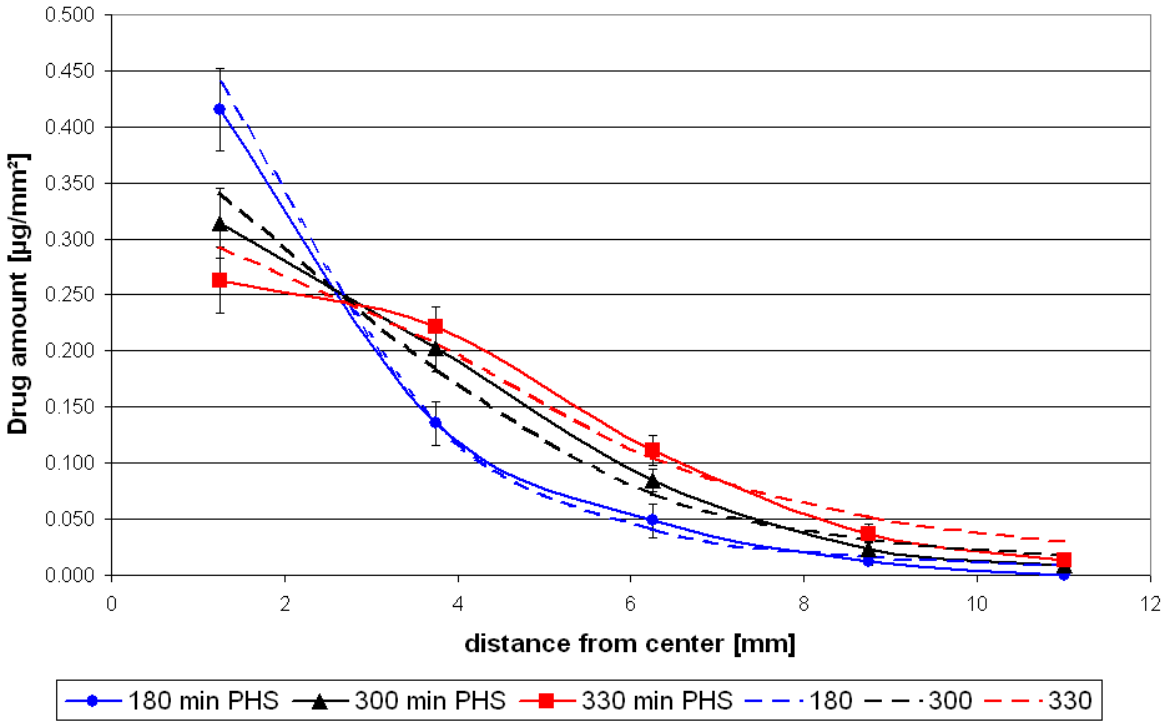

Fig. 4.38: Comparison of experimental results from Ibutop + DMSO on PHS to the respective time points in the mathematical fit

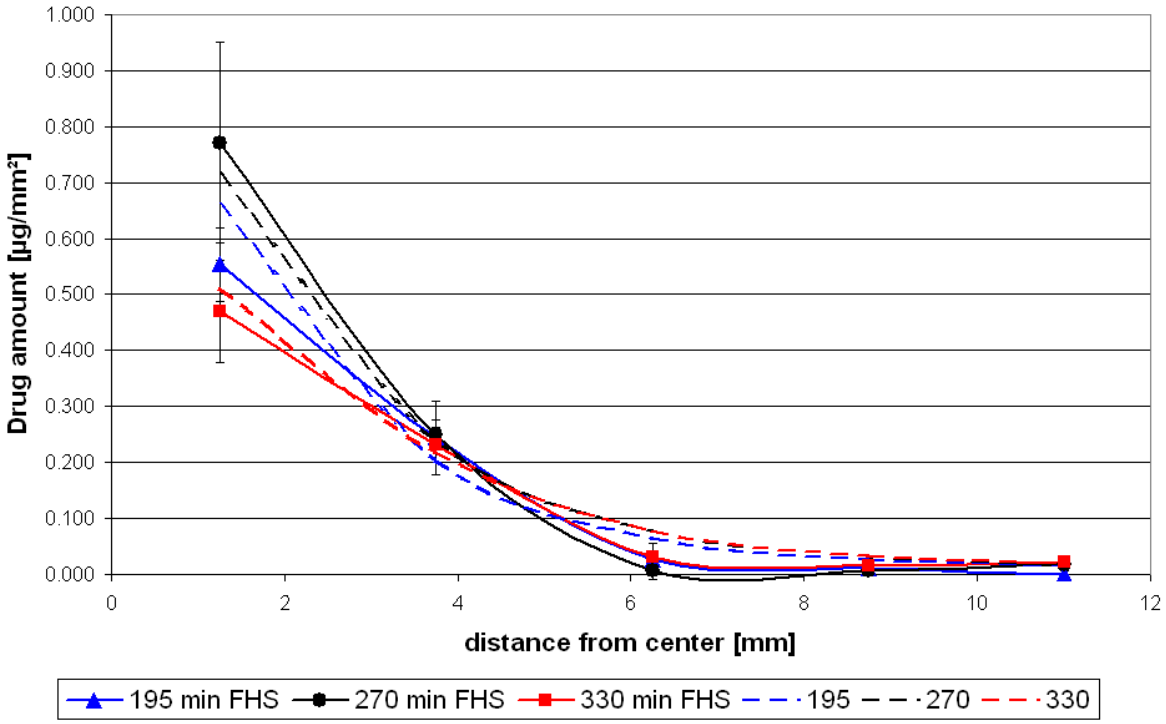

Fig. 4.39: Comparison of experimental results from Ibutop on FHS to the respective time points in the mathematical fit

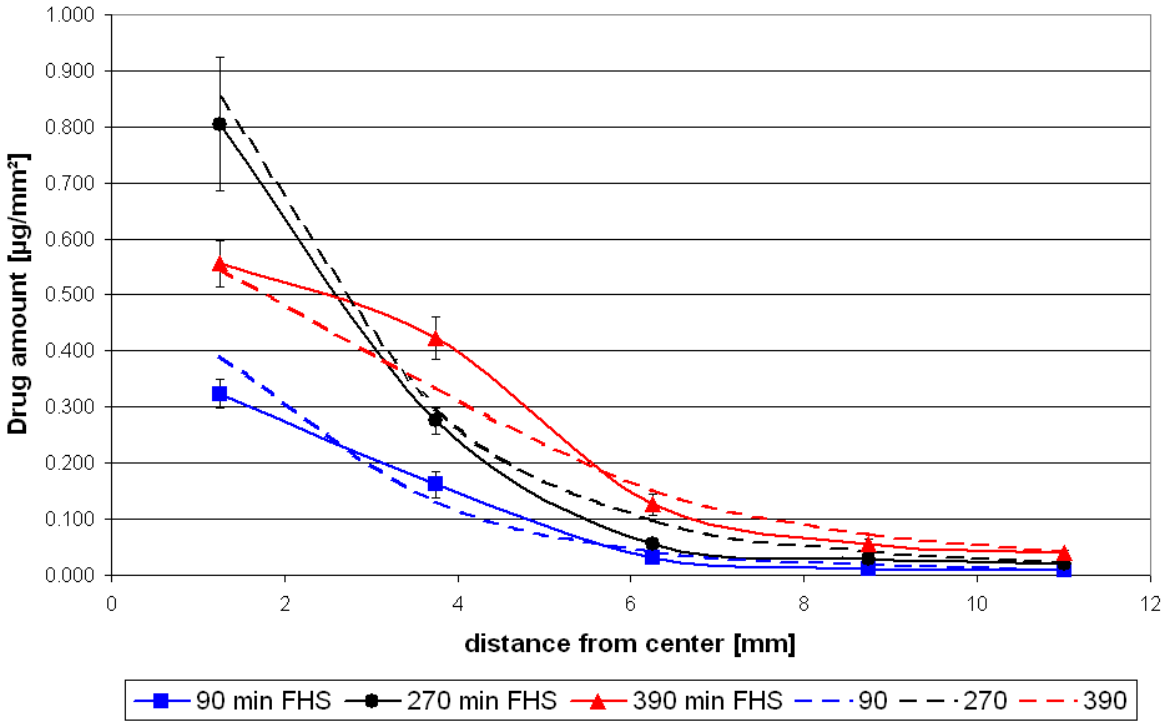

Fig. 4.40: Comparison of experimental results from Ibutop + DMSO on FHS to the respective time points in the mathematical fit

Regarding the curves obtained with Ibutop + DMSO on FHS (fig. 4.40) especially the deviation from the sigmoidal shape for the 390 minutes attracts attention. Although most of the practically determined ring segment contents are in good agreement with the fitted graph, ring segment #2 contained relevantly greater amounts of ibuprofen than were calculated. Even for later simulated time points this level would not be reached using the same parameters matching the curves from the other time points.

The parameters used for the best fit of the functional values from equation 4.1 to the respective experimental data set are given in the following table.

Table 4.3: Values for the several parameters used to fit to experimental results

	ASC		**PHS**		**FHS**	
	Ibutop	Ibutop + DMSO	Ibutop	Ibutop + DMSO	Ibutop	Ibutop + DMSO
C_{max} [µg/mm²]	0.51	0.52	0.48	0.5	0.85	0.95
t_{max} [min]	100	95	200	200	240	260
a	12000	15000	20000	25000	15000	25000
b	1.026	1.030	1.035	1.034	1.026	1.028
s	2.6	2.5	2.8	2.8	2.7	2.7
r	15	15	15	15	13	15

Comparing the parameters listed in table 4.3 across the different skin types and formulations especially two parameters stand out due to a systematic difference between formulations on the same type of skin. Firstly the C_{max} value always was slightly higher using the DMSO containing formulation which supports the findings and interpretation from 4.2.4 that DMSO slightly improves the solubility of ibuprofen in the skin and secondly for the parameter *a,* influencing mainly the accumulation

phase, greater values had to be chosen so a connection with skin permeability is assumed.

For t_{max} no systematic trend within one type of skin is detectable. Using the chosen values for the evaluation of the missing shoulder for ASC (see 4.2.4, table 4.1) leads to the same conclusion.

The remaining parameters only show slight skin type related differences (*b* and *s*) or appear to be almost constant (*r*).

Overall the model allows to fit content profiles over time and distance with sufficient congruence to the experimental data set and to deduct some comparative parameters for each set.

4.4 Permeation experiments

The permeation experiments (3.2.8) characterize mainly the barrier function of the different types of skin by the determination of the respective ibuprofen flux and permeation coefficient in dependence of the donor formulation. From these results a quantitative comparison of the barrier function (2.2) as well as the efficacy of the permeation enhancers (2.2.2.3) can be estimated.

4.4.1 Determination of flux and permeation coefficient

While numerous permeation studies also with ibuprofen are available from literature [Hadgraft et al., 2003; Gonzales and Sumano, 2007] the aim for these experiments is to generate supportive data for the interpretation of the results from the lateral diffusion experiments. The experimental set up as described in 3.2.8 was therefore chosen in order to be identical to the diffusion experiments and thus to deviate from the classic modified Franz diffusion cell set up by intention. From the experimental results the cumulated amount of permeated ibuprofen per skin surface in contact with

the donor [µg/cm²] is calculated and plotted over permeation time [min]. The linear slope of the resulting diagram allows a calculation of the effective drug flux (2.3.1, equation 2.3) leading to the permeation coefficient (2.3.1, equation 2.4) taking the drug concentration in the formulation into account.

4.4.1.1 Full thickness human skin

FHS (3.2.5) is not suitable for permeation experiments due to the thickness of the material. During a for the diffusion experiments relevant period of eight hours no detectable amount of ibuprofen was found in the buffer medium. It must be concluded that penetration takes place but all active substance remains within the skin sample. This result is in good agreement with Hadgraft et al. [2003].

4.4.1.2 Planed human skin

Reducing the thickness of the skin by removing large parts of the hydrophilic viable tissue leads to an analytically accessible permeation through the native skin (3.2.6). The lag-time of the experiments lies within a normal range of about 30 minutes for all formulations and a sufficient relative standard deviation for n = 6 experiments is obtained.

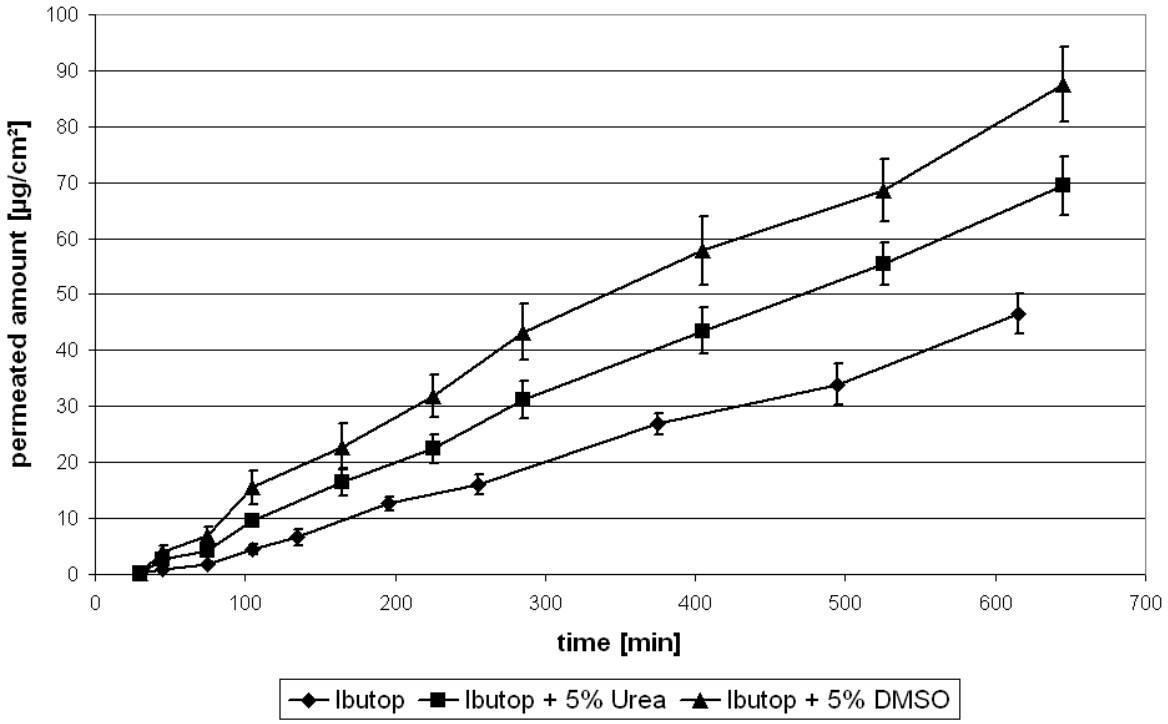

Fig. 4.41: Permeation of ibuprofen acid from Ibutop, Ibutop + Urea and Ibutop + DMSO through planed human skin

The diagram 4.41 gives a comparative overview on the ibuprofen permeation through PHS from the three formulations plotting the permeated drug amount [µg/cm²] over time [min].

It can clearly be observed that both enhancers improve the drug permeation to a significant degree. DMSO is obviously more effective in reducing the diffusion barrier compared to urea.

From the slope of a linear fit to each graph the flux and permeation coefficient was calculated and the respective results are presented in the table 4.4.

The results for permeation from Ibutop are reasonably close to previously published results for ibuprofen permeation from Ibutop on fully hydrated excised human stratum corneum showing a flux (J) of $1.85 \cdot 10^{-9}$ [g/cm²·s] [Stoye, 1997] and a permeation coefficient (P) of $3.70 \cdot 10^{-8}$ [cm/s] [Specht et al., 1998 a].

Table 4.4: Ibuprofen flux and permeation coefficient for PHS

Formulation	**Flux** J [g/cm²·s]	**Permeation coefficient** P [cm/s]
Ibutop [n=6]	$1.32 \cdot 10^{-9} \pm 0.11 \cdot 10^{-9}$	$2.63 \cdot 10^{-8} \pm 0.22 \cdot 10^{-8}$
Ibutop + 5% urea [n=6]	$1.87 \cdot 10^{-9} \pm 0.14 \cdot 10^{-9}$	$3.75 \cdot 10^{-8} \pm 0.22 \cdot 10^{-8}$
Ibutop + 5% DMSO [n=6]	$2.32 \cdot 10^{-9} \pm 0.16 \cdot 10^{-9}$	$4.65 \cdot 10^{-8} \pm 0.32 \cdot 10^{-8}$

4.4.1.3 Artificial skin construct

Since the quality of the barrier function of the ASC (3.2.4) might differ in between batches some permeation experiments were carried out several times using different ASC batches to provide information of the reproducibility of the barrier function. In such cases the individual results are displayed in the table accompanied by an average result in the table in bold print.

The average values are in good agreement with the results reported by Specht [1998 b] of $J=3.81 \cdot 10^{-8} \pm 0.55 \cdot 10^{-8}$ [g/cm²·s] and $P=7.62 \cdot 10^{-7} \pm 1.1 \cdot 10^{-7}$ [cm/s] [Specht et al., 1998 a] also produced with Ibutop on ASC using a similar experimental set up, yet with a slightly bigger donor contact area. Using a modified Franz cell Winkler [2005] obtained an average permeation coefficient of $P=8.70 \cdot 10^{-7} \pm 0.92 \cdot 10^{-7}$ [cm/s] for the permeation of ibuprofen from Ibutop through ASC.

Table 4.5: Ibuprofen flux and permeation coefficient for ASC from Ibutop

Formulation	**Flux** J [g/cm²·s]	**Permeation coefficient** P [cm/s]
Ibutop [n=6]	$3.07 \cdot 10^{-8} \pm 0.47 \cdot 10^{-8}$	$6.14 \cdot 10^{-7} \pm 0.94 \cdot 10^{-7}$
Ibutop [n=6]	$4.81 \cdot 10^{-8} \pm 0.87 \cdot 10^{-8}$	$9.61 \cdot 10^{-7} \pm 1.75 \cdot 10^{-7}$
Ibutop [n=5]	$3.86 \cdot 10^{-8} \pm 0.39 \cdot 10^{-8}$	$7.71 \cdot 10^{-7} \pm 0.77 \cdot 10^{-7}$
Average [n=17]	$\mathbf{3.91 \cdot 10^{-8} \pm 0.95 \cdot 10^{-8}}$	$\mathbf{7.83 \cdot 10^{-7} \pm 1.89 \cdot 10^{-7}}$

Also the permeation from Ibutop + DMSO was carried out in duplicate which produced the results given in table 4.6.

For the visual comparison in figure 4.42 only one representative graph deriving from one set of experimental results per formulation is shown since an averaging of the individual sets of cumulated drug amounts versus time is not feasible.

Again clearly DMSO increases the permeated amount of ibuprofen to a greater extent than urea. This is also expressed by the results from the following table 4.7.

Table 4.6: Ibuprofen flux and permeation coefficient for ASC from Ibutop + 5% DMSO

Formulation	**Flux** J [g/cm²·s]	**Permeation coefficient** P [cm/s]
Ibutop + 5% DMSO [n=6]	$5.79 \cdot 10^{-8}$ $\pm 0.66 \cdot 10^{-8}$	$1.16 \cdot 10^{-6}$ $\pm 0.13 \cdot 10^{-6}$
Ibutop + 5% DMSO [n=6]	$7.45 \cdot 10^{-8}$ $\pm 0.76 \cdot 10^{-8}$	$1.49 \cdot 10^{-6}$ $\pm 0.15 \cdot 10^{-6}$
Average [n=12]	**$6.62 \cdot 10^{-8}$ $\pm 1.10 \cdot 10^{-8}$**	**$1.32 \cdot 10^{-6}$ $\pm 0.22 \cdot 10^{-6}$**

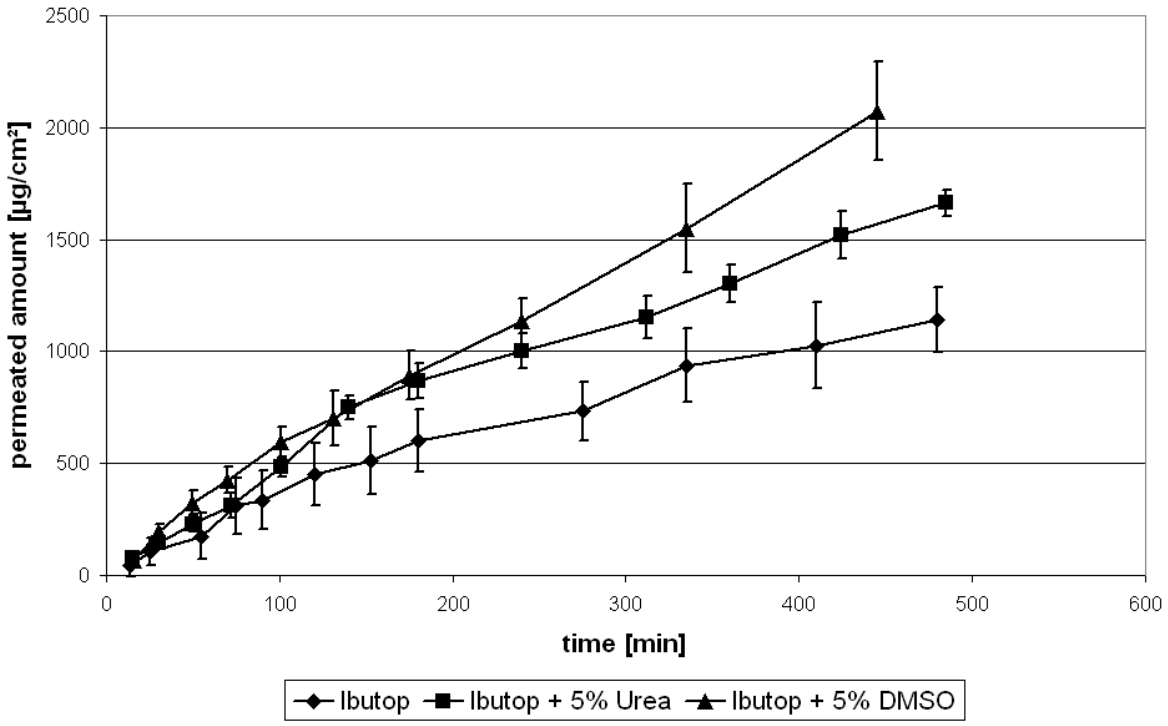

Fig. 4.42: Permeation of ibuprofen acid from Ibutop, Ibutop + Urea and Ibutop + DMSO through the artificial skin construct

Table 4.7: Ibuprofen flux and permeation coefficient for ASC

Formulation	**Flux** J [g/cm²·s]	**Permeation coefficient** P [cm/s]
Ibutop [n=17]	$3.91 \cdot 10^{-8}$ $\pm 0.95 \cdot 10^{-8}$	$7.83 \cdot 10^{-7}$ $\pm 1.89 \cdot 10^{-7}$
Ibutop + 5% urea [n=6]	$5.59 \cdot 10^{-8}$ $\pm 0.28 \cdot 10^{-8}$	$1.12 \cdot 10^{-6}$ $\pm 0.\cdot 06^{-6}$
Ibutop + 5% DMSO [n=12]	$6.62 \cdot 10^{-8}$ $\pm 1.10 \cdot 10^{-8}$	$1.32 \cdot 10^{-6}$ $\pm 0.22 \cdot 10^{-6}$

4.4.2 Comparison of the barrier function

The comparison of PHS to ASC using the calculated fluxes for the respective formulations allows an evaluation of the transferability of results obtained with one skin type towards the other. Therefore the ratio of the flux obtained from ASC to PHS is calculated and presented in the following table 4.8.

Table 4.8: Ratio of the flux J from ASC/PHS for the three formulations

Flux J [g/cm²·s]	**ASC**	**PHS**	**Ratio J_{ASC} / J_{PHS}**
Ibutop	$3.91 \cdot 10^{-8}$	$1.32 \cdot 10^{-9}$	29.7
Ibutop + 5% urea	$5.59 \cdot 10^{-8}$	$1.87 \cdot 10^{-9}$	29.8
Ibutop + 5% DMSO	$6.62 \cdot 10^{-8}$	$2.32 \cdot 10^{-9}$	28.5

For all three formulations an about thirty fold higher barrier function for the native skin PHS is detected in comparison to the diffusion barrier of ASC. The influence of the permeation enhancers urea and DMSO respectively is seen to an equal extent for both skin types.

4.4.3 Relative permeation enhancement

Taking the flux J [g/cm²·s] obtained from the permeation of Ibutop for each skin type individually as reference value, the relative permeation enhancement by the addition of 5% urea or DMSO can be calculated.

It can clearly be seen from the results given in table 4.9 that for both skin types a permeation enhancement by the factor of about 1.4 for the addition of 5 % urea and about 1.7 for the addition of 5 % DMSO is registered.

Table 4.9: Relative permeation enhancement by urea or DMSO for ASC and PHS

	ASC	**PHS**
Ibutop	1.00	1.00
Ibutop + 5% urea	1.43	1.43
Ibutop + 5% DMSO	1.69	1.77

The finding that DMSO is the more effective permeation enhancer compared to urea was expected since DMSO is known to act on multiple sites [Barry, 1991] (see 2.5.2.1) creating synergistic effects as previously described in 2.2.2 and 2.2.2.3 while the mode of action for urea is the keratolytic effect reducing the keratinocyte and corneocyte coherence (see 2.5.2.2).

4.5 Total drug amount from diffusion and permeation experiments

Due to the finding, that decisive differences in drug concentrations within the first two ring segments (#1 and #2) were seen between FHS and PHS (see 4.2.4) although both are native human tissues and similar barrier properties are to be assumed, the total absolute amount of penetrated / permeated ibuprofen over time was calculated from the previous data. For this the determined drug amounts per ring segment at a certain time point were summed for each type of skin in order to give the total amount of drug substance in the skin. Additionally the total permeated ibuprofen amount for each diffusion time point was calculated using the in 4.4.1.2 and 4.4.1.3 determined flux (J) for each skin and formulation combination, respectively (see annex 8.2).

4.5.1 Comparison of FHS to PHS

The effect of the previous finding of greater drug amounts in ring #1 and #2 for FHS can be comprehended from figure 4.43 showing the increase of total drug amount in the skin sample over time for FHS and PHS.

While the overlapping error bars indicate no relevant difference for the diffusion experiments using Ibutop only as donor formulation, for the comparison of both skin types using Ibutop + DMSO significantly different drug amounts are seen throughout the complete time scale ($\rho < 0.001$ at 180 min; $\rho < 0.001$ at 330 min). Furthermore it can be clearly seen that for FHS using Ibutop a constant drug level after 270 minutes is reached in contrast to the DMSO containing formulation with steadily increasing drug amounts leading to significantly greater total drug amounts ($\rho < 0.001$ at 330 min). This could be explained by decreasing sink conditions within the FHS over time using Ibutop in contrast to the effect of improved solubility of ibuprofen due to DMSO especially in the hydrophilic viable parts of the epidermis and dermis.

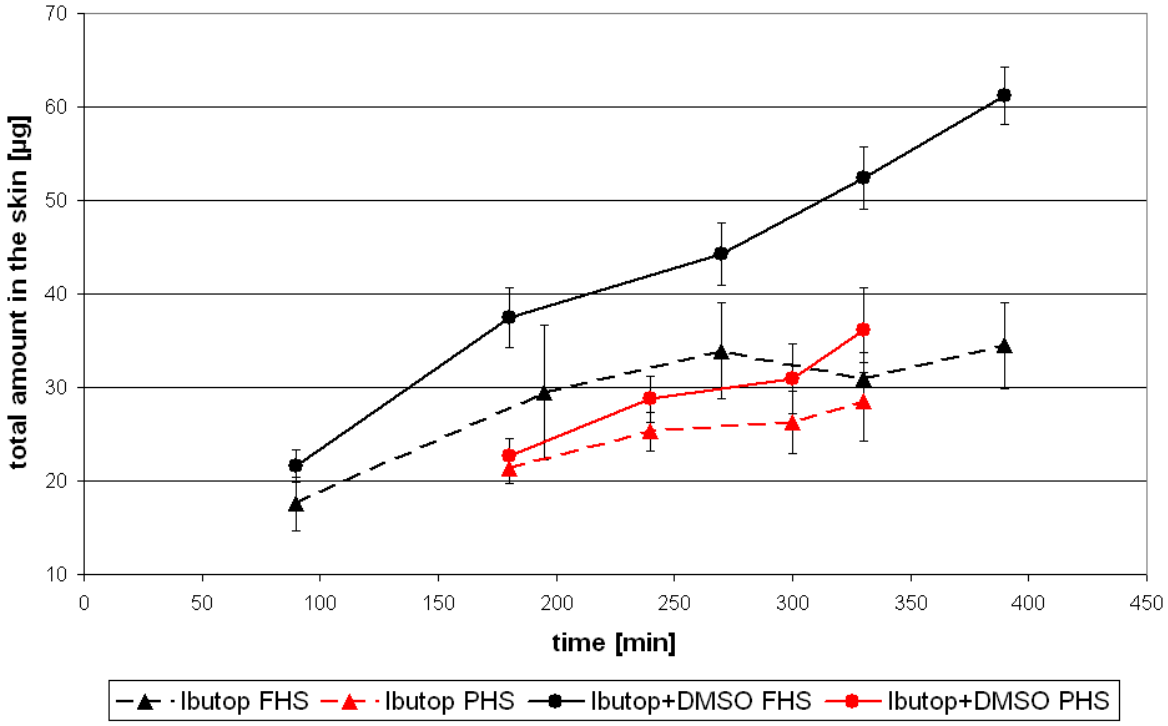

Fig. 4.43: Development of total ibuprofen amount within the complete skin samples of FHS and PHS depending on the respective formulation

Adding the total permeated drug amount at each time point to the amount contained in the skin itself for PHS a direct comparability to the results from FHS showing no drug permeation is reached. This summation shifts the curves for PHS towards greater drug amounts as can be seen in figure 4.44 and indicates greater equality of the results obtained from FHS and PHS. The differences between the respective skin curves belonging to one formulation type are not significant anymore and can be explained by tissue donor differences.

It can also be seen that the distance between the PHS curves for the two formulations increases by addition of the permeation values due to DMSO's permeation enhancing effects. This on the other hand indicates that the difference between the PHS curves in figure 4.43 is mainly connected to the enhancer action on lateral diffusion and improved solubility of ibuprofen in the skin.

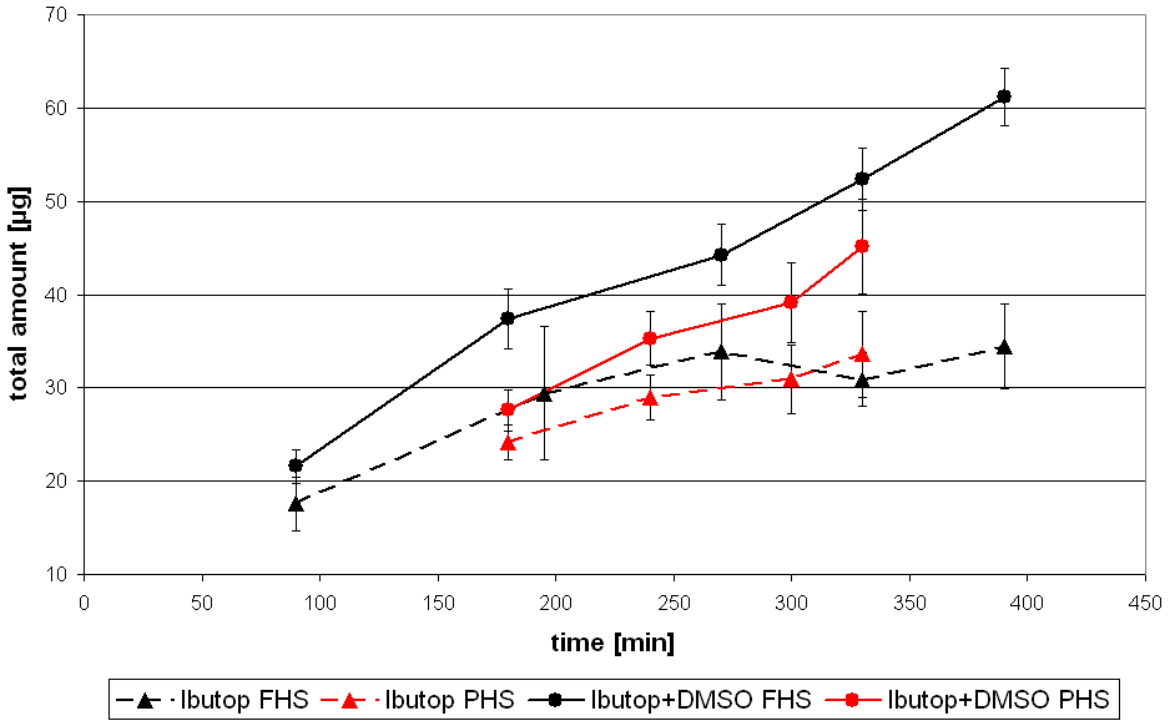

Fig. 4.44: Development of total ibuprofen amount in the acceptor medium and the complete skin samples depending on the respective formulation

4.5.2 Comparison of ASC to PHS

As was already noted in 4.2.4 quite similar drug levels were determined during the two phases of diffusion development using both formulations on ASC and PHS, respectively. So it is not surprising that the total drug amount in the complete skin samples (sum of ring #1 to #5) also develop similarly, yet with different timing. For the display in figure 4.45 the curves for PHS results were shifted by -120 minutes (which is roughly the time difference between the modeled t_{max} values from table 4.3) and then closely match the curves obtained from ASC.

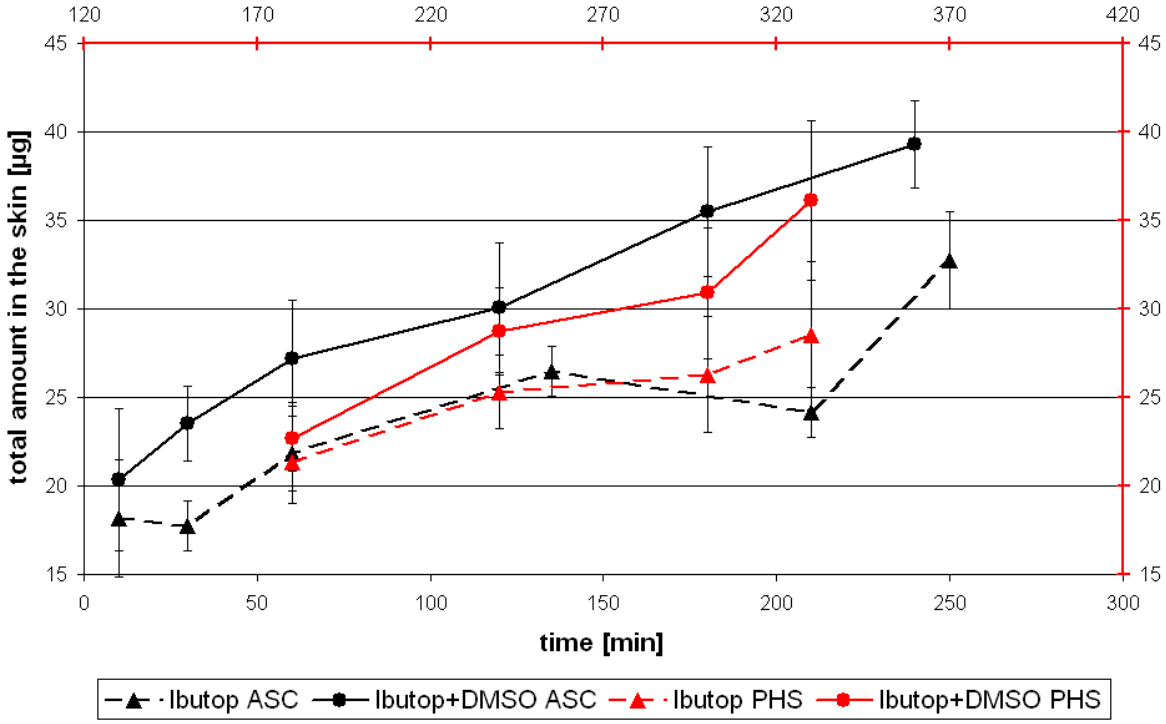

Fig. 4.45: Development of total ibuprofen amount within the complete skin sample depending on the respective formulation (PHS on secondary axes of coordinates in red)

Although no significant difference can be shown, overall a good tendency for higher ibuprofen content in the skin samples is achieved using the DMSO containing formulation with both, ASC and PHS. This congruence demonstrates the similarity of enhancer effects on the lateral diffusion for the two types of skin.

While the summation of the permeated drug amount to the skin content leads to better comparability between FHS and PHS this clearly is not the case for ASC and PHS as can be seen in figure 4.46. Due to the lower permeation barrier properties of the ASC a different magnitude of permeated drug amounts separates the curves of two types of skin.

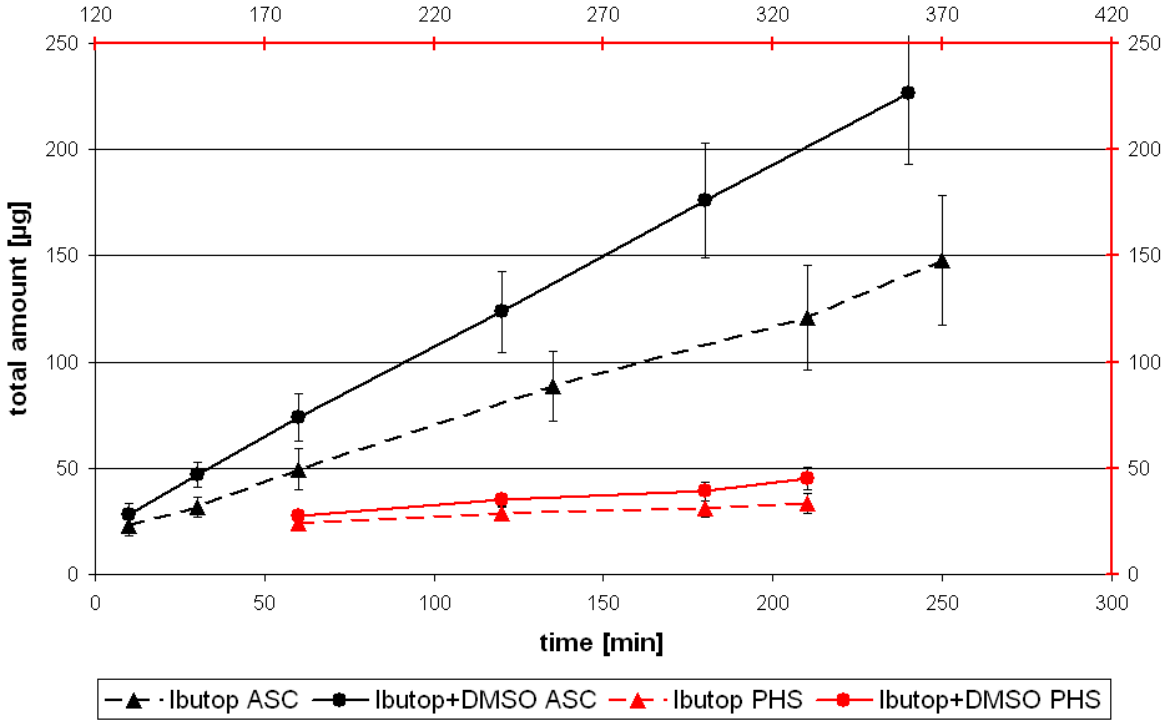

Fig. 4.46: Development of total ibuprofen amount in the acceptor medium and the complete skin samples depending on the respective formulation (PHS on secondary axes of coordinates in red)

Most interestingly the development of drug amounts in the skin is apparently not directly connected to the permeation characteristics of the skin type. Although the amount of drug substance permeating in vertical direction per time unit is largely different for the two skin types no relevant difference regarding the total amount of drug substance in the total skin compartment is observed. This is already comprehendible from the similar maximal drug concentrations in ring #1 for both PHS and ASC effective as driving force for the lateral diffusion process. It can therefore be concluded that the increase in the drug content of the skin is solely depending on the lateral diffusion of the active substance in combination with its solubility in the skin. Based on this it can be shown that all three types of skin demonstrate that DMSO not only enhances the drug permeation but, moreover, also the lateral diffusion leading to greater ibuprofen content in the skin and thus enhances forming of a drug depot.

The comparison of the drug contents in the skin indicates that ASC is well capable to produce directly comparable results to human derived skin, also with good differentiation between formulation effects, despite its lower permeation barrier.

5 Conclusion

The effects of lateral diffusion on drug depot building within skin after dermal application with focus on spatiotemporal development were studied.

The characteristics of this process taking place in an artificial skin construct in comparison to two types of human skin (full thickness and planed) using the active substance ibuprofen from different formulations were investigated.

As far as possible also permeation experiments were carried out in order to further characterize the barrier properties of the different types of skin and to allow a better interpretation of differences seen in the diffusion experiments.

5.1 Lateral diffusion process

5.1.1 Process mechanism

The results produced using the artificial skin construct (ASC) principally show the same time dependent drug concentration per distance gradient development as also seen with the full thickness human skin (FHS) and the planed human skin (PHS).

This over all development is characterized by two phases. The first phase (accumulation) is dominated by a drug concentration increase mainly in the central skin area either with direct formulation contact or in direct vicinity to the formulation application area. Then a maximal concentration in the central area is observed and the second phase (redistribution) starts, which is characterized by decreasing central drug concentration in contrast to an increase in concentration in the distal skin area.

Based on the determination of similar drug amounts within the ASC and the PHS in spite of the large difference in permeability of the skin types, it must be concluded that the main driving force for the lateral diffusion within the skin is not the

permeation coefficient but more likely the resulting concentration of drug in the skin at the site of formulation application. This concentration is certainly depending on the permeation coefficient as velocity parameter but moreover on the total solubility of the drug substance in the skin.

The observation of a concentration maximum in the central segment indicates that the lateral diffusion of ibuprofen starts with a certain time lag. Before the lateral diffusion is fully established the drug substance accumulates in the skin and is only reduced by effective permeation into the acceptor medium. Thus, a sole vertical transport route (one dimensional) is predominant in that phase. When the lateral diffusion becomes relevant after the lag time two additional directions in the plane of the skin surface are available for drug wash-out from the central segment. This then three dimensional drainage causes the decrease in central drug content until steady state equilibrium is reached with the rate limiting step for drug influx of either penetration into the stratum corneum or even release from the formulation. The latter is assumed to be the case for diffusion using ASC since the results from the permeation experiments with ASC show a slight bend towards smaller slope in the permeation diagrams at about 100 - 120 minutes especially noticeable for the additional enhancer containing formulations. The timing of this bend coincides with the estimated time for maximal drug concentration in ASC from the fitted mathematical model. Hence the bend is a direct result from the additional competitive lateral diffusion. This bend in permeation curves was also observed by Specht [1998 b] at the same time point using a similar methodological set up for permeation experiments with a slightly larger application surface but still with sufficient surrounding skin to allow for lateral diffusion.

The lag time for effective lateral diffusion should depend largely on the co-diffusion of solubility increasing excipients like in this case propylene glycol from the Ibutop formulation. This assumption is in good agreement with the finding of Nicoli et al. [2009] demonstrating that clearance of ibuprofen from the stratum corneum is significantly reduced if the propylene glycol containing formulation is removed from the skin and the treated area is left unoccluded so that the volatile propylene glycol can evaporate from the skin.

The results from penetration studies with ibuprofen presenting depth profiles obtained by tape stripping show, that the drug concentration declines exponentially within the 15 - 20 µm distance of the stratum corneum [Bock et al., 2004; Nicoli et al., 2009]. A similar exponential decline is seen with the results of this work but over a lateral distance of several millimeters. This emphasizes the proposal of Johnson et al. [1997] that the lateral diffusion in the stratum corneum lipid bilayers is the main transport mechanism for lipophilic drugs. The findings of Ashworth et al. [1988] that higher concentrations of clobetasol 17-propinate in upper stratum corneum layers correlate with larger lateral drug transport compared to a second formulation showing the greater drug amounts in lower stratum corneum layers with less lateral diffusion indicate that this phenomenon is depending on the formulation.

5.1.2 Relevance

While in typical studies the occurrence of lateral diffusion is considered as a possible cause of error [Dreher et al., 2002; Weigmann et al., 1999] for inaccurate penetration rates during this investigation it was intently included. The results from this study show that the lateral drug diffusion must not be disregarded for in vitro experiments using significantly larger skin sample sizes than required for donor contact area.

The relevance of lateral diffusion for in vivo experiments is even greater. In therapeutic use the topical application of a drug loaded vehicle normally takes place by localized administration. So there will always be untreated adjacent sites functioning as possible compartments for laterally diffused substances. This has been impressively demonstrated by Simonsen et al. [2002] and Weigmann et al. [1999]. Furthermore the comparison of the permeated drug amounts to the amounts found in the skin using PHS in this work underlines that during treatment times of up to five hours 4 – 5 fold larger drug amounts accumulate in the skin, building a depot with a large quantity of drug contained in lateral skin areas.

The relevance of the lateral diffusion process on the dermal absorption depending on the spatial distribution has been described mathematically by Reddy and Bunge [2000] emphasizing that when the area fraction of the exposed skin in contact with the chemical is held constant, dermal absorption is larger from many small piles without being in close contact to each other than from a few large piles close together.

This interrelation has been demonstrated by Karande and Mitragotri [2003] investigating the relative permeation increase of model drug when multiple small circular compartments were used instead of one big circular compartment of the same total surface area. But the results have not been explained by the effects of lateral diffusion but by a lateral strain in the skin due to preferential swelling of the skin. This is in contrast to the findings from Lévêque et al. [2002 b] indicating that skin deformation does not have a significant impact on permeability.

Yet the experimentally determined results from Karande can easily be explained by the influence of lateral diffusion. The fragmentation of the one big reference area into

multiple smaller areas practically enlarges the available surface of tissue for lateral diffusion over the same distance *w* as can be seen in figure 5.1.

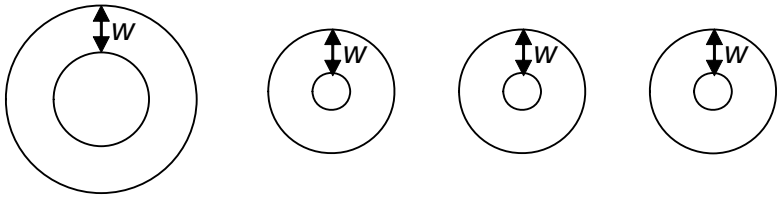

Fig. 5.1: Visualization of the relative increase of surface for lateral diffusion by fragmentation of the donor area

This relative lateral surface increase (matching the normalized permeation enhancement $PE_{(r)}$ used by Karande) can be calculated using equation 5.1 which expresses the surface ratio of *n* lateral rings of width *w* around the small donors with radius *r* to one lateral ring of width *w* around one large donor with radius r_{ref}.

$$PE_{(r)} = \frac{n \cdot \left(\pi \cdot \left(r + w\right)^2 - \pi \cdot r^2\right)}{\pi \cdot \left(r_{ref} + w\right)^2 - \pi \cdot {r_{ref}}^2} \qquad \text{Eq. 5.1}$$

$n = \frac{\pi \cdot {r_{ref}}^2}{\pi \cdot r^2}$ (Ratio of reference donor area to smaller donor area)

$r =$ Radius of smaller donors

$r_{ref} =$ Radius of reference donor

$w =$ Virtual width of the lateral ring

After integrating the term for *n* into equation 5.1 the function can be simplified to equation 5.2.

$$PE_{(r)} = \frac{{r_{ref}}^2 \cdot \left(2 \cdot r + w\right)}{r^2 \cdot \left(2 \cdot r_{ref} + w\right)} \qquad \text{Eq. 5.2}$$

The virtual width of the lateral ring should be an indirect parameter for effectiveness of lateral diffusion and thus be specific for a certain drug formulation.

The comparison of the experimental results from Karande to the mathematical fit using equation 5.2 (with w = 6 mm) is given in figure 5.2 displaying the normalized permeation enhancement over the inverse radius of the several application reservoirs.

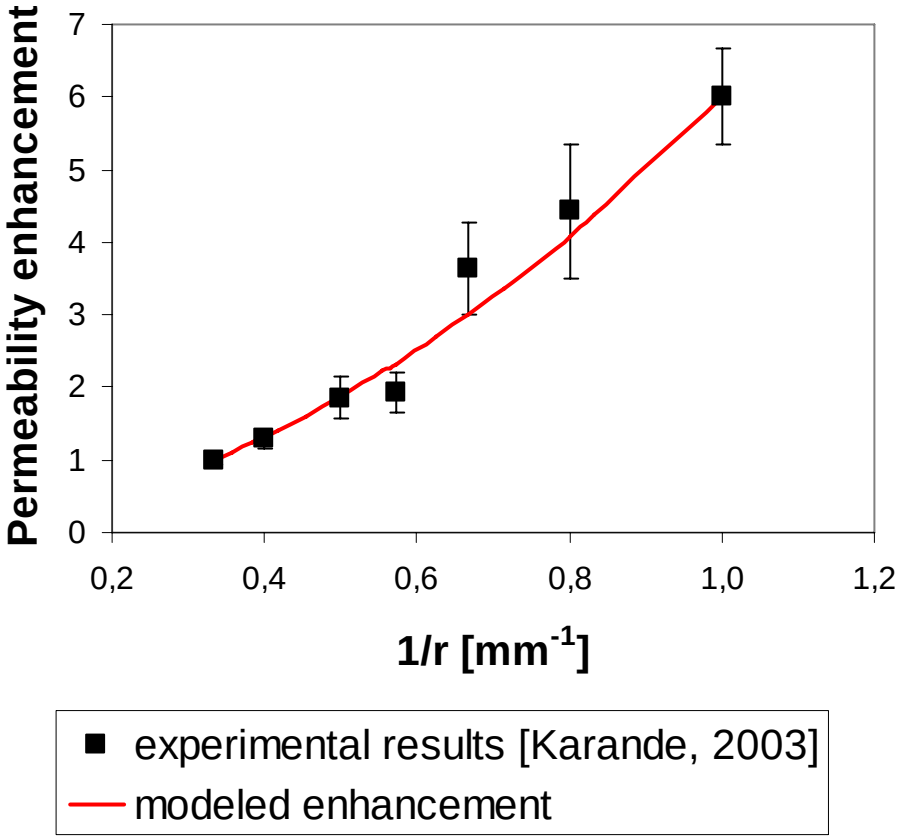

Fig. 5.2: Comparison of the experimentally determined dependence of skin permeability (relative to that of a 6 mm reservoir) to the modeled enhancement on the basis of relative lateral surface increase

This observation indicates special relevance for systemically administered drugs, for instance from a transdermal therapeutic system of the matrix type. These matrix patches are often cut to a specific area for dose adaptation. If the dissected patch

fragment is kept and later applied together with other fragments giving the same total area a significantly greater total dose may be applied.

A study about ketoprofen permeation / penetration conducted by Bock et al. [2004] showed a maximal concentration in the in vivo experiments at the treated site after 3 h while the 6 h results were noticeably lower. The authors attribute this observation (similar to the observed maxima in this work) to the effects of skin hydration after the 6 h occlusion on the tape stripping leading to non-uniform strips and excluded the results from further evaluation. Yet this finding could principally also be explained by lateral diffusion reducing the drug concentration as shown in this work. Since the adjacent sites were not included in the tape stripping this cannot be finally evaluated.

5.2 Comparison of the artificial skin construct to human skin types

5.2.1 Lateral diffusion

Good comparability using ASC can be shown to PHS while the influence on skin's drug content by permeation into the acceptor medium is neglected using the FHS leading to greater contained amounts.

The two phase (accumulation / redistribution) process develops more quickly in ASC compared to the two human skin types. So the occurrence of the maximum concentration in the central area is observed in less than half of the duration. This difference is attributed to the lower permeation barrier of the ASC compared to human stratum corneum as is known from Specht et al. [1998 a] and Winkler and Müller-Goymann [2002] making a quicker invasion of ibuprofen reasonable.

Another difference between ASC and the human skins is seen during the redistribution phase. Typically the concentration gradient curve in the human skins develops from an exponentially shaped decrease over rings one to three to a shape

forming a shoulder due to concentration decrease in ring one while rings two and three maintain their concentration or even increase, respectively. This development is not observed to the same extent in ASC. Here the decline in the central ring segment is relatively smaller so that the exponential shape is maintained and at the same time the increase in distal concentration is increased suggesting larger lateral diffusion.

With regard to the larger increase in lateral drug amounts for the ASC an error source due to a lateral spreading of the formulation on the skin as described by Giese et al. [2000] of up to 20 mm in 11 min can be excluded. It is rather to be suspected that a reuptake of ibuprofen from the acceptor medium into the skin could take place which would be more pronounced for ASC compared to PHS since significantly greater amounts of drug permeate into the acceptor compartment. The more distal ring segments should be most affected due to their lower intrinsic drug concentration. This potential artifact could be avoided by increasing the volume of the acceptor medium by the ratio of permeation coefficients from ASC to PHS and requires further investigation. With regard to the total drug amounts contained in the complete skin sample, irrespective if central or lateral, this deviation is of minor influence.

Over all a good analogy could be shown for the concentration development in ASC and PHS. Furthermore the use of the formulations Ibutop and Ibutop + 5 % DMSO on both ASC and PHS allow highly similar differentiation of the enhancer effect with regard to the total drug amounts in the several skin segments and thus the depot building. In a principal differentiation between the two formulations all three skin types show the trend to reach a plateau of drug content in the skin using Ibutop only while with Ibutop + 5 % DMSO a continuous increase in drug amounts over time is

seen. This continuous increase is explicable from the increased permeation rate in combination with improved drug solubility in the skin.

Regarding the comparison to FHS no direct comparability of drug amounts per segment is seen due to the distortion of the results by lack of drug permeation in FHS. Yet in the relative, percental comparison of laterally diffused drug amounts good comparison for all three skin types is shown.

5.2.2 Permeation results

Although Specht et al. [1998 a] have already shown that the ASC differentiates between permeation rates from formulations comparably to stratum corneum, the permeation from Ibutop and the two additional enhancer (urea / DMSO) containing variations was investigated using the set up from the diffusion experiments. These results should provide comparability to PHS and give insight into the influence of the permeation coefficient on the lateral diffusion. The high similarity of relative permeation enhancement between ASC and PHS in combination with the similarity of the lateral diffusion results provides a good predictability of depot effects from ASC results despite the roughly 30-fold lower diffusion barrier for all three formulations.

5.2.3 Diffusion model fitting

Based on the obtained results from the diffusion experiments a mathematical function was developed empirically allowing to match the observed results from multiple experiments belonging to one result set for lateral diffusion using the parameters C_{max} and t_{max}.

Although the function has a general tendency to overestimate early and underestimate late ring #1 drug concentration the model is able to describe the concentration gradient development within the standard deviation as seen from the

experimental results over time and distance within the timeframe of the experiments. The deviation in early and late estimation is deriving from the term describing the accumulation phase which produces a bell shaped curve returning to almost zero for large diffusion times which should be incorrect for late diffusion times but steady state equilibrium significantly greater than zero should be reached. The parameter *a* largely controls the shape of this term and therefore the speed of concentration increase and decrease in the central ring segment. Interestingly the parameter ratio (Ibutop / Ibutop + DMSO) for this factor *a* from the parametrical fit is exactly identical for ASC and PHS. This and the only minimal variability of the other remaining parameters indicate the high similarity of the lateral diffusion or depot building process between ASC and the human skin in vitro.

6 Summary

The aim of this study is to investigate the spatial drug concentration development within skin focusing especially on effects of lateral drug diffusion and the accompanying drug depot formation. Furthermore a comparison of the effects seen within an artificial skin construct (ASC) to the development in human skin is carried out in order to evaluate the suitability of the ASC for more complex diffusion studies.

For this an experimental set up especially provoking a larger influence of lateral diffusion was developed. Diffusion experiments with ASC, planed human skin (PHS) and full thickness human skin (FHS) were carried out using the ibuprofen containing commercial formulation Ibutop Creme, Ibutop + 5 % urea and Ibutop + 5 % DMSO for several time points. The drug concentration profile was then determined by dissecting the skin sample into five concentric rings which were analyzed separately on their ibuprofen content.

It was shown that the spatial concentration development in all skin types follows the same principal pattern characterized by an initial increase in the central skin section which is in direct contact with the formulation and only slight lateral diffusion into the two directly adjacent skin segments so that larger drug amounts accumulate in the central area. Then the effect of lateral diffusion increases and the drug concentration in the central segment decreases while the lateral diffusion leads to a continuous increase in the lateral skin segments by redistribution. The observed concentration maximum for the central skin segment is explained by the lag time for the effective lateral diffusion leading then to a three dimensional drainage compared to the mainly vertical (one dimensional) diffusion during the accumulation phase.

From these observations a relevant depot building in the skin areas adjacent to the site of application can be proven. The comparison of the total drug amount in the

complete skin sample (sum of rings #1 to #5 of PHS) in relation to the amount permeated through PHS during the time frame of the experiments reveals the relevance of this depot building since 4 – 5 times greater amounts of drug than found in the acceptor medium were determined in the skin with a large fraction in the lateral skin segments.

The use of the additional permeation enhancers mainly lead to larger amounts in the skin but not to a relatively greater lateral diffusion.

The comparison of the results obtained with ASC to those from PHS and FHS show some skin type dependent differences. So the time frame for the concentration profile development as observed in the human skins is largely reduced in ASC which is attributed to the lower permeation barrier. On the other hand the results obtained with FHS show significantly larger amounts of ibuprofen in the skin. This can be explained by the lack of drug permeation using this skin so that also the amounts otherwise found in the acceptor were retained in the skin. Hence a direct comparison of ASC to FHS is not feasible but the comparison to PHS shows that very close resemblance between these two skin types is obtained. This is true for the individual skin segment concentration as well as for the total amount in the skin with a similar differentiation between enhancer containing formulation to Ibutop alone. This high similarity might mainly be based on the very good comparability of the relative permeation enhancing effect of the respective formulations that could be shown in the permeation experiments.

A parametric fit of an empirically developed function to the diffusion results supports that the mechanisms within ASC and human skin responsible for lateral diffusion and thus depot building are highly similar and the use of ASC for studies on drug diffusion in and through skin is reasonable.

7 References

ABDATA API dossier on ibuprofen, state of 10/2007

Abraham, M. H., Chadha, H. S., Mitchell, R. C., The factors that influence skin penetration of solutes, J Pharm Pharmacol 47 (1995) 8-16

Abraham, M. H., Martins, F., Human skin permeation and partition: general linear free-energy relationship analyses, J Pharm Sci 93 (2004) 1508-1523

Ainsworth, M., Methods for measuring percutaneous absorption, J Soc Cosmet Chem 11 (1960) 69-78

Akimoto, T., Nagase, Y., Novel transdermal drug penetration enhancer: synthesis and enhancing effect of alkyldisiloxane compounds containing glucopyranosyl group, J Control Release 88 (2003) 243-252

Alonso, A., Meirelles, M. C., Tabak, M., Effect of hydration upon the fluidity of intercellular membrane of stratum corneum: an EPR study, Biochem Biophys Acta 1237 (1995) 6-15

Ashworth, J., Watson, W. S., Finlay, A. Y., The lateral spread of clobetasol 17-propionate in the stratum corneum in vivo, Br J Dermatol 119 (1988) 351-358

Barbero, A. M., Frasch, H. F., Transcellular route of diffusion through stratum corneu: results from finite element models, J Pharm Sci 95 (2006) 2186-2194

Barry, B. W., Dermatological formulations, Marcel Dekker, INC., 1983

Barry, B. W., Mode of action of penetration enhancers in human skin, J Control Release 6 (1987) 85-97

Bauer, J., Bahmer, F. A., Wörl, J., Neuhuber, W., Schuler, G., Fartasch, M., A strikingly constant ratio exists between Langerhans cells and other epidermal cells

in human skin. A stereologic study using the optical disector method and the confocal laser scanning microscope, J Invest Dermatol 116 (2001) 313-318

Bell, E., Ehrlich, H. P., Buttle, D. J., Nakatsuji, T., Living tissue formed in vitro and accepted as skin-equivalent tissue of full thickness, Science 211 (1981) 1052-1054

Bernard, D., Méhul, B., Schmidt, R., Update on desquamation and first evidence for the presence of the endoglycosidase heparanase 1 in the human stratum corneum, in The Essential Stratum Corneum, Martin Duniz Ltd., (2002) 17-24

Bernard, D., Méhul, B., Thomas-Collignon, A., Simonetti, L., Remy, V., Bernard, M. A., Schmidt, R., Analysis of proteins with caseinolytic activity in a human stratum corneum extract revealed a yet unidentified cysteine protease and identified the so-called "Stratum Corneum Thiol Protease" as Cathepsin L2, J Invest Dermatol 120 (2003) 592-600

Berner, G., Wagener, H. H., The percutaneous kinetics of ibuprofen from a cream formulation, Drug Res 37 (1987) 814-816

Bock, U., Krause, W., Otto, J., Haltner, E., Comparative in vitro and in vivo studies on the permeation and penetration of ketoprofen and ibuprofen in human skin, Drug Res 54 (2004) 522-529

Bouchard, G., Galland, A., Carrupt, P.-A., Gulaboski, R., Mirčeski, V., Scholz, F., Girault, H. H., Standard partition coefficients of anionic drugs in the n-octanol/water system determined by voltammetry at three phase electrodes, Phys Chem Chem Phys 5 (2003) 3748-3751

Boukamp, P., Petrussevska, R. T., Breitkreutz, D., Hornung, J., Markham, A., Fusenig, N. E., Normal keratinization in a spontaneously immortalized aneuploid human keratinocyte cell line, J. Cell. Biol. 106 (1988) 761-771

Bouwstra, J. A., Dubbelaar, F. E., Gooris, G. S., Ponec, M., The sandwich model, Perspectives in Percutaneous Penetration, Vol. 7A (2000) 16

Bronaugh, R. L., Stewart, R. F., Methods for in vitro percutaneous absorption studies. VI. Preparation of the barrier layer, J Pharm Sci 75 (1986) 487-491

Bunge, A. L., Cleek, R. L., A new method for estimating dermal absorption from chemical exposure: 2. Effect of molecular weight and octanol-water partitioning, Pharm Res 12 (1995) 88-95

Cevc, G., Mazgareanu, S., Rother, M., Vierl, U., Occlusion effect on transcutaneous NSAID delivery from conventional and carrier-based formulations, Int J Pharm 359 (2008) 190-197

Chandrasekaran, S. K., Bayne, W., Shaw, J. E., Pharmacokinetics of drug permeation through human skin, J Pharm Sci 67 (1978) 1370-1374

Chapman, S. J., Walsh, A., Desmosomes, corneosomes and desquamation, Arch Dermatol Res 282, (1990) 304-310

Chesnoy, S., Durand, D., Doucet, J., Couarraze, G., Effect of iontophoresis in combination with ionic enhancers on the lipid structure of the stratum corneum: an X-ray-diffraction study, Pharm Res 13 (1996) 1581-1584

Chilcott, R.P., Emanuel, A.J., Is transepidermal water loss a true measure of skin barrier function?, Perspectives in Percutaneous Penetration, Vol. 7A (2000) 49

Coceani, N., Colombo, I., Grassi, M., Acyclovir permeation through rat skin: mathematical modelling and in vitro experiments, Int J Pharm 254 (2003) 197-210

Cullander, C., Guy, R. H., Visualising the pathways of iontophoretic current flow in real time with laser scanning confocal microscopy and the vibrating probe electrode, in Scott, R. C., Guy, R. H., Hadgraft, J., Bodde H. E., Prediction of percutaneous

penetration methods, measurements, modeling, London, IBC technical services 2 (1991) 229-237

Doucet, O., Garcia, N., Zastrow, L., Skin culture model: a possible alternative to the use of excised human skin for assessing in vitro percutaneous absorption, Toxicol in Vitro 12 (1998) 423-430

Dreher, F., Patouillet, C., Fouchard, F., Zanini, M., Messager, A., Roguet, R., Cottin, M., Leclaire, J., Benech-Kieffer, F., Improvement of the experimental setup to assess cutaneous bioavailability on human skin models: Dynamic protocol, Skin Pharmacol Appl Skin Physiol 15 (suppl 1) (2002) 31-39

Elias, P. M., Epidermal lipids, membranes, and keratinization, Int J Dermatol 20 (1981) 1-19

Forslind, B., A domain mosaic model of the skin barrier, Acta Derm Venereol 74 (1994) 1-6

Franz, T. J., Percutaneous absorption. On the relevance of in vitro data, J. Invest. Dermatol. 64 (1975) 190-195

Freshney, R. I., Tierische Zellkulturen: ein Methoden-Handbuch, de Gruyter, Berlin, New York (1990)

Gaede, H. C., Gawrisch, K., Lateral diffusion rates of lipid, water and a hydrophobic drug in a multilamellar liposome, Biophys J 85 (2003) 1734-1740

Giese, K., Neudecker, B.A., Schüle, G., Fluorescence spectroscopy: a rapid, non invasive method for measurement of spreading behaviour and skin penetration of topically applied drugs, Perspectives in Percutaneous Penetration, Vol. 7A (2000) 39

Glombitza, B., Müller-Goymann, C. C., Investigation of interactions between silicones and stratum corneum lipids, Int J Cosmet Sci 23 (2001) 25-34

González, N., Sumano, H., Design of two liquid ibuprofen-poloxamer-limonene or menthol preparations for dermal administration, Drug Deliv 14 (2007) 287-293

Gu, X., Dannefaer, J. L., Collins, B. R., In vitro permeation characterisation of the analgesic ibuprofen and the sunscreen oxybenzone, Drug Dev Ind Pharm 34 (2008) 845-852

Guy, R. H., Hadgraft, J., Prediction of drug disposition kinetics in skin and plasma following topical administration, J Pharm Sci 73 (1984) 883-887

Guy, R. H., Potts, R. O., Structure-permeability relationship in percutaneous penetration, J Pharm Sci 81 (1992) 603-604

Gysler, A., Kleuser, B., Sippl, W., Lange, K., Korting, H. C., Höltje, H. D., Schäfer-Korting, M., Skin penetration and metabolism of topical glucocorticoids in reconstructed epidermis and in excised human skin, Pharm Res 16 (1999) 1386-1391

Hadgraft, J., Passive enhancement strategies in topical and transdermal drug delivery, Int J Pharm 184 (1999) 1-6

Hadgraft, J., Crossing the barrier, in The essential stratum corneum Martin Duniz Ltd., (2002) 103-109

Hadgraft, J., **Whitefield, M., Rosher, P. H**., Skin penetration of topical formulations of ibuprofen 5%: an in vitro comperative study, Skin Pharmacol Appl Skin Physiol 16 (2003) 137-142

Haftek, M., Ultrastructural aspects of the stratum corneum, in The essential stratum corneum Martin Duniz Ltd., (2002) 3-15

Herkenne, C., Naik, A., Kalia, Y. N., Hadgraft, J., Guy, R. H., Ibuprofen transport into and through skin from topical formulations: in vitro - in vivo comparison, J Invest Dermatol 127 (2007) 135-142

Hirvonen, J., Rytting, J.H., Paronen, P., Urtti, A., Dodecyl N,N-dimethylamino acetate and azone enhance drug penetration across human, snake and rabbit skin, Pharm Res 8 (1991) 933-937

Hoath, S. B., Leahy, D. G., Formation and function of the stratum corneum, in The Essential Stratum Corneum, Martin Duniz Ltd., (2002) 31-40

Holbrook, K., Odland, G., Regional differences in the thickness (cell layers) of the human stratum corneum: an ultrastrucural analysis, J Invest Dermatol 62 (1974) 415-422

Johnson, M. E., Berk, D. A., Blankschtein, D., Golan, D. E., Jain, R. K., Langer, R. S., Lateral diffusion of small compounds in human stratum corneum and model lipid bilayer systems, Biophys J 71 (1996) 2656-2668

Johnson, M. E., Blankschtein, D., Langer, R., Evaluation of solute permeation through the stratum corneum: lateral bilayer diffusion as the primary transport mechanism, J Pharm Sci 86 (1997) 1162- 1172

Karande, P., Mitragotri, S., Dependence of skin permeability on contact area, Pharm Res 20 (2003) 257-263

Kitson, N., Thewalt, J., Lafleur, M., Bloom, M., A model membrane approach to the epidermal permeability barrier, Biochemistry 33 (1994) 6707-6715

Kietzmann, M., Löscher, W., Arens, D., Maaß, P., Lubach, D., The isolated perfused bovine udder as an in vitro model of percutaneous drug absorption. Skin

viability and percutaneous absorption of dexamethasone, benzoyl peroxide and etofenamate, J Pharmacol Toxicol Methods 30 (1993) 75-84

Knorr, F., Lademann, J., Patzelt, A., Sterry, W., Blume-Peytavi, U., Vogt, A., Follicular transport route – research progress and future perspectives, Eur. J. Pharm. Biopharm 71 (2009) 173-180

Kuntsche, J., Bunjes, H., Fahr, A., Pappinen, S., Rönkkö, S., Suhonen, M., Urtti, A., Interaction of lipid nanoparticles with human epidermis and an organotypic cell culture model, Int J Pharm 354 (2008) 180-195

Lampe, M. A:, Williams, M. L., Elias, P. M., Human stratum corneum lipids: characterization and regional variations; J Lipid Res 24 (1983) 120-130

Landmann, L., Epidermal permeability barrier: transformation of lamellar granule-disks into intercellular sheets by a membrane fusion process, a freeze fracture study, J Invest Dermatol 87 (1986) 202-209

Landmann, L., Die Permeabilitätsbarriere der Haut, Pharmazie in unserer Zeit, 20 (1991) 155-163

Lee, A. J., King, J. R., Rogers, T. G., A multiple-pathway model for the diffusion of drugs in skin, J Math Appl Med Bio 13 (1996) 127-150

Lee, K. J., Hwang, S. J., Kim, J. S., Kim, D. D., Shin, Y. H., Lee, C. H., Effects of HPE-101, a skin penetration enhancer, on human erythrocyte membranes, Int J Pharm 285 (2004) 43-49

Lévêque, J.-L., Lipid organization and barrier function, in The Essential Stratum Corneum, Martin Duniz Ltd., (2002 a) 111-117

Lévêque, J.-L., Hallégot, P., Doucet, J., Piérard, G., Structure and function of human stratum corneum under deformation, Dermatology 205 (2002 b) 353-357

Lombardi Borgia, S., Schlupp, P., Mehnert, W., In vitro skin absorption and drug release - A comparison of six commercial prednicarbate preparations for topical use, Eur J Pharm Biopharm 68 (2008) 380-389

Lotte, C., Rougier, A., Wilson, D.R., Maibach, H.I., In vivo relationship between transepidermal water loss and percutaneous penetration of some organic compounds in man: effect of anatomic site, Arch Dermatol Res 279 (1987) 351-356

Lundström, A., Serre, G., Haftek, M., Egelrud, T., Evidence for a role of corneodesmosine, a protein which may serve to modify desmosomes during cornification, in stratum corneum cell cohesion and desquamation, Arch Dermatol Res 286 (1994) 369–375

Meshali, M. M., Abdel-Aleem, H. M., Sakr, F. M., Nazzal, S., El-Malah, Y., In vitro phonophoresis: effect of ultrasound intensity and mode at high frequency on NSAIDs transport across cellulose and rabbit skin membranes, Pharmazie 63 (2008) 49-53

Mitragotri, S., A theoretical analysis of permeation of small hydrophobic solutes across the stratum corneum based on Scaled Particle Theory, J Pharm Sci 91 (2002) 744-752

Mitragotri, S., Modeling skin permeability to hydrophilic and hydrophobic solutes based on four permeation pathways, J Control Release 86 (2003) 69-92

Moll, I., Unsere dynamische Haut, Chapter 1 in Jung, E. G., Dermatologie, Hippokrates Verlag GmbH, Stuttgart 1989

Netzlaff, F., Lehr, C.-M., Wertz, P. W., Schaefer, U. F., The human epidermis models EpiSkin SkinEthic and EpiDerm: An evaluation of morphology and their suitability for testing phototoxicity, irritancy, corrosivity and substance transport, Eur J Pharm Biopharm 60 (2005) 167-178

Netzlaff, F., Kaca, M., Bock, U., Haltner-Ukomadu, E., Meiers, P., Lehr, C.-M., Schaefer, U. F., Permeability of the reconstructed human epidermis model Episkin in comparison to various human skin preparations, Eur J Pharm Biopharm 66 (2007) 127-134

Nicolazzo, J. A., Morgan, T. M., Reed, B. L., Finnin, B. C., Synergistic enhancement of testosterone transdermal delivery, J Control Release 103 (2005) 577-585

Nicoli, S., Bunge, A. L., Delgado-Charro, M., Guy, R. H., Dermatopharmacokinetics: factors influencing drug clearance from the stratum corneum, Pharm Res 26 (2009) 865-871

Norlen, L., Skin barrier structure and function: the single gel phase model, J Invest Dermatol 117 (2001) 830-836

Öhman, H., Vahlquist, A., In vivo studies concerning a pH gradient in human stratum corneum and upper epidermis, Acta Derm Venereol 74 (1994) 375–379

Pfeifer, S., Pflegel, P., Borchert, H.-H., Grundlagen der Biopharmazie, Verlag Volk und Gesundheit, Berlin (1984) 72

Pinkus, H., The direction of growth of human epidermis, Br J Dermatol 83 (1970) 556-564

Potts, R. O., Guy, R. H., A predictive algorithm for skin permeability: the effects of molecular size and hydrogen bond activity, Pharm Res 12 (1995) 1628-1633

Reddy, M. B., Bunge, A. L., Dermal absorption of chemicals deposited on the skin surface: effects of spatial distribution, Perspectives in Percutaneous Penetration, Vol 7a (2000) 21

Ryan, T. J., The direction of growth of epithelium, Br J Dermatol 78 (1966) 403-415

Savi, S., Savi, M., Tamburi, S., Vuleta, G., Vesi, S., Müller-Goymann, C. C., An alkylpolyglucoside surfactant as a prospective pharmaceutical excipient for topical formulations: the influence of oil polarity on the colloidal structure and hydrocortisone in vitro/in vivo permeation, Eur J Pharm Sci 30 (2007) 441-450

Schendzielorz, A., Neubert, R., Muck, A., Reconstituted stratum corneum as model membrane for penetration studies/preparation and characterization, Pharm Ind 59 (1997) 712-717

Scheuplein, R. J., Robert, J., Permeability of the skin: a review of major concepts and some new developments, J Invest Dermatol 67 (1976) 672-676

Schmook, F. G., Meingassner, J. G., Billich, A., Comparison of human skin or epidermis models with human and animal skin in vitro percutaneous absorption, Int J Pharm 215 (2001) 51-56

Sekkat, N., Kalia, Y. N., Guy, R. H., Biophysical study of porcine ear skin in vitro and its comparison to human skin in vivo, J Pharm Sci 91 (2002) 2376-2381

Shah, S. N., Rabbani, M., Amir, M. F., Effect of urea on topical absorption of diclofenac diethylamine through hairless rabbit skin, J Res Sci 17 (2006) 165-171

Shimada, K., Yoshihara, T., Yamamoto, M., Konno, K., Momoi, Y., Nishifuji, K., Iwasaki, T., Transepidermal water loss (TEWL) reflects skin barrier function of dog, J Vet Med Sci 70 (2008) 841-843

Simonsen, L., Petersen, M. B., Benfeldt, E., Serup, J., Development of an in vivo animal model for skin penetration in hairless rats assessed by mass balance, Skin Pharmacol Appl Skin Physiol 15 (2002) 414-424

Sparr, E., Wennerström, H., Responding phospholipids membranes – interplay between hydration and permeability, Biophys J 81 (2001) 1014-1028

Specht, C., Stoye, I., Müller-Goymann, C. C., Comparative investigations to evaluate the use of organotypic cultures of transformed and native dermal and epidermal cells for permeation studies, Eur. J. Pharm. Biopharm. 46 (1998 a) 273-278

Specht, C., Entwicklung organotypischer Hautäquivalente und ihre Testung auf Eignung für Permeationsuntersuchungen von Arzneistoffen aus dermalen Zubereitungen, Dissertation Technische Universität Braunschweig (1998 b)

Stoye, I., Permeabilitätsveränderung von humanem Stratum corneum nach Applikation nicht-steroidaler Antirheumatika in verschiedenen kolloidalen Trägersystemen, Dissertation Technische Universität Braunschweig (1997)

Suzuki, Y., Nomura, J., Koyama, J., Horii, I., The role of proteases in stratum corneum: involvement in stratum corneum desquamation, Arch Dermatol Res 286 (1994) 249-253

Sweeney, T. M., Downing, D. T., The role of lipids in the epidermal barrier to water diffusion, J Invest Dermatol 55 (1970) 135-140

Takahashi, M., Marks, R., Conformational and functional changes in the stratum corneum after forced extension, Bioeng Skin 2 (1985) 39-48

Tang, H., Mitragotri, S., Blankschtein, D., Langer, R., Theoretical description of transdermal transport of hydrophilic permeants: application to low-frequency sonophoresis, J Pharm Sci 90 (2001) 545-568

Tang, H., Blankschtein, D., Langer, R., Prediction of steady-state skin permeabilities of polar and nonpolar permeants across excised pig skin based on measurements of transient diffusion: Characterization of hydration effects on the skin porous pathway, J Pharm Sci 91 (2002) 1891-1907

Tayar, N., Tsai, R.-S., Testa, B., Carrupt, P.-A., Hansch, C., Leo, A., Percutaneous penetration of drugs: a quantitative structure-permeability relationship study, J Pharm Sci 80 (1991) 744-749

Tegtmeyer, S., Papantoniou, I., Müller-Goymann, C. C., Reconstruction of an in vitro cornea and ist use for drug permeation studies from different formulations containing pilocarpine hydrochloride, Eur J Pharm Biopharm 51 (2001) 119-125

Tezel, A., Mitragotri, S., On the origin of size-dependent tortuosity for permeation of hydrophilic solutes across the stratum corneum, J Control Release 86 (2003) 183-186

Tojo, K., Chiang, C. C., Chien, Y. W., Drug permeation across the skin: effect of penetrant hydrophilicity, J Pharm Sci 76 (1987) 123-126

Treffel, P., Muret, P., Muret-D'Aniello, P., Coumes-Marquet, S., Agache, P., Effect of occlusion on in vitro percutaneous absorption of two compounds with different physicochemical properties, Skin Pharmacol 5 (1992) 108-113

Vávrová, K., Lorencová, K., Klimentová, J., Novotný, J., Holý, A., Hrabálek, A., Transdermal and dermal delivery of adefovir: Effects of pH and permeation enhancers, Eur J Pharm Biopharm 69 (2008) 597-604

Wagner, H., Kostka, K.-H., Lehr, C.-M., Schaefer, U. F., Ex vivo skin models for the study of drug penetration and permeation, Proc. 2nd World Meeting APGI/APV, Paris, 25/28 May 1998, 831-832

Wagner, H., Kostka, K.-H., Lehr, C.-M., Schaefer, U. F., Interrelation of permeation and penetration parameters obtained from in vitro experiments with human skin and skin equivalents, J Control Release 75 (2001) 283-295

Wagner, H., Kostka, K.-H., Lehr, C.-M., Schaefer, U. F., Human skin penetration of flufenamic Acid: in vivo/in vitro correlation (deeper skin layers) for skin samples from the same subject, J Invest Dermatol 118 (2002) 540-544

Walters, K. A., Brain, K. R., Skin permeation predictions and databases – what are their limitations?, , Perspectives in Percutaneous Penetration, Vol 7a (2000) 15

Warner, K. S., Li S. K., He K., Suhonen T. M., Chantasart D., Bolikal D., Higuchi W. I., Structure-activity relationship for chemical skin permeation enhancers: probing the chemical microenvironment of the site of action, J Pharm Sci 92 (2003) 1305-1322

Wassermann, K., Müller-Goymann, C. C., Standardized cultivation of artificial skin constructs for drug permeation studies, Arch. Pharm. Pharm. Med. Chem. 333 (Suppl. 1) (2000) 34

Weigmann, H.-J., Lademann, J., v.Pelchrzim, R., Sterry, W., Hagemeister, T., Molzahn, R., Schaefer, M., Lindscheid, M., Schaefer, H., Shah, V. P., Bioavailability of clobetasol proprionate – quantification of drug concentrations in the stratum corneum by dermatopharmacokinetics using tape stripping, Skin Pharmacol Appl Skin Physiol. 12 (1999) 46-53

Wheater, P. R., Burkitt, H. G., Daniels, V. G., Funktionelle Histologie, Urban & Schwarzenberg, (1987) 131

Wiechers, J. W., The barrier function of the skin in relation to percutaneous absorption of drugs, Pharm Weekbl Sci Ed 11 (1989) 185-198

Winkler, A., Müller-Goymann, C. C., Comperative permeation studies for δ-aminolevulinic acid and its n-butyl ester through stratum corneum and artificial skin constructs, Eur J Pharm Biopharm 53 (2002) 281-287

Winkler, A., Untersuchungen zur Permeation von 5-Aminolävulinsäure (ALA) und ALA-*n*-butylester durch excidiertes humanes Stratum corneum und organotypisches Hautkonstrukt, Dissertation Technische Universität Braunschweig (2005); http://www.digibib.tu-bs.de/?docid=00001726

Yourick, J. J., Jung, C. T., Bronaugh, R. L., In vitro and in vivo percutaneous absorption of retinol from cosmetic formulations: Significance of the skin reservoir and prediction of systemic absorption, Toxicol Appl Pharmacol 231 (2008) 117-121

Yu, B., Kim, K. H., So, P. T. C., Blankschtein, D., Langer, R., Visualization of oleic acid-induced transdermal diffusion pathway using two-photon fluorescence microscopy, J Invest Dermatol 120 (2003) 448-455

Zesch, A., Schaefer, H., Penetrationskinetik von radiomarkiertem Hydrocortison aus verschiedenartigen Salbengrundlagen in die menschliche Haut, Arch Derm Forsch 252 (1975) 245-256

Zgoda, M. M., Kolodziejska, J., Nachajski, M. J., Viscosity of hydrogel pharmaceutical products and the rate of diffusion of ibuprofen hydrotropic binding through model phase boundary in vitro, Polim Med 37 (2007) 3-24

Zobel, H. P., Brinkmann, I., Fröstl, B., Heim, S., Müller, C., Van Nguyen, TH., Prescher, K., Zimmer, A., Alternativen zum Salbenrühren im Vergleich, PZ, 35 (1997) 2944-2951

Zuurmond, W. W., Langendijk, P. N., Bezemer, P. D., Brink, H. E., de Lange, J. J., van loenen, A. C., Treatment of acute reflex sympathetic dystrophy with DMSO 50% in a fatty cream, Acta Anaesthesiol Scand 40 (1996) 364-367

8 Annex

The data in this annex provides the basis for the diagrams which were presented in the results and discussion section (4.2 and 4.5) and are included for consultation in case a more detailed comparison of results than possible from the graphs is needed.

8.1 Data from diffusion experiments

8.1.1 Full thickness human skin (FHS)

8.1.1.1 Ibutop on FHS

Table 8.1: Ibuprofen content of the ring segments in [µg/mm^2] for the respective diffusion experiment time periods using Ibutop on FHS

Ibutop on FHS		Ring #1 [1.25 mm]	Ring #2 [3.75 mm]	Ring #3 [6.25 mm]	Ring #4 [8.75 mm]	Ring #5 [11.0 mm]
Duration	**n=**	**Ø ± SD**	**Ø ± SD**	**Ø ± SD**	**Ø ± SD**	**Ø ± SD**
90 min	4	0.283 ±0.040	0.157 ±0.040	0.021 ±0.002	0.005 ±0.007	0.000 ±0.000
195 min	5	0.554 ±0.065	0.244 ±0.065	0.027 ±0.030	0.011 ±0.003	0.000 ±0.000
270 min	5	0.771 ±0.179	0.249 ±0.026	0.007 ±0.016	0.007 ±0.010	0.018 ±0.011
330 min	5	0.470 ±0.091	0.231 ±0.031	0.031 ±0.007	0.015 ±0.014	0.021 ±0.009
390 min	6	0.355 ±0.068	0.275 ±0.036	0.060 ±0.007	0.020 ±0.011	0.018 ±0.008

8.1.1.2 Ibutop + 5 % urea on FHS

Table 8.2: Ibuprofen content of the ring segments in [µg/mm^2] for the respective diffusion experiment time periods using Ibutop + 5 % urea on FHS

Ibutop+urea on FHS		Ring #1 [1.25 mm]	Ring #2 [3.75 mm]	Ring #3 [6.25 mm]	Ring #4 [8.75 mm]	Ring #5 [11.0 mm]
Duration	**n=**	**Ø ± SD**	**Ø ± SD**	**Ø ± SD**	**Ø ± SD**	**Ø ± SD**
90 min	6	0.322 ±0.034	0.159 ±0.029	0.030 ±0.005	0.008 ±0.003	0.009 ±0.003
180 min	6	0.624 ±0.080	0.265 ±0.042	0.040 ±0.007	0.014 ±0.003	0.011 ±0.004
270 min	6	0.803 ±0.126	0.269 ±0.039	0.054 ±0.011	0.026 ±0.006	0.018 ±0.006
300 min	6	0.781 ±0.098	0.315 ±0.036	0.074 ±0.010	0.033 ±0.007	0.025 ±0.006
330 min	6	0.495 ±0.058	0.330 ±0.031	0.080 ±0.010	0.038 ±0.008	0.029 ±0.006
390 min	6	0.483 ±0.068	0.370 ±0.037	0.105 ±0.015	0.046 ±0.008	0.034 ±0.006

8.1.1.3 Ibutop + 5 % DMSO on FHS

Table 8.3: Ibuprofen content of the ring segments in [µg/mm^2] for the respective diffusion experiment time periods using Ibutop + 5 % DMSO on FHS

Ibutop+DMSO on FHS		Ring #1 [1.25 mm]	Ring #2 [3.75 mm]	Ring #3 [6.25 mm]	Ring #4 [8.75 mm]	Ring #5 [11.0 mm]
Duration	**n=**	**Ø ± SD**	**Ø ± SD**	**Ø ± SD**	**Ø ± SD**	**Ø ± SD**
90 min	6	0.324 ±0.026	0.162 ±0.024	0.031 ±0.004	0.010 ±0.003	0.009 ±0.002
180 min	6	0.640 ±0.086	0.279 ±0.026	0.044 ±0.005	0.017 ±0.003	0.013 ±0.004
270 min	6	0.805 ±0.119	0.276 ±0.024	0.055 ±0.009	0.029 ±0.003	0.021 ±0.004
300 min	6	0.747 ±0.067	0.320 ±0.037	0.080 ±0.011	0.036 ±0.005	0.026 ±0.006
330 min	6	0.609 ±0.061	0.349 ±0.037	0.101 ±0.009	0.041 ±0.009	0.032 ±0.006
390 min	6	0.556 ±0.041	0.424 ±0.038	0.126 ±0.019	0.055 ±0.010	0.039 ±0.006

8.1.2 Planed human skin (PHS)

8.1.2.1 Ibutop on PHS

Table 8.4: Ibuprofen content of the ring segments in [µg/mm^2] for the respective diffusion experiment time periods using Ibutop on PHS

Ibutop on PHS		Ring #1 [1.25 mm]	Ring #2 [3.75 mm]	Ring #3 [6.25 mm]	Ring #4 [8.75 mm]	Ring #5 [11.0 mm]
Duration	**n=**	**Ø ± SD**	**Ø ± SD**	**Ø ± SD**	**Ø ± SD**	**Ø ± SD**
180 min	6	0.405 ±0.052	0.128 ±0.026	0.044 ±0.019	0.011 ±0.004	0.000 ±0.000
240 min	6	0.443 ±0.044	0.151 ±0.025	0.057 ±0.016	0.014 ±0.004	0.001 ±0.001
300 min	6	0.288 ±0.033	0.182 ±0.024	0.069 ±0.013	0.019 ±0.007	0.003 ±0.002
330 min	6	0.231 ±0.034	0.181 ±0.037	0.092 ±0.017	0.023 ±0.008	0.008 ±0.005

8.1.2.2 Ibutop + 5 % DMSO on PHS

Table 8.5: Ibuprofen content of the ring segments in [µg/mm^2] for the respective diffusion experiment time periods using Ibutop + 5 % DMSO on PHS

Ibutop+DMSO on PHS		Ring #1 [1.25 mm]	Ring #2 [3.75 mm]	Ring #3 [6.25 mm]	Ring #4 [8.75 mm]	Ring #5 [11.0 mm]
Duration	**n=**	**Ø ± SD**	**Ø ± SD**	**Ø ± SD**	**Ø ± SD**	**Ø ± SD**
180 min	6	0.415 ±0.036	0.136 ±0.019	0.049 ±0.015	0.013 ±0.004	0.000 ±0.000
240 min	6	0.459 ±0.048	0.159 ±0.017	0.072 ±0.008	0.019 ±0.005	0.005 ±0.003
300 min	6	0.314 ±0.031	0.203 ±0.021	0.085 ±0.010	0.024 ±0.006	0.009 ±0.005
330 min	6	0.263 ±0.030	0.222 ±0.018	0.112 ±0.013	0.037 ±0.008	0.013 ±0.006

8.1.3 Artificial skin construct (ASC)

8.1.3.1 Ibutop on ASC

Table 8.6: Ibuprofen content of the ring segments in [µg/mm^2] for the respective diffusion experiment time periods using Ibutop on ASC

Ibutop on ASC		Ring #1 [1.25 mm]	Ring #2 [3.75 mm]	Ring #3 [6.25 mm]	Ring #4 [8.75 mm]	Ring #5 [11.0 mm]
Duration	**n=**	**Ø ± SD**	**Ø ± SD**	**Ø ± SD**	**Ø ± SD**	**Ø ± SD**
10 min	5	0.224 ±0.050	0.117 ±0.025	0.031 ±0.008	0.016 ±0.005	0.011 ±0.008
30 min	5	0.298 ±0.031	0.126 ±0.017	0.028 ±0.006	0.009 ±0.002	0.003 ±0.004
60 min	5	0.436 ±0.069	0.137 ±0.034	0.037 ±0.013	0.012 ±0.004	0.000 ±0.000
135 min	3	0.409 ±0.005	0.139 ±0.010	0.050 ±0.007	0.030 ±0.006	0.009 ±0.004
210 min	4	0.347 ±0.057	0.106 ±0.036	0.045 ±0.006	0.049 ±0.004	0.000 ±0.000
250 min	3	0.263 ±0.012	0.127 ±0.000	0.075 ±0.017	0.054 ±0.000	0.039 ±0.007

8.1.3.2 Ibutop + 5 % DMSO on ASC

Table 8.7: Ibuprofen content of the ring segments in [µg/mm^2] for the respective diffusion experiment time periods using Ibutop + 5 % DMSO on ASC

Ibutop+DMSO on ASC		Ring #1 [1.25 mm]	Ring #2 [3.75 mm]	Ring #3 [6.25 mm]	Ring #4 [8.75 mm]	Ring #5 [11.0 mm]
Duration	**n=**	**Ø ± SD**	**Ø ± SD**	**Ø ± SD**	**Ø ± SD**	**Ø ± SD**
10 min	6	0.243 ±0.046	0.131 ±0.022	0.039 ±0.008	0.020 ±0.008	0.010 ±0.005
30 min	6	0.314 ±0.042	0.155 ±0.022	0.045 ±0.008	0.023 ±0.007	0.005 ±0.003
60 min	6	0.466 ±0.051	0.163 ±0.023	0.041 ±0.008	0.019 ±0.006	0.013 ±0.007
120 min	6	0.440 ±0.069	0.176 ±0.018	0.052 ±0.011	0.025 ±0.008	0.018 ±0.008
180 min	6	0.376 ±0.046	0.183 ±0.022	0.078 ±0.011	0.047 ±0.012	0.024 ±0.010
240 min	6	0.311 ±0.038	0.177 ±0.016	0.086 ±0.010	0.062 ±0.015	0.042 ±0.011

8.2 Data for total drug amount from diffusion and permeation experiments

8.2.1 Ibutop on FHS, PHS and ASC

Table 8.8: Amount of ibuprofen as sum from the ring segments' content and the respective permeated amount in [µg] for the several diffusion experiment time periods using Ibutop on all three skin types

	Ibutop			
Skin type	**Time [min]**	**Skin content Ø ± SD [µg]**	**Permeated amount Ø ± SD [µg]**	**Total Ø ± SD [µg]**
FHS	**90**	17.58 ± 2.87	—	17.58 ± 2.87
	195	29.43 ± 7.18	—	29.43 ± 7.18
	270	33.87 ± 5.13	—	33.87 ± 5.13
	330	30.90 ± 2.86	—	30.90 ± 2.86
	390	34.48 ± 4.57	—	34.48 ± 4.57
PHS	**180**	21.36 ± 1.65	2.79 ± 0.23	24.15 ± 1.89
	240	25.30 ± 2.09	3.72 ± 0.31	29.02 ± 2.40
	300	26.28 ± 3.28	4.65 ± 0.39	30.93 ± 3.67
	330	28.50 ± 4.18	5.11 ± 0.43	33.62 ± 4.61
ASC	**10**	18.17 ± 3.28	4.61 ± 1.12	22.77 ± 4.40
	30	17.74 ± 1.41	13.82 ± 3.36	31.56 ± 4.77
	60	21.86 ± 2.87	27.64 ± 6.72	49.51 ± 9.59
	135	26.49 ± 1.39	62.20 ± 15.11	88.69 ± 16.50
	210	24.16 ± 1.38	96.75 ± 23.50	120.92 ± 24.89
	250	32.77 ± 2.75	115.18 ± 27.98	147.95 ± 30.73

8.2.2 Ibutop + 5 % DMSO on FHS, PHS and ASC

Table 8.9: Amount of ibuprofen as sum from the ring segments' content in [µg] and the respective permeated amount in [µg] for the several diffusion experiment time periods using Ibutop + 5 % DMSO on all three skin types

	Ibutop + 5 % DMSO			
Skin type	**Time [min]**	**Skin content Ø ± SD [µg]**	**Permeated amount Ø ± SD [µg]**	**Total Ø ± SD [µg]**
FHS	**90**	21.60 ± 1.78	—	21.60 ± 1.78
	180	37.45 ± 3.21	—	37.45 ± 3.21
	270	44.26 ± 3.28	—	44.26 ± 3.28
	330	52.41 ± 3.34	—	52.41 ± 3.34
	390	61.21 ± 3.05	—	61.21 ± 3.05
PHS	**180**	22.67 ± 1.84	4.93 ± 0.34	27.60 ± 2.18
	240	28.74 ± 2.46	6.57 ± 0.45	35.30 ± 2.91
	300	30.91 ± 3.70	8.21 ± 0.57	39.12 ± 4.26
	330	36.10 ± 4.50	9.03 ± 0.62	45.13 ± 5.13
ASC	**10**	20.36 ± 4.03	7.80 ± 1.30	28.16 ± 5.33
	30	23.50 ± 2.13	23.40 ± 3.89	46.90 ± 6.01
	60	27.20 ± 3.29	46.79 ± 7.78	74.00 ± 11.07
	120	30.09 ± 3.65	93.59 ± 15.55	123.68 ± 19.21
	180	35.51 ± 3.67	140.38 ± 23.33	175.89 ± 26.99
	240	39.29 ± 2.45	187.18 ± 31.10	226.47 ± 33.55

Lebenslauf

Name	Guido Lutz Schicksnus
Geburtsdatum	21.08.71
Geburtsort	Wolfsburg
Staatsangehörigkeit	deutsch
Familienstand	verheiratet, 2 Kinder

Schulbildung	1977 - 1980	Kardinal Galen Schule, Hannover
	1981 - 1982	Ludwig Windhorst Schule, Hannover
	1983 - 1988	Gymnasium Schillerschule, Hannover
	1988 - 1989	Besuch der San Simon High School in San Simon, Arizona, USA mit Abschluss
	1989 - 1991	Gymnasium Schillerschule, Hannover (allg. Hochschulreife)
Wehrdienst	10/1991 - 09/1992	Sanitätssoldat der Luftwaffe
Ausbildung	10/1992 - 09/1997	Studium der Pharmazie an der Technischen Universität (TU) Braunschweig
	21/03/1996	1. Abschnitt der Pharmazeutischen Prüfung
	28/10/1997	2. Abschnitt der Pharmazeutischen Prüfung
	12/1997 - 05/1998	Praktikum bei der Salutas Pharma GmbH in Barleben bei Magdeburg
	06/1998 - 11/1998	Praktikum in der Löwen-Apotheke in Hannover
	11/12/1998	3. Abschnitt der Pharmazeutischen Prüfung
	12/01/1999	Erteilung der Approbation
	12/1998 - 02/2004	Promotionsarbeit am Institut für Pharmazeutische Technologie, TU Braunschweig, unter Leitung von Frau Prof. Dr. C. Müller-Goymann
Berufliche Tätigkeit	12/1998 - 02/2004	Wissenschaftlicher Mitarbeiter am o.g. Institut
	05/2004 - 07/2008	Leiter der analytischen Chemie bei der Hameln pharmaceuticals GmbH, Hameln
	07/2006	Benennung zum Leiter der Qualitätskontrolle und zur Sachkundigen Person (Qualified Person) bei Hameln pharmaceuticals
	08/2008 - 02/2010	Chemical and Pharmaceutical Project Leader bei der Solvay pharmaceuticals GmbH, Hannover
	02/2010 - heute	Product Development Manager bei der Abbott products GmbH, Hannover